LOW REYNOLDS NUMBER FLOW PAST AN INFINITE ROW OF CIRCULAR CYLINDERS WITH SURFACE MASS TRANSFER

A THESIS

Presented to

The Faculty of the Division of Graduate Studies

by

Ta-Yeh J. Fang

In Partial Fulfillment

of the Requirements for the Degree

Doctor of Philosophy

in the School of Chemical Engineering

Georgia Institute of Technology

June, 1975

LOW REYNOLDS NUMBER FLOW PAST AN

INFINITE ROW OF CIRCULAR CYLINDERS

WITH SURFACE MASS TRANSFER

Approved:

Dr. Henderson C. Ward, Chairman

Dr. Charles W. Gorton

Dr. Jade T. Sommerfeld

Date Approved by Chairman: 5/2/25

ACKNOWLEDGEMENTS

The author wishes to express his sincere appreciation to Dr. Henderson C. Ward, his thesis advisor, for suggesting this problem and for his advice and guidance throughout the progress of this study. He is also indebted to Dr. Charles W. Gorton and Dr. Jude T. Sommerfeld who served as members of the thesis committee, for their many helpful suggestions and careful review of the entire thesis. In addition, appreciation is extended to Dr. Homer V. Grubb and Dr. Dar-Veig Ho for having served on the orals committee.

Particular appreciation is expressed to Dr. Waldemar T. Ziegler for his valuable guidance and advice during the course of the graduate studies.

Thanks are also extended to Dr. Joseph J. Smrekar for his help in arranging the use of the computer and to Mrs. Nancy Price for her excellent work in the typing of the final draft of this thesis.

Acknowledgement is also due to the office of Computing Services, Georgia Institute of Technology for their great help and instructions.

I also wish to thank my family for giving their encouragement and financial support throughout my graduate study at the Georgia Institute of Technology.

TABLE OF CONTENTS

Page

LIST OF TABLES

LIST OF ILLUSTRATIONS

LIST OF ILLUSTRATIONS (Continued)

LIST OF ILLUSTRATIONS (Continued)

LIST OF ILLUSTRATIONS (Concluded)

NOMENCLATURE

a	radius of a circular cylinder
A	component A of binary solution
B	component B of binary solution
C	dimensionless mass concentration of component A
C_D	total drag coefficient
C_{DF}	friction drag coefficient
C_{DP}	pressure drag coefficient
C_P	pressure coefficient
D	diameter
$\mathscr{D}$	diffusivity of binary solution
f	function of a variable or friction factor
G	radial suction mass flux in gallons/ft^2/day (gfd)
I	positive integer in angular direction
J	positive integer in radial direction
$k_{x,loc}$	local mass transfer coefficient
M	number of grid spacings in angular direction
N	number of grid spacings in radial direction
n_{Ao}	radial mass flux of component A at the surface
n_{Bo}	radial mass flux of component B at the surface
Nu_{loc}	local Nusselt number, $\frac{2ak_{x,loc}}{C\mathscr{D}}$
$Nu_{overall}$	overall Nusselt number
p	dimensional pressure
P	dimensionless pressure with respect to ρU_∞^2

NOMENCLATURE (Continued)

P_o	dimensionless pressure at front stagnation point
P_∞	dimensionless pressure in uniform stream
Pe	Peclet number, $\frac{2aU_\infty}{\mathcal{D}}$
Pt	transverse opening ratio, the ratio of the shortest center-to-center distance between adjacent cylinders to the outside diameter of the cylinder
r	radial distance in cylindrical coordinates, dimensional or dimensionless
r_∞	outer boundary position
Δr	mesh size in radial direction
R	Reynolds number, $\frac{2aU_\infty \rho}{\mu}$
Sc	Schmidt number, $\frac{\nu}{\mathcal{D}}$
U_∞	uniform stream velocity
v_o	dimensional radial velocity at the surface
v_r	dimensional radial velocity
v_θ	dimensional angular velocity
V_o	dimensionless radial velocity at the surface
V_x	dimensionless angular velocity
V_z	dimensionless radial velocity
x	angle in cylindrical coordinates, same as θ
Δx	mesh size in angular direction
z	axial distance normal to flow direction or radial distance from the cylinder wall
Δz	mesh size in radial direction
α	relaxation factor in stream equation
β	relaxation factor in vorticity equation

NOMENCLATURE (Concluded)

τ	concentration polarization
ϵ	a small dimensionless quantity, 10^{-6}
ζ	vorticity
θ	angle in cylindrical coordinates
μ	viscosity
ν	kinematic viscosity
π	3.14159
ρ	mass density of binary solution
ρ_A	mass concentration of component A
ψ	stream function
ω_A	mass fraction of component A

Subscript

o	quantity evaluated at the surface of the cylinder
∞	quantity in the uniform stream
I	positive integer denotes a grid point whose angular coordinate is $x = I\Delta x$
J	positive integer denotes a grid point whose radial coordinate is $z = J\Delta z$

Note: Symbols that appear infrequently are defined in the text and are not listed here.

SUMMARY

A study of low Reynolds number flow past an infinite row of circular cylinders with constant radial suction mass flux at the cylinder walls was carried out by a finite difference numerical method. A pure fluid and a binary solution were studied separately to determine the characteristic flow parameters at Reynolds number of 0.1 to 1.0 and opening ratios of 1.25, 1.50 and 1.75.

Because of the difficulty of modeling the whole flow field, a surface-interaction model is proposed. In this model, each cylinder is assumed to be surrounded by a rectangular envelope of fluid and uncoupled from the flow field. The value of the opening ratio is used to locate the centerline between the cylinders. In order to examine closely the region near the cylinder wall, the flow field of the model was transformed from the cylindrical grid system into a rectangular grid system with the centerline becoming a curved boundary.

The governing Navier-Stokes equations and the diffusion equation were modified at the grid points near the curved boundaries. The stream function and the vorticity were introduced to reduce the complexity of the equations of motion. The resulting fourth-order partial differential equation (PDE) was split into two second-order PDEs which were then approximated by finite difference equations. Hence the values of the stream function and the vorticity were considered as point functions at the grid points. The successive over-

relaxation (SOR) method together with empirical relaxation factors were employed to achieve fast rates of convergence in the calculations.

Further flow characteristic parameters were then calculated from the known values of the stream function and the vorticity. The flow patterns are almost symmetrical fore and aft with no radial mass flux at the wall at low Reynolds numbers. As the Reynolds number increases the vorticity is drifted farther downstream by convection. The maximum surface vorticity and the maximum rate of change of surface pressure occurred at 90° from the front stagnation point.

With radial suction mass flux, the curved streamlines move closer to the cylinders, their locations being dependent upon the magnitude of the radial suction flux. As the suction velocity at the surface increases, the asymmetry becomes more pronounced and affects the flow near the body. In all cases the pressure drag had more effect on the total drag than the friction drag due to the presence of the neighboring tubes.

For the binary solution study, the Crank-Nicholson implicit finite difference method along with some of the techniques which were found to be useful in dealing with irregular grid spacings was employed to approximate the convective diffusion equation. The total Nusselt number was found to increase slowly in the upstream direction. It reached its maximum at the minimum clearance between the cylinders, and then decreased sharply. The contribution of the rear region to the overall mass transfer is very small. The overall Nusselt number can be approximated by

$$Nu_{overall}/Sc^{1/3} = 1.53\ R^{1/3} + k_1 \quad \text{(for Pt=1.75)}$$

and

$$Nu_{overall}/Sc^{1/3} = 1.68\ R^{1/3} + k_2 \quad \text{(for Pt=1.50)}$$

where k_1 and k_2 depend on the magnitude of the radial suction mass flux.

Over the entire Reynolds number range investigated, characteristic flow parameters, such as the drag coefficient, pressure coefficient, streamline pattern and Nusselt number, compare favorably with available experimental data and numerical solution results.

CHAPTER I

INTRODUCTION

Recent advances in membrane technology have stimulated the development of separation processes using single or multiple hollow-fiber tubes in which the fluid mixture to be separated flows perpendicular to the tube or tubes at low Reynolds numbers. To aid in the design of such process, this study was undertaken to determine the fluid dynamics and mass transfer mechanisms which occur in low Reynolds number flow past an infinite row by cylinders with constant radial suction mass flux at the surface.

Literature Survey

One Cylinder

Theoretical Study. For years, many investigators have studied the case of viscous, incompressible flow at low Reynolds number past circular cylinders. Because of the difficulty of finding an analytic solution to the complete Navier-Stokes equations, Stokes[1] neglected the convective terms in the equations, thereby obtaining a linear governing equation for the stream function. No solution could be found to satisfy the uniform free stream condition far from the body. This is the famous Stokes' paradox. Oseen[2] suggested approximating the inertia terms by their linearized forms valid far from the body. Soon thereafter, Lamb[3] solved Oseen's equations, employing an approximate boundary condition at the body surface. This work was

extended by Tomotika and Aoi[4]. Their results showed that a pair of standing eddies were formed behind the cylinder even at a Reynolds number of 0.05. Yamada[5] concluded that Oseen's equation is valid only at very low Reynolds numbers. Hence Tomotika and Aoi's results are wrong.

With the aid of a high speed digital computer, Thom[6] was the first to solve numerically the Navier-Stokes equations using approximation methods. He divided the fourth-order differential equation in the stream function into two second-order equations. After approximating both elliptic partial differential equations with finite difference equations, solutions for the stream function and the vorticity were obtained using an iteration technique at Reynolds numbers of 10 and 20. Kawaguti[7] did a similar study at a Reynolds number of 40.

When a viscous fluid flows past a circular cylinder in an infinite domain, the outer boundary is considered to be at infinity. Accurate results of the flow parameters are obtained using an extrapolation procedure. Hamielec and Raal[8] found that the drag coefficient should be a monotonic function of the outer bound of the computation field. This finding was considered inadequate by Keller and Takami[9] who assumed that the drag coefficient should fit a quadratic polynomial in $1/r_\infty$ (i.e. $C_D = a_o + a_1/r_\infty + a_2/r_\infty^2$ where r_∞ is the outer boundary position). Later, Wu[10] studied numerically the flow past a cylinder with constant radial suction mass flux at the surface and used a finite difference method to solve the Navier-Stokes equations and the diffusion equation. He found that the drag coefficient is a linear function

of the reciprocal of the radial position of the outer boundary Y_∞.

With surface mass transfer, Wu found that the surface pressure distribution is relatively insensitive to the effect of the radial suction flux at low Reynolds numbers. The drag coefficient increases as the suction flux is increased. The friction drag also increases more rapidly than the pressure drag does. The maximum local Nusselt number occurred at the front stagnation point, then decreased with increasing distance from there and would continue to decrease if there were no flow separation which occurred above a Reynolds number of 7.0. The overall Nusselt number was found to be approximated by

$$Nu_{overall}/Sc^{1/3} = b + 0.75\ R^{1/2}$$

where b depends on the magnitude of the radial suction flux.

Experimental Study. Taneda[11] photographed the flow pattern and obtained the Reynolds number above which separation occurs and the length of the standing vortices behind the cylinder. Tritton[12] observed the bending of quartz fibers in a stream at Reynolds numbers of 0.5 to 100 and measured, extensively and carefully, the drag coefficient. Nishioka and Sato[13] measured the velocity in the flow field behind a circular cylinder at Reynolds numbers of 10 to 80. Their results showed good agreement with Keller and Takami's solution[9] at low Reynolds numbers and fair agreement at high Reynolds numbers.

Multiple Cylinders

Theoretical Study. Fujikawa[14] used Oseen's linearized equations of motion in an early study to simplify the case of crossflow

past two cylinders. He found that on increasing the distance between the cylinders, the drag on one cylinder increased and approached that of a single cylinder in an unlimited stream. In 1957, Tamada and Fujikawa[15] studied the steady two-dimensional flow of a viscous fluid past an infinite row of equal parallel circular cylinders regularly spaced. They found that the interference effect among the cylinders in the row was appreciable at low Reynolds numbers and predicted that there is an essential difference between the cases when the number of cylinder is infinite and when large but finite. In the latter case, the flow may pass round the system of cylinders, leaving the fluid inside the system almost at rest. Thus in such a case the drag on a cylinder inside the system is expected to be very small.

Kuwabara[16] used a zero vorticity model for the study of a viscous flow through randomly distributed parallel cylinders at small Reynolds numbers. Almost at the same time, Happel[17] proposed a free-surface model to solve the problem of creeping flow normal to arrays of cylinders and calculated the forces at the surfaces of the cylinders. Both models have been used in solving complicated problems. Considering each cylinder from an assemblage of uniform circular cylinders separately, LeClair and Hamielec[18] introduced a surface-interaction model to study the interaction effect between the cylinders. The resulting drag and heat transfer coefficients for assemblages of cylinders showed satisfactory agreement with other experimental data for fiber bundles and tube banks.

Ishihara[19] studied the case of steady flow across banks of tubes arranged in-line at Reynolds numbers of 1 to 100 and pitch

ratios of 1.25 and 1.50. He found that there are eddy regions between the tube rows at all Reynolds numbers studied, but the wake-bubble behind the last (i.e. the third)tube row appears only after the Reynolds number exceeds 20. He also found that for all rows the ratio of the form drag to the total drag is almost constant at approximately 0.7 for Pt (pitch ratio) = 1.50 and approximately 0.8 for Pt = 1.25. He concluded that no simplified flow model would be satisfactory in predicting the friction factor of the tube bank.

Experimental Study. Most experiments reported are for turbulent flow. The most extensive and useful data came from the University of Delaware research program.[20] It was designed to provide correlations between fluid friction and heat transfer for flow across tube banks at Reynolds numbers in the turbulent regime. Correlations are presented in graphical form for different tube layouts.

Recently, Honji[21] studied two-dimensional laminar wakes of multiple cylinders aligned in a row normal to the flow using visualization techniques. He observed that an isolated symmetrical vortex pair formed at a distance downstream. The length of standing eddies behind the cylinder group increases with the Reynolds number based on the width of the group and decreases with the opening ratio and the Reynolds number based on the diameter of a single cylinder.

CHAPTER II

MATHEMATICAL DESCRIPTION OF THE PROBLEM

Statement of the Problem

The system considered consists of a binary solution of component B (say, water) and component A (salt)* and a single row of an infinite number of equal circular porous-walled cylinders of infinite length. When the solution flows past the cylinders, component B is sucked, uniformly but not completely, through the wall into the cylinder and component A is rejected outside completely. Other assumptions are as follows:

(1) The flow is steady, isothermal and two-dimensional with uniform approaching stream velocity and concentration

(2) The fluid is Newtonian with constant physical properties (i.e. viscosity, density and diffusivity).

(3) The Schmidt number is high (Sc for a dilute salt-water solution at 25°C is 560).

(4) There is no wall slip in the case of no radial suction mass flux.

Fluid Flow Equations

Under these assumptions, the governing differential equations in cylindrical coordinates (see Figure 1) can be expressed as

*Component A may not be present when the case of no radial suction mass flux is considered.

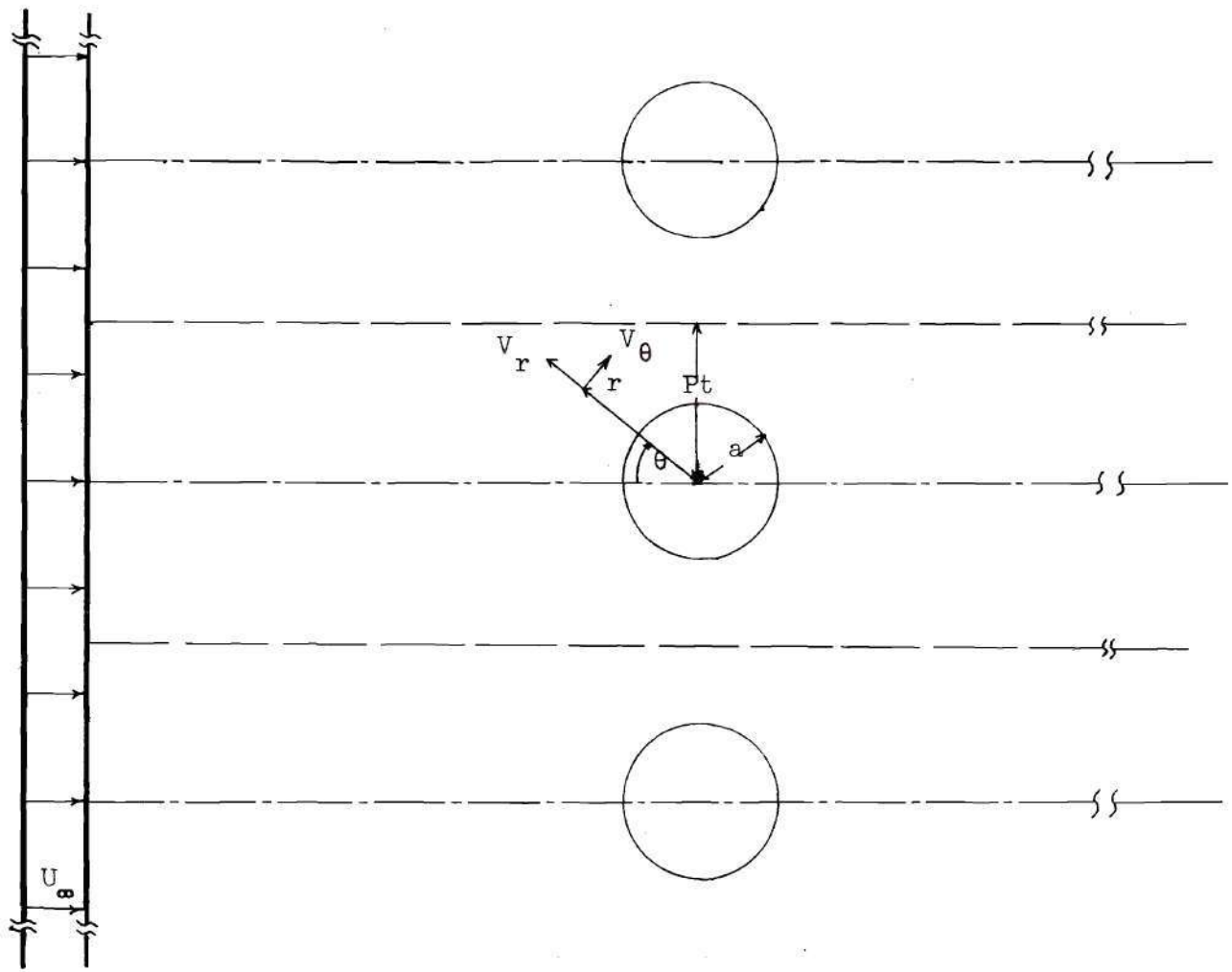

Figure 1. Cylindrical Coordinate System.

Equation of Continuity

$$\frac{\partial v_r}{\partial r'} + \frac{v_r}{r'} + \frac{1}{r'} \frac{\partial v_\theta}{\partial \theta} = 0 \qquad (2\text{-}1)$$

Equation of Motion in the r-direction

$$\rho\left(v_r \frac{\partial v_r}{\partial r'} + \frac{v_\theta}{r'} \frac{\partial v_r}{\partial \theta} - \frac{v_\theta^2}{r'} \right) = - \frac{\partial p}{\partial r'} + \mu\left(\frac{\partial^2 v_r}{\partial r'^2} + \frac{1}{r'} \frac{\partial v_r}{\partial r'} - \frac{v_r}{r'^2} - \frac{1}{r'} \frac{\partial^2 v_r}{\partial \theta} - \frac{2}{r'^2} \frac{\partial v_\theta}{\partial \theta} \right) \qquad (2\text{-}2)$$

Equation of Motion in the θ-Direction

$$\rho\left(v_r \frac{\partial v_\theta}{\partial r'} + \frac{v_\theta}{r'} \frac{\partial v_\theta}{\partial \theta} - \frac{v_r v_\theta}{r'} = - \frac{1}{r'} \frac{\partial p}{\partial \theta} \right.$$

$$\left. + \mu\left(\frac{\partial^2 v_\theta}{\partial r'^2} + \frac{1}{r'} \frac{\partial v_\theta}{\partial r'} - \frac{v_\theta}{r'^2} + \frac{1}{r'^2} \frac{\partial^2 v_\theta}{\partial \theta^2} + \frac{2}{r'^2} \frac{\partial v_r}{\partial \theta} \right) \right. \qquad (2\text{-}3)$$

Dimensionless Forms of Flow Equations

In the general case, the uniform approaching velocity U_∞ and a cylinder radius a were chosen as reference quantities. The dimensionless variables can be expressed as

$$V_r = v_r/U_\infty \qquad V_\theta = v_\theta/U_\infty \qquad V_o = v_o/U_\infty$$

$$P = p/\rho U_\infty^2 \qquad R = 2aU_\infty\rho/\mu \qquad r = r'/a \tag{2-4}$$

where R is the Reynolds number based on the diameter of a cylinder.

Substituting the above dimensionless variables into Equations (2-1) through (2-3), the dimensionless forms of the equations of continuity and motion become

Equation of Continuity

$$\frac{\partial V_r}{\partial r} + \frac{V_r}{r} + \frac{1}{r}\frac{\partial V_\theta}{\partial \theta} = 0 \tag{2-5}$$

Equation of Motion in the r-direction

$$Vr\ \frac{\partial V_r}{\partial r} + \frac{V_\theta}{r}\frac{\partial V_r}{\partial \theta} - \frac{V_\theta^2}{r} = -\frac{\partial P}{\partial r}$$

$$+ \frac{2}{R}\left(\frac{\partial^2 V_r}{\partial r^2} + \frac{1}{r}\frac{\partial V_r}{\partial r} - \frac{V_r}{r^2} + \frac{1}{r^2}\frac{\partial^2 V_r}{\partial \theta^2} \right. \tag{2-6}$$

$$\left. - \frac{2}{r^2}\frac{\partial V_\theta}{\partial \theta} \right)$$

Equation of Motion in the θ-Direction

$$V_r \frac{\partial V_\theta}{\partial r} + \frac{V_\theta}{r} \frac{\partial V_\theta}{\partial \theta} + \frac{V_r V_\theta}{r} = -\frac{1}{r} \frac{\partial P}{\partial \theta}$$

$$+ \frac{2}{R} \left(\frac{\partial^2 V_\theta}{\partial r^2} + \frac{1}{r} \frac{\partial V_\theta}{\partial r} - \frac{V_\theta}{r^2} + \frac{1}{r^2} \frac{\partial^2 V_\theta}{\partial \theta^2} + \frac{2}{r^2} \frac{\partial V_r}{\partial \theta} \right) \qquad (2\text{-}7)$$

Dimensionless Forms of Equations of Motion in Terms of the Stream Function and Vorticity

Introducing the stream function ψ defined as

$$V_r = -\frac{1}{r} \frac{\partial \psi}{\partial \theta}$$

$$V_\theta = \frac{\partial \psi}{\partial r} \qquad (2\text{-}8)$$

the equation of continuity (2-5) is satisfied. Cross-differentiating the equations of motion, in the r- and θ-directions, with respect to θ and r, respectively, the terms containing the pressure components can be eliminated, giving (as shown on the following page):

$$\nabla^4\psi + \frac{R}{2r}\left(\frac{\partial\psi}{\partial\theta}\frac{\partial}{\partial r} - \frac{\partial\psi}{\partial r}\frac{\partial}{\partial\theta}\right)\nabla^2\psi = 0 \qquad (2\text{-}9)$$

where ∇^2 is the Laplacian operator defined as

$$\nabla^2 = \frac{\partial^2}{\partial r^2} + \frac{1}{r}\frac{\partial}{\partial r} + \frac{1}{r^2}\frac{\partial^2}{\partial\theta^2}$$

Defining the vorticity ζ, in dimensionless form, as

$$\zeta = \nabla^2\psi \qquad (2\text{-}10)$$

Equation (2-9) then can be rewritten as

$$\nabla^2\zeta + \frac{R}{2r}\left(\frac{\partial\psi}{\partial\theta}\frac{\partial}{\partial r} - \frac{\partial\psi}{\partial r}\frac{\partial}{\partial\theta}\right)\zeta = 0 \qquad (2\text{-}11)$$

Since most of the interesting phenomena occur in the opening between the cylinders and in the region near the surfaces, a careful examination of this region can be achieved by defining the radial distance as

$$r = e^z \qquad (2\text{-}12)$$

Setting $\theta = x$ and substituting Equation (2-12) in Equations (2-11), (2-10) and (2-8), the resulting dimensionless flow equations can be rewritten in terms of the new set of dependent variables (ψ, ζ, z and x) as follows:

Stream Function Equation

$$\frac{\partial^2\zeta}{\partial x^2} + \frac{\partial^2\zeta}{\partial z^2} + \frac{R}{2}\left(\frac{\partial\psi}{\partial x}\frac{\partial\zeta}{\partial z} - \frac{\partial\psi}{\partial z}\frac{\partial\zeta}{\partial x}\right) = 0 \qquad (2\text{-}13)$$

Vorticity Equation

$$\frac{\partial^2 \psi}{\partial x^2} + \frac{\partial^2 \psi}{\partial z^2} = e^{2z} \zeta \qquad (2\text{-}14)$$

Velocity Equation

$$V_x = \frac{1}{e^z} \frac{\partial \psi}{\partial z}$$

$$V_z = -\frac{1}{e^z} \frac{\partial \psi}{\partial x} \qquad (2\text{-}15)$$

Geometry and Boundary Conditions

Because of the difficulty of modeling the whole flow field, a surface-interaction model is proposed. In this model, each cylinder is assumed to be surrounded by a rectangular envelope of fluid and uncoupled from the flow field. The interaction effect causes the boundary near the cylinder to coincide with the upper symmetry line which is considered to extend to infinity. The value of the opening ratio (Pt) is used to locate the upper symmetry line and the stream function on this boundary is equal to Pt. The uniform flow condition is satisfied on the outer boundary far from the cylinder. Zero vorticity condition is set on the boundary except on the tube surface where the vorticity is determined by the stream function.

With suction, an additional term is added on the boundary condition to allow for the effect of mass transfer on the flow field. This effect depends on the magnitude of the surface mass velocity and the opening ratio.

The geometry of half ot the model and the boundary conditions involved in the computation are illustrated in the schematic diagram of Figure 2. The characteristic length is the radius a and for simplicity a is assumed equal to 1. The distance between the upper and lower symmetry lines is the opening ratio Pt.

The following boundary conditions are as follows:

Tube Surface

at $z = 0$, $V_z(z,x) = V_o$,

$(V_z(z,x) = 0)$*

and

$V_x(z,x) = 0$

thus $\psi = -V_o x$,

$(\psi = 0)$

and $\zeta = \frac{\partial^2 \psi}{\partial x^2} + \frac{\partial^2 \psi}{\partial z^2}$

Incoming and Outgoing Flow

at $z = \infty$, $V_z(z,x) = -\cos x$

and $V_x(z,x) = \sin x$

thus $\psi = e^z \sin x - V_o x$,

$(\psi = e^z \sin x)$

and $\zeta = 0$

*The boundary conditions enclosed in parentheses are for the case of no radial suction mass flux at the surface.

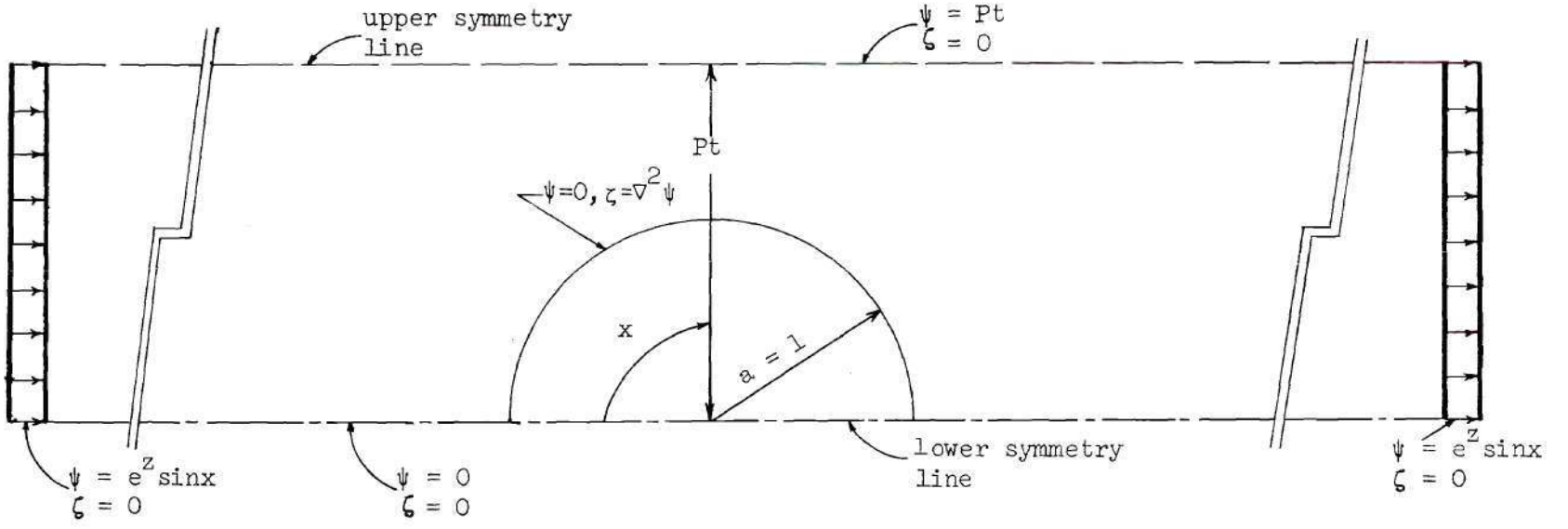

Figure 2. Geometry and Boundary Conditions

Upper Symmetry Line

at $z = \ln (Pt/\sin x)$, $\psi = Pt - V_o \pi/2$,

$(\psi = Pt)$

and $\zeta = 0$

Lower Symmetry Line

at $x = 0$, $\psi = 0$

and $\zeta = 0$

at $x = \pi$, $\psi = -V_o \pi$,

$(\psi = 0)$

and $\zeta = 0$

Diffusion Equation and Boundary Conditions

The equation of continuity of component A (salt) in the binary solution can be expressed as

$$v_r \frac{\partial \rho_A}{\partial r} + \frac{v_\theta}{r} \frac{\partial \rho_A}{\partial \theta} = \left(\frac{\partial^2 \rho_A}{\partial r^2} + \frac{1}{r} \frac{\partial \rho_A}{\partial r} + \frac{1}{r^2} \frac{\partial^2 \rho_A}{\partial \theta^2} \right) \tag{2-16}$$

with the boundary conditions:

Incoming and Outgoing Flow

at $r = \infty$, $\rho_A(r,\theta) = \rho_{A\infty}$

Upper Symmetry Line

Since no mass transfer occurs across the axis of symmetry

at $r = \frac{Pt}{\sin\theta}$, $\frac{\partial \rho_A}{\partial n} = 0$

where $\partial\rho_A/\partial n$ is the normal derivative of the mass concentration of component A.

Lower Symmetry Line

$$\text{at } \theta = 0, \qquad \frac{\partial \rho_A}{\partial \theta} = 0$$

Tube Surface

According to Fick's first law of diffusion, the mass flux of component A at the surface of the cylinder can be expressed as

$$n_{Ao} = \omega_{Ao}(n_{Ao} + n_{Bo}) - \rho\mathscr{D}\left(\frac{\partial \omega_A}{\partial r}\right)_{r=a} \tag{2-17}$$

Since component A is not sucked into the cylinder through the wall, n_{Ao} must be zero. From the definitions of $n_{Bo} = \rho v_o$ and $\omega_A = \rho_A/\rho$, Equation (2-17) becomes

$$\frac{1}{\rho_A}\left(\frac{\partial \rho_A}{\partial r}\right)_{r=a} = \frac{v_o}{\mathscr{D}}$$

Dimensionless Forms of Diffusion Equation and Boundary Conditions

Defining the dimensionless mass concentration as

$$C = \rho_A/\rho_{A\infty}$$

the diffusion equation together with its boundary conditions can be made dimensionless and becomes

$$V_r \frac{\partial C}{\partial r} + \frac{V_\theta}{r}\frac{\partial C}{\partial \theta} = \frac{2}{Pe}\left(\frac{\partial^2 C}{\partial r^2} + \frac{1}{r}\frac{\partial C}{\partial r} + \frac{1}{r^2}\frac{\partial^2 C}{\partial \theta^2}\right) \tag{2-18}$$

$$\begin{aligned}
&\text{at } r = \infty, && C(r,\theta) = 1.0 \\
&\text{at } r = \frac{Pt}{\sin\theta}, && \frac{\partial C}{\partial n} = 0 \\
&\text{at } \theta = 0, && \frac{\partial C}{\partial \theta} = 0 \\
&\text{at } r = 1, && \frac{1}{C}\frac{\partial C}{\partial r} = \frac{aV_o}{\mathscr{D}}
\end{aligned} \tag{2-19}$$

where Pe is the Peclet number defined as

$$Pe = 2aU_\infty/\mathcal{D}$$

Further simplification of Equation (2-18) is made by assuming that diffusion in the angular direction can be neglected at high Schmidt numbers[22]. Hence

$$V_r \frac{\partial C}{\partial r} + \frac{V_\theta}{r} \frac{\partial C}{\partial \theta} = \frac{2}{Pe} \left(\frac{\partial^2 C}{\partial r} + \frac{1}{r} \frac{\partial C}{\partial r} \right) \qquad (2\text{-}20)$$

Dimensionless Diffusion Equation in Terms of New Variables

Setting $\theta = x$ and substituting Equation (2-12) in Equations (2-20) and (2-19), the dimensionless diffusion equation may be expressed in terms of the new set of dependent variables (C, z and x) as follows:

$$V_z e^z \frac{\partial C}{\partial z} + V_x e^z \frac{\partial C}{\partial x} = \frac{2}{Pe} \frac{\partial^2 C}{\partial z^2} \qquad (2\text{-}21)$$

with the boundary conditions:

Incoming and Outgoing Flow

at $z = \infty$, $\qquad C = 1$

Upper Symmetry Line

After transformation:

$$\frac{\partial C}{\partial n} = e^{-z} \left(\frac{\partial C}{\partial x} \cos x + \frac{\partial C}{\partial z} \sin x \right)$$

thus

$$\text{at } z = \ln (Pt/\sin x), \qquad \frac{\partial C}{\partial x} \Big/ \frac{\partial C}{\partial z} = -\tan x \qquad (2\text{-}22)$$

Lower Symmetry Line

at $x = 0$, $\quad \frac{\partial C}{\partial x} = 0$

Tube Surface

at $z = 0$, $\quad \frac{1}{C} \frac{\partial C}{\partial z} = \frac{aV_o}{\mathscr{D}}$

Other Flow Characteristics

Pressure Distribution on the Surface of the Cylinder

At the front stagnation line, both V_θ and $\partial V_r/\partial\theta$ are equal to zero because of symmetry. The equation of motion in the r-direction is simplified to

$$V_r \frac{\partial V_r}{\partial r} + \frac{\partial P}{\partial r} = \frac{2}{R} \left(\frac{\partial^2 V_r}{\partial r^2} + \frac{1}{r} \frac{\partial V_r}{\partial r} - \frac{V_r}{r^2} + \frac{1}{r^2} \frac{\partial^2 V_r}{\partial \theta^2} - \frac{2}{r^2} \frac{\partial V_\theta}{\partial \theta} \right)$$

Substituting Equation (2-8) into the above equation and rearranging gives

$$V_r \frac{\partial V_r}{\partial r} + \frac{\partial P}{\partial r} = - \frac{2}{Rr} \left(\frac{\partial \zeta}{\partial \theta} \right)_{\theta=0}$$

Integrating with respect to r and transforming with $r = e^z$,

$$P_o - P_\infty = \frac{1}{2} \left(1 - V_o^2 \right) + \frac{2}{R} \int_o^\infty \left(\frac{\partial \zeta}{\partial \theta} \right)_{\theta=0} dz \qquad (2\text{-}23)$$

where P_o is the pressure at the front stagnation point of the cylinder and P_∞ is the pressure in the plane $\theta = 0$ far from the cylinder.

Since V_θ and all derivatives with respect to θ are zero on the surface of the cylinder, the equation of motion in the θ-direction

is simplified to

$$V_r \frac{\partial V_\theta}{\partial r} + \frac{1}{r} \frac{\partial P}{\partial \theta} = \frac{2}{R} \left(\frac{\partial^2 V_\theta}{\partial r^2} + \frac{1}{r} \frac{\partial V_\theta}{\partial r} \right)$$

On the surface

$$\left(\frac{\partial V_\theta}{\partial r} \right)_{r=1} = \zeta_{z=o}$$

Hence

$$\left(\frac{\partial P}{\partial \theta} \right)_{z=o} = \frac{2}{R} \left(\frac{\partial \zeta}{\partial z} \right)_{z=o} - V_o \zeta_{z=o}$$

Integrating with respect to θ

$$P - P_o = \frac{2}{R} \int_o^\theta \left(\frac{\partial \zeta}{\partial z} \right)_{z=o} d\theta - V_o \int_o^\theta \zeta_{z=o} d\theta \qquad (2\text{-}24)$$

where P is the pressure at any point on the cylinder surface.

Combining Equations (2-23) and (2-24), the pressure distribution around the cylinder surface can be expressed in terms of the pressure coefficient defined as

$$C_P = \frac{P - P_\infty}{\frac{1}{2} \rho U_\infty^2} \qquad (2\text{-}25)$$

Drag Coefficient

In past studies of low Reynolds number flows past submerged bodies, the drag coefficient has been one of the most carefully examined flow characteristics. The total drag coefficient is

$$C_D = C_{DP} + C_{DF} \qquad (2\text{-}26)$$

where C_{DP} and C_{DF} are the pressure and the friction drag coefficients respectively given by the relations

$$C_{DP} = 2 \int_{o}^{\pi} P\cos\theta \, d\theta \qquad (2\text{-}27)$$

and

$$C_{DF} = \frac{4}{R} \int_{o}^{\pi} \zeta_{z=0} \sin\theta \, d\theta \qquad (2\text{-}28)$$

A relation between the isothermal friction factor f and the total drag coefficient C_D was reported[19] as

$$f = \frac{C_D}{4\,Pt} \qquad (2\text{-}29)$$

Mass-Transfer Coefficient

It is convenient to express the rate of mass transfer in terms of the local mass-transfer coefficient

$$k_{x,loc} = -\mathscr{D} \frac{C \cdot C_\infty}{a(C_o - C_\infty)} \left(\frac{\partial C}{\partial r}\right)_{r=1}$$

The corresponding local Nusselt number for mass transfer is

$$Nu_{loc} = \frac{2ak_{x,loc}}{C\mathscr{D}} = -2\left(\frac{1}{C-1}\frac{\partial C}{\partial r}\right)_{r=1} \qquad (2\text{-}30)$$

and the overall Nusselt number is

$$Nu_{overall} = \frac{1}{A}\int_{o}^{A} Nu_{loc}\, dA = -\frac{2}{\pi} \cdot \int_{o}^{\pi} \left(\frac{1}{C-1}\frac{\partial C}{\partial r}\right)_{r=1} d\theta \qquad (2\text{-}31)$$

CHAPTER III

TECHNIQUE FOR NUMERICAL SOLUTION

It is difficult to obtain analytical solutions for flows over submerged objects beyond the creeping flow regime because of the presence of nonlinear convective effects and eddy formation behind the bodies. However, with the advent of high speed electronic computers, numerical approximation techniques, such as finite differences, finite element methods etc., are practical and powerful tools in theoretical research in fluid dynamics. These methods can (i) give the minute details of the flow phenomena, (ii) reduce the experimental effort needed for the evaluation of design parameters, and (iii) suggest new approaches to analytical solutions. However, they can also (i) result in serious errors if the step size used is not small enough or the convergence criteria required are not strict enough, and (ii) become very time-consuming in obtaining accurate results due to the limitation of the computer capacity available.

System of Grid Points

The flow field covered by the cylindrical grid system (Figure 3) can be transformed to the rectangular grid system (Figure 4) by the relations

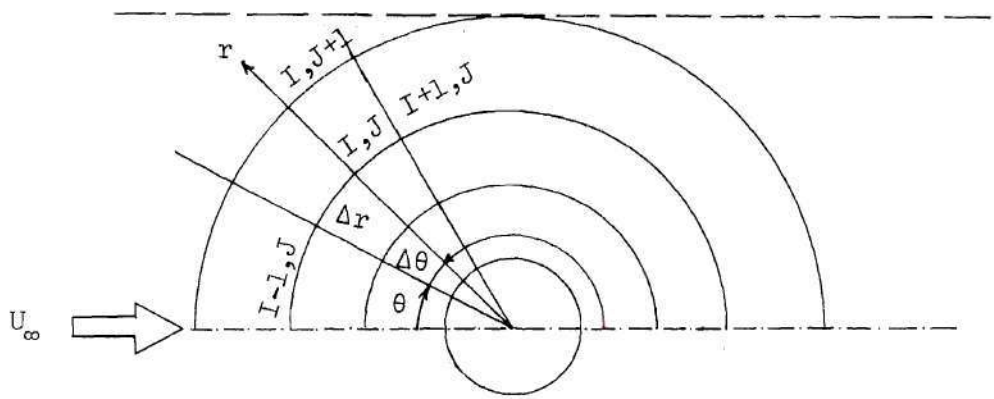

Figure 3. Cylindrical Grid System.

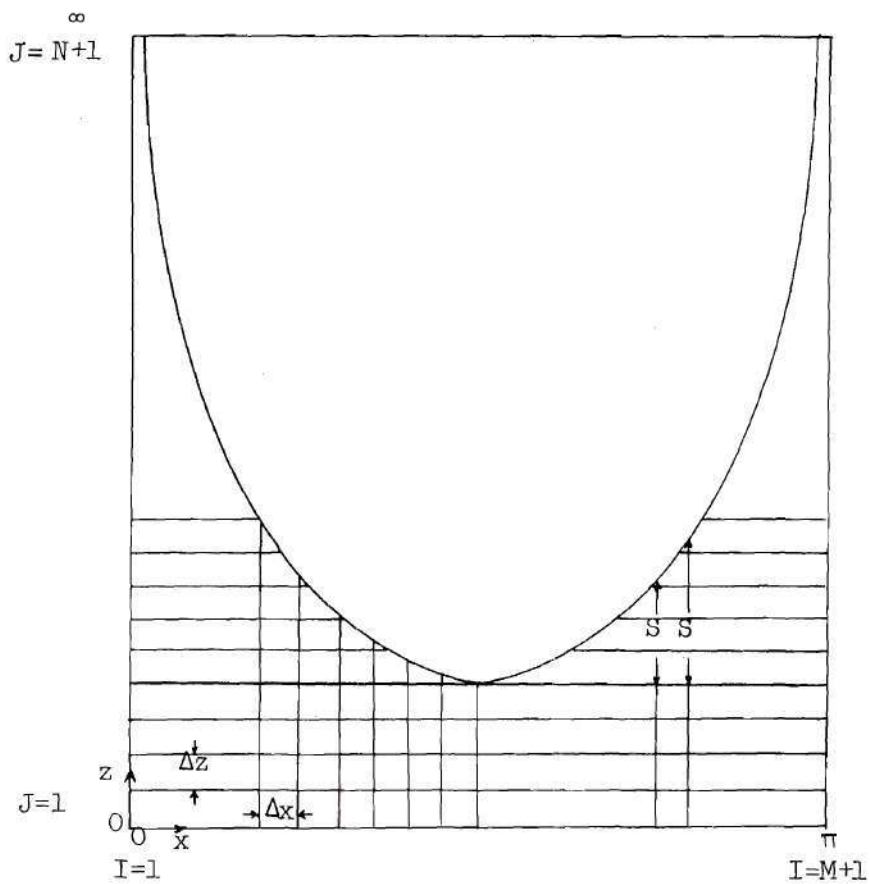

Figure 4. Rectangular Grid System.

$$r = e^{z}$$

$$\theta = x$$

Thus a grid point represented by (I,J) has the space coordinates $x = I\Delta x$ and $z = J\Delta z$. The value of a variable is then considered as a point function on these grid points, $f_{I,J} = f(I\Delta x, J\Delta z)$.

In problems dealing with but one cylinder, the geometry is so simple that regular grid points can be arranged to lie on the boundaries. However, since in this study part of the boundary does not fall on regular grid points (Figure 4), the boundary is considered to be irregular. The boundary points can be placed into four categories and require individual treatment, as described in Figure 5.

Approximation of Derivatives by Finite Differences

There are many finite difference approximations for derivatives of different orders. The choice of the approximation to be used depends on the accuracy desired and the grid points involved. The following different approximations of $\partial f/\partial x$ and $\partial^2 f/\partial x^2$ were employed in the governing flow equations, diffusion equation and boundary conditions at each regular point:

Two-point formula

$$\frac{\partial f}{\partial x}\Big|_{I,J} = \frac{1}{\Delta x}\left(f_{I+1,J} - f_{I,J}\right) + O(\Delta x)$$

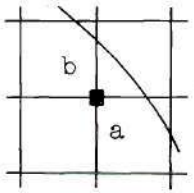

Type I

$\epsilon < a < 1$

$\epsilon < b < 1$

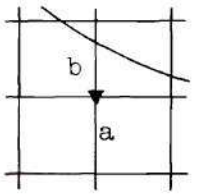

Type II

$a = 1$

$\epsilon < b < 1$

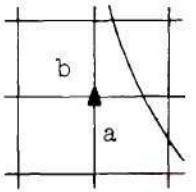

Type III

$\epsilon < a < 1$

$b = 1$

Type IV

$0 \leq |a| < \epsilon$

$0 \leq |b| < \epsilon$

Figure 5. Types of Boundary Points.

Three-point formulas

$$\frac{\partial f}{\partial x}\Big|_{I,J} = \frac{1}{2\Delta x}\left(f_{I+1,J} - f_{I-1,J}\right) + O(\Delta x^2)$$

$$\frac{\partial f}{\partial x}\Big|_{I,J} = \frac{1}{2\Delta x}\left(-3f_{I,J} + 4f_{I+1,J} - f_{I+2,J}\right) + O(\Delta x^2)$$

Four-point formulas

$$\frac{\partial f}{\partial x}\Big|_{I,J} = \frac{1}{6\Delta x}\left(-2f_{I-1,J} - 3f_{I,J} + 6f_{I+1,J} - f_{I+2,J}\right) + O(\Delta x^3)$$

$$\frac{\partial f}{\partial x}\Big|_{I,J} = \frac{1}{6\Delta x}\left(-11f_{I,J} + 18f_{I+1,J} - 9f_{I+2,J} + 2f_{I+3,J}\right) + O(\Delta x^3)$$

Five-point formulas

$$\frac{\partial f}{\partial x}\Big|_{I,J} = \frac{1}{12\Delta x}\left(f_{I-2,J} - 8f_{I-1,J} + 8f_{I+1,J} - f_{I+2,J}\right) + O(\Delta x^4)$$

$$\frac{\partial f}{\partial x}\Big|_{I,J} = \frac{1}{12\Delta x}\left(-3f_{I-1,J} - 10f_{I,J} + 18f_{I+1,J} - 6f_{I+2,J} + f_{I+3,J}\right) + O(\Delta x^4)$$

$$\frac{\partial f}{\partial x}\Big|_{I,J} = \frac{1}{12\Delta x}\left(-25f_{I,J} + 48f_{I+1,J} - 36f_{I+2,J} + 16f_{I+3,J} - 3f_{I+4,J}\right) + O(\Delta x^4)$$

Three - point formula

$$\left.\frac{\partial^2 f}{\partial x^2}\right|_{I,J} = \frac{1}{(\Delta x)^2}\left(f_{I+1,J} - 2f_{I,J} + f_{I-1,J}\right) + O(\Delta x^2)$$

where $O(\Delta x^n)$ is the truncation error of the order of Δx^n. For irregular boundary points, the following were used:

Three-point formulas

$$\left.\frac{\partial f}{\partial x}\right|_{BDR} = \frac{1}{a(1+a)\Delta x}\left[(1+2a)f_{BDR} - (1+a)^2 f_{I,J} + a^2 f_{I-1,J}\right] + O(\Delta x^2)$$

$$\left.\frac{\partial f}{\partial x}\right|_{I,J} = \frac{1}{a(1+a)\Delta x}\left[f_{BDR} - (1-a^2)f_{I,J} - a^2 f_{I-1,J}\right] + O(\Delta x^2)$$

$$\left.\frac{\partial f}{\partial x}\right|_{I-1,J} = \frac{1}{a(1+a)\Delta x}\left[-f_{BDR} + (1+a)^2 f_{I,J} - a(2+a)f_{I-1,J}\right] + O(\Delta x^2)$$

Four-point formulas

$$\left.\frac{\partial f}{\partial x}\right|_{BDR} = \frac{1}{S\Delta x}\left[2(2+6a+3a^2)f_{BDR} - (1+a)^2(2+a)^2 f_{I,J} + 2a^2(2+a)^2 f_{I-1,J} - a^2(1+a)^2 f_{I-2,J}\right] + O(\Delta x^3)$$

$$\frac{\partial f}{\partial x}\Big|_{I,J} = \frac{1}{S\Delta x}\Big[\, 4f_{BDR} - (1+a)(2+a)(2-3a)f_{I,J} - 4a^2(2+a)f_{I-1,J} + a^2(1+a)f_{I-2,J}\,\Big] + O(\Delta x^3)$$

$$\frac{\partial f}{\partial x}\Big|_{I-1,J} = \frac{1}{S\Delta x}\Big[\, 2f_{BDR} - (1+a)^2(2+a)f_{I,J} + 2a(2+a)f_{I-1,J} + a(1+a)^2 f_{I-2,J}\,\Big] + O(\Delta x^3)$$

$$\frac{\partial f}{\partial x}\Big|_{I-2,J} = \frac{1}{S\Delta x}\Big[\, 4f_{BDR} - (1+a)(2+a)^2 f_{I,J} + 4a(2+a)^2 f_{I-1,J} - a(1+a)(8+3a)f_{I-2,J}\,\Big] + O(\Delta x^3)$$

Three-point formula

$$\frac{\partial^2 f}{\partial x^2}\Big|_{I,J} = \frac{2}{a(1+a)(\Delta x)^2}\Big[\, f_{BDR} + af_{I-1,J} - (1+a)f_{I,J}\,\Big] + O(\Delta x)$$

where the subscript BDR refers to the quantity evaluated at the boundary, and a = fractional length of mesh size Δx and $S = 2a(1+a)(2+a)$.

Similar formulas can be used for $\partial f/\partial z$ and $\partial^2 f/\partial z^2$ by making the appropriate change of the variable from x to z and from a to b.

Finite Difference Forms of the Stream Function and Vorticity Equations and the Boundary Conditions

According to the grid points involved, the finite difference forms of the governing flow equations can be subdivided into three main categories:

I. Interior Points

Using the approximation formulas with second order accuracy, Equations (2-14) and (2-13) with variable rectangular mesh sizes in the x- and z-directions may be expressed as follows:

$$\psi_{I,J} = \frac{1}{2\left(1 + \frac{\Delta x^2}{\Delta z^2}\right)} \left[\psi_{I+1,J} + \psi_{I-1,J} + \left(\psi_{I,J+1} + \psi_{I,J-1}\right) \frac{\Delta x^2}{\Delta z^2} - \Delta x^2 e^{2z} \zeta_{I,J} \right]$$

and

$$\zeta_{I,J} = \frac{1}{2\left(1+\frac{\Delta x^2}{\Delta z^2}\right)} \left\{ \zeta_{I+1,J} + \zeta_{I-1,J} + \left(\zeta_{I,J+1} + \zeta_{I,J-1}\right) \frac{\Delta x^2}{\Delta z^2} + \frac{R}{8} \frac{\Delta x}{\Delta z} \left[\left(\psi_{I+1,J} - \psi_{I-1,J}\right) \left(\zeta_{I,J+1} - \zeta_{I,J-1}\right) - \left(\psi_{I,J+1} - \psi_{I,J-1}\right)\left(\zeta_{I+1,J} - \zeta_{I-1,J}\right) \right] \right\}$$

or

$$\psi'_{I,J} = \psi_{I,J} + \frac{\alpha}{2\left(1+\frac{\Delta x^2}{\Delta x^2}\right)} \Big[\psi_{I+1,J} - \psi_{I-1,J} + (\psi_{I,J+1} + \psi_{I,J-1}) \frac{\Delta x^2}{\Delta z^2} - \Delta x^2 e^{2z} \zeta_{I,J} - 2\left(1 + \frac{\Delta x^2}{\Delta z^2}\right) \psi_{I,J} \Big] \tag{3-1}$$

and

$$\zeta'_{I,J} = \zeta_{I,J} + \frac{\beta}{2\left(1 + \frac{\Delta x^2}{\Delta z^2}\right)} \Big\{ \zeta_{I+1,J} + \zeta_{I-1,J} + (\zeta_{I,J+1} + \zeta_{I,J-1}) \frac{\Delta x^2}{\Delta z^2} + \frac{R}{8} \frac{\Delta x}{\Delta z} \Big[(\psi_{I+1,J} - \psi_{I-1,J})(\zeta_{I,J+1} - \zeta_{I,J-1}) - (\psi_{I,J+1} - \psi_{I,J-1})(\zeta_{I+1,J} - \zeta_{I-1,J}) \Big] - 2\left(1 + \frac{\Delta x^2}{\Delta z^2}\right) \zeta_{I,J} \Big\} \tag{3-2}$$

where α and β are relaxation factors (found by trial). The successive over-relaxation method was introduced to achieve fast convergence. Some quantitative tests of this method against the ordinary iterative computation have been made. The results indicated just what was expected - fewer iterations and less computing time.

II. Points Near the Left Half of the Upper Symmetry Line

Substituting the approximation formulas for irregular boundary points into Equations (2-14) and (2-13), there results

$$\Psi'_{I,J} = \Psi_{I,J} + \frac{\alpha}{\frac{1}{b}\frac{\Delta x^2}{\Delta z^2} + \frac{1}{a}} \left[e\Psi_A + c\Psi_{I-1,J} + (f\Psi_B + d\Psi_{I,J-1}) \right.$$

$$\left. \frac{\Delta x^2}{\Delta z^2} - \frac{1}{2}\Delta x^2 e^{2z}\zeta_{I,J} - \left(\frac{1}{b}\frac{\Delta x^2}{\Delta z^2} + \frac{1}{a} \right) \Psi_{I,J} \right] \qquad (3\text{-}3)$$

and

$$\zeta'_{I,J} = \zeta_{I,J} + \frac{\beta}{t} \left\{ \frac{1}{\frac{\Delta x^2}{\Delta z^2}} (e\zeta_A + c\zeta_{I-1,J}) + f\zeta_B + d\zeta_{I,J-1} \right.$$

$$+ \frac{R}{4\frac{\Delta x}{\Delta z}} \left[(f\zeta_B - h\zeta_{I,J-1})(e\Psi_A - g\Psi_{I-1,J} - p\Psi_{I,J}) \right. \qquad (3\text{-}4)$$

$$\left. - (e\zeta_A - g\zeta_{I-1,J})(f\Psi_B - h\Psi_{I,J-1} - q\Psi_{I,J}) \right]$$

$$\left. - t\zeta_{I,J} \right\}$$

where a = fractional length of mesh size Δx

b = fractional length of mesh size Δz

c = 1/(1+a)

d = 1/(1+b)

e = 1/a(1+a)

f = 1/b(1+b)

g = 1/e = a(1+a)

h = 1/f = b(1+b)

$$p = (1-a)/a$$

$$q = (1-b)/b$$

$$t = \frac{1}{a\left(\frac{\Delta x^2}{\Delta z^2}\right)} + \frac{1}{b} + \frac{R}{4\left(\frac{\Delta x}{\Delta z}\right)} \left[q \left(e\Psi_A - g\psi_{I-1,J} - p\Psi_{I,J}\right) - p \left(f\Psi_B - h\Psi_{I,J-1} - q\Psi_{I,J}\right)\right]$$

Since $\Psi_A = \Psi_B = \Psi_{BDR}$ and $\zeta_A = \zeta_B = \zeta_{BDR}$ at the upper symmetry line, the following special cases of Equations (3-1) and (3-2) at the various types of boundary points are listed in Table 1.

Table 1. Special Cases at Boundary Points (Left Half).

Type of Point (I,J)	Ψ_A	Ψ_B	ζ_A	ζ_B	a	b
I	Ψ_{BDR}	Ψ_{BDR}	ζ_{BDR}	ζ_{BDR}	a	b
II	$\Psi_{I+1,J}$	Ψ_{BDR}	$\zeta_{I+1,J}$	ζ_{BDR}	1	b
III	Ψ_{BDR}	$\Psi_{I,J+1}$	ζ_{BDR}	$\zeta_{I,J+1}$	a	1

III. Points near the Right Half of the Upper Symmetry Line

Changing the signs and the grid points involved in the approximation formula of $\partial f/\partial x$ for irregular boundary points and substituting into Equations (2-14) and (2-13) there results the same equation for the stream function together with

$$\zeta'_{I,J} = \zeta_{I,J} + \frac{\beta}{t}\left\{\frac{1}{\frac{\Delta x^2}{\Delta z^2}}\left[e\zeta_A + c\zeta_{I+1,J}\right] + f_B + d\zeta_{I,J-1}\right.$$

$$- \frac{R}{4\frac{\Delta x}{\Delta z}}\left[(f\zeta_B - b\zeta_{I,J-1})(e\Psi_A - g\Psi_{I+1,J} - p\Psi_{I,J})\right. \tag{3-5}$$

$$\left. - (e\zeta_A - g\zeta_{I+1,J})(f\Psi_B - h\Psi_{I,J-1} - q\Psi_{I,J})\right]$$

$$\left. - t\zeta_{I,J}\right\}$$

where

$$t = \frac{1}{a\left(\frac{\Delta x^2}{\Delta z^2}\right)} + \frac{1}{b} - \frac{R}{4\left(\frac{\Delta x}{\Delta z}\right)}\left[q(e\Psi_A - g\Psi_{I-1,J} - p\Psi_{I,J}) - p(f\Psi_B\right.$$

$$\left. - h\Psi_{I,J-1} - q\Psi_{I,J})\right]$$

Similar cases in Table 1 can be applied to Equation (3-5) except Type II in which the subscript I+1 should be changed to I-1.

It is necessary to estimate the vorticity distribution around the surface of the cylinder before further calculations can be made. This can be done by assuming the stream function Ψ as a polynomial function of z, as was done by Jenson [23]

$$\Psi_{I,J} = a+bz+cz^2+dz^3$$

Since $\Psi_{I,1} = -V_o x$ and $V_x = 0$ (i.e. $\partial\Psi/\partial z = 0$) on the cylinder surface ($z = 0$), the polynomial function of z becomes

$$\Psi_{I,J} = -V_o x+cz^2+dz^3$$

From the boundary condition at z = 0, the vorticity distribution becomes

$$\zeta_{I,1} = \left(\frac{\partial^2 \Psi}{\partial x^2} + \frac{\partial^2 \Psi}{\partial z^2} \right)_{z=0} = 2c$$

Solving simultaneously the equations for $\Psi_{I,3}$ $\Psi_{I,2}$ and $\Psi_{I,1}$ gives

$$\zeta_{I,1} = \frac{8\Psi_{I,2} - \Psi_{I,3} - 7\Psi_{I,1}}{2\Delta z^2} \qquad (3\text{-}6)$$

Finite Difference Forms of the Diffusion Equation and the Boundary Conditions

The Crank-Nicholson implicit finite difference method[24] is used to approximate the diffusion equation over the first angular increment (i.e. I=2). The numerical differentiation formulas employed are

$$\frac{\partial c}{\partial x} = \frac{C_{I+1,J} - C_{I,J}}{\Delta x} + O(\Delta x^2)$$

$$\frac{\partial c}{\partial z} = \frac{1}{2}\left(\frac{C_{I+1,J+1} - C_{I+1,J-1}}{2\Delta z} + \frac{C_{I,J+1} - C_{I,J-1}}{2\Delta z}\right) + O(\Delta z^2)$$

$$\frac{\partial^2 c}{\partial z^2} = \frac{1}{2}\left(\frac{C_{I+1,J+1} - 2C_{I+1,J} + C_{I+1,J-1}}{\Delta z^2} + \frac{C_{I,J+1} - 2C_{I,J} + C_{I,J-1}}{\Delta z^2}\right) + O(\Delta z^2)$$

Substituting these approximating formulas into Equation (2-21) the following finite difference equation is obtained:

$$(T1 + T3)C_{I+1,J-1} - (2T1 + T4)C_{I+1,J} + (T1 - T3)C_{I+1,J+1} =$$

$$- (T1 + T3)C_{I,J-1} + (2T1 - T4)C_{I,J} - (T1 - T3)C_{I,J+1} \qquad (3\text{-}7)$$

where

$$T1 = 1/(Pe\Delta z^2)$$

$$T3 = e^z(V_{z_{I+1,J}} + V_{z_{I,J}})/(8\Delta z)$$

$$T4 = e^z(V_{x_{I+1,J}} + V_{x_{I,J}})/(2\Delta x)$$

At the front stagnation line (I=1), the above equation can be simplified to

$$(T1 + T2)C_{1,J-1} - 2T1\ C_{1,J} + (T1 - T2)C_{1,J+1} = 0$$

where $$T2 = e^z V_{z_{1,J}}/(4\Delta z)$$

Because of the characteristics of the implicit procedure and the existence of the irregular boundary, further calculations from this point will be subdivided into three cases. The differentiation formulas together with the finite difference approximations of Equation (2-21) can be expressed as follows:

I. Interior Points

$$\frac{\partial C}{\partial x} = \frac{3C_{I+1,J} - 4C_{I,J} + C_{I-1,J}}{2\Delta x} + O(\Delta x^2)$$

$$\frac{\partial C}{\partial z} = \frac{C_{I+1,J+1} - C_{I+1,J-1}}{2\Delta z} + O(\Delta z^2)$$

$$\frac{\partial^2 C}{\partial z^2} = \frac{C_{I+1,J+1} - 2\,C_{I+1,J} + C_{I+1,J-1}}{\Delta z^2} + O(\Delta z^2)$$

$$(2T1 + T3/2)\, C_{I+1,J-1} - (4T1 + 3T4/2) C_{I+1,J}$$

$$+ (2T1 - T3/2)\, C_{I+1,J+1} = (T4/2)\, C_{I-1,J} - 2C_{I,J} \qquad (3\text{-}8)$$

II. Points near the Upper Symmetry Line in the Upstream

$$\frac{\partial C}{\partial x} = \frac{3C_{BDR} - 4\, CITPZ_I + CITPZ_{I-1}}{2\Delta x} + O(\Delta x^2)$$

$$\frac{\partial C}{\partial z} = \frac{(1+2b)C_{BDR} + b^2 C_{I+1,J-1} - (1+b)^2 C_{I+1,J}}{b(1+b)\Delta z} + O(\Delta z^2)$$

From Equation (2-24) the concentration on the boundary is

$$C_{BDR} = \frac{(4TB1)CITPZ_I - (TB1)\, CITPZ_{I-1} + \tan(x)\,[-b^2 C_{I+1,J-1}}{3\, TB1 + (1 + 2b)\, \tan(x)}$$

$$\underline{+ (1+b)^2 C_{I+1,J}]}$$

where b = fractional length of mesh size Δz

TB1 = $b(1+b)\Delta z/2\Delta x$

CITPZ = the interpolated value of the concentration in the radial direction.

The governing diffusion equation can be expressed as

$$[b^2 TB2 + b\, TB3 + b^2 TB5\, \tan(x)]\, C_{I+1,J-1}$$

$$- [(b^2-1)\, TB2 + (1+b)TB3 + 3TB4 + (1+b)^2\, TB5\, \tan(x)]\, C_{I+1,J} \qquad (3\text{-}9)$$

$$= TB4 \cdot (C_{I-1,J} - 4C_{I,J}) + TB1TB5(4CITPZ_I - CITPZ_{I-1})$$

where

$$TB2 = e^{z}V_{z_{I+1,J}} / [b(1+b)\Delta z]$$

$$TB3 = 4/[Pe\ b(1+b)\Delta z^2]$$

$$TB4 = e^{z}V_{x_{I+1,J}} /2\Delta x$$

$$TB5 = (TB2-TB3)/[3TB1 + (1+2b)\ \tan(x)]$$

III. Points Near the Symmetry Line in the Downstream

$$\frac{\partial C}{\partial x} = \frac{3C_{BDR} - 4CITPZ_{I+1} + CITPZ_{I+2}}{2\Delta x} + O(\Delta x^2)$$

$$\frac{\partial C}{\partial z} = \frac{2(2+6S + 3S^2)\ C_{BDR} -[(1+S)^2(2+S)^2]\ C_{I+1,J} +}{2S(1+S)(2 + S)\ \Delta z}$$

$$\frac{[2(2+S)^2S^2]\ C_{I+1,J-1} - [S^2(1 + S)^2]\ C_{I+1,J-2}}{} + O(\Delta z^3)$$

Similarly, the concentration on the boundary can be obtained as

$$C_{BDR} = \{\tan(x)\ [S1^2\ S2^2\ C_{I+1,J} - 2S^2S2^2C_{I+1,J-1}$$

$$+ S^2S1^2C_{I+1,J-2}] + TB6\ (4CITPZ_{I+2} - CITPZ_{I+3})\}/$$

$$[3TB6 + 2\tan(x)(2+6S + 3S^2)]$$

where

S = distance between the boundary and the position-fixed boundary points (see Figure 4).

$S1 = S + 1$

$S2 = S + 2$

$SB = (S)(S2)$ $\qquad$ $TB6 = (SB)\ \Delta z/\Delta x$

The governing diffusion equation becomes

$$[TB12\ S1^2S2^2 + TB8\ (6 + 7S - S^3) + 3TB9 - TB7\ S1\ S2\ (2 - 3S)]\ C_{I+1,J}$$
$$- [2TB12\ S^2S2^2 + 4TB7\ S^2S2 + 2\ TB8\ S\ (4 - S^2)]\ C_{I+1,J-1}$$
$$+ [TB12\ S^2S1^2 + TB7\ S^2S1 + TB8\ S\ (1-S^2)]\ C_{I+1,J-2}$$
$$= TB9\ (4C_{I,J} - C_{I-1,J}) - TB6\ TB11\ (4\ CITPZ_{I+2} - CITPZ_{I+3}) \qquad (3\text{-}10)$$

where

$$TB7 = e^{z}V_{z_{I+1,J}}/2(SB)\Delta z$$

$$TB8 = 2/[Pe(SB)(\Delta z)^2]$$

$$TB9 = e^{z}V_{x_{I+1,J}}/2\Delta x$$

$$TB11 = (4TB7 - 6TB8)/[3TB6 + 2\tan(x)(2+6S+3S^2)]$$

$$TB12 = (TB11)\tan(x)$$

Note that, in the last two cases, the points of type III were neglected due to the use of a regular step size in the angular direction.

At the last angular increment, the Crank-Nicholson method is modified to approximate the diffusion equation over the points near the boundary:

$$(2TB16-BCP)C_{I+1,J} - (ACP)C_{I+1,J-1} + (EC)C_{I+1,J-2}$$
$$= (BCP)C_{I,J} + (ACP)C_{I,J-1} - (EC)C_{I,J-2} + 12TB15 - 8TB14 \qquad (3\text{-}11)$$

where

$$ACP = 4S^2(S2)(TB14) + 2S(4-S^2)(TB15)$$

$$BCP = (S1)(S2)(2-3S)(TB14) - (6+7S-S^3)(TB15) + TB16$$

$$EC = S^2(S1)(TB14) + S(1-S^2)(TB15)$$

with

$$TB14 = e^z(V_{z_{I+1,J}} + V_{z_{I,J}})/(SB)(8\Delta z)$$

$$TB15 = 1/(SB)(Pe\Delta z^2)$$

$$TB16 = e^z(V_{x_{I+1,J}} + V_{x_{I,J}})/(2\Delta x)$$

Table 2 summarizes the various difference systems used for Equation (2-23).

Computational Procedures

The computer program used to perform the calculations is presented in Appendix C. The desired quantity is obtained through the following steps:

(1) In order to reduce the number of iterations needed, the initial guess of the stream function Ψ at each interior point is set as $\Psi = e^z \sin x$ and the vorticity ζ as $\zeta = 0$. Once a solution is obtained for a given Reynolds number, then this is used as the starting solution for the next lower value of Reynolds number.

(2) Stream functions within the specified boundaries are first calculated roughly until the first convergence criterion is met. This occurs when the sum of the

Table 2. Finite-Difference Approximations to the Diffusion Equation.

Mnemonic Scheme	Position of Points	Equation No.	Remark
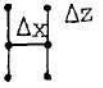	I = 2 Interior	(3-6)	
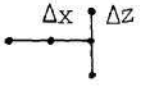	I = 3 to N Interior	(3-7)	
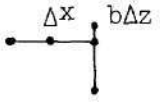	I = 3 to N/2 + 1 Boundary in Upstream	(3-8)	b < 1
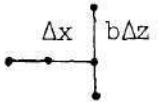	I = N/2 + 2 to N Boundary in Downstream	(3-9)	or b < 1 b ≥ 1
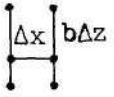	I = N + 1	(3-10)	b > 1

difference in the values of Ψ between two successive iterative steps is less than 1.0×10^{-3}.

(3) The values of ζ around the surface of the cylinder are then calculated by substituting the improved values of Ψ into Equation (3-6).

(4) New values of ζ around the surface of the cylinder are then calculated by substituting the improved values of Ψ and surface vorticity into Equation (3-2) with the appropriate boundary conditions.

(5) Subsequently, new values of Ψ are then calculated by substituting the improved values of ζ into Equation (3-1) with the appropriate boundary conditions.

(6) Step (3) is repeated.

(7) Repeat step (4) through (6) until the second convergence criterion is met. This occurs when the sums of the difference in the values of both Ψ and ζ between two successive iterative steps are less than 1.0×10^{-4} respectively.

(8) Drag coefficients and surface pressure distribution are then calculated from the convergent values of the stream function and vorticity.

(9) Angular and radial velocities (V_x and V_z) are calculated from Equation (2-15) by using the differentiation approximation formulas of higher order.

(10) The concentration on the cylinder surface, C^*, is guessed first to start the calculation of the concentration profile.

(11) At each angular increment, the combined equations of diffusion for both interior and boundary points are written once. Their unknown coefficients can be arranged as a lower-triangular matrix. After simplification, the Thomas method[25] is employed to solve these special simultaneous equations (See Appendix A).

(12) An improved value of C^* is then calculated from the last one of Equation (2-22) by substituting the results of step (11).

(13) Repeat steps (11) and (12) for the points in the upstream until the change in C^* at each angular increment is less than 1.0×10^{-5}.

(14) In the downstream, the boundary concentration, C_{BDR}, is calculated from Equation (2-22) which requires interpolating the predicted concentration over the next two angular increments. Therefore, repeat steps (11) through (13) until changes in the values of the concentration at each point in the downstream are less than 1.0×10^{-5}.

(15) The local and overall Nusselt numbers are obtained using Equations (2-30) and (2-31).

CHAPTER IV

RESULTS AND DISCUSSION

Introduction

With the aid of a Univac-1108 electronic digital computer, a series of calculations was made at Reynolds numbers from 0.1 to 1.0 and opening ratios of 1.25, 1.50 and 1.75. For higher Reynolds numbers, the outer boundary position must be moved further out to obtain converged results. This requires larger core memory to accommodate the increase of grid points involved in the computation. Hence, calculations at Reynolds numbers of 2, 3 and 5 at different opening ratios were attempted but would not converge due to the insufficient core memory capacity (65K words, 36 bits/word).

Partial differential equations of elliptical form, such as the stream function and vorticity equations, are usually solved by a successive over-relaxation technique. In order to achieve fast rates of convergence, a relaxation factor must be introduced. In regular domains, there are methods available for determining relaxation factors. However in irregular domains such as encountered in this study, there appears to be no method available for finding relaxation factors. Therefore, a trial and error technique was used.

Various angular and radial step sizes were used to test the accuracy of the calculations. It was found that 60 grid points in the angular direction were sufficiently small to obtain excellent results.

The presentation of the results are divided into two sections: zero radial mass flux and constant radial suction mass flux. Since no results of the latter case are available for comparison, the study of zero radial mass flux was undertaken to verify that the flow parameters obtained in the present study were in good agreement with those of other similar numerical studies and experimental investigations.

Zero Radial Mass Flux

Drag Coefficient

Drag coefficients calculated in the present study together with other related variables are summarized in Tables 3-5. It is known that the outer boundary position (r_∞) depends on the number of increments in both the angular and radial directions (M and N). As the opening ratio gets smaller, the number N increases rapidly. The value of the opening ratio is divided evenly into a number of radial increments (10 in all cases) and this increment is defined as the radial step size (Δz).

Various angular step sizes (Δx) and a constant radial step size (Δz) were used to test the effect of the position of the outer boundary, where uniform flow is assumed, on the accuracy of the drag coefficients. As can be seen from Tables 3-5, the values of the outer boundary positions (r_∞) make little difference in the resulting total drag coefficients (C_D) when Reynolds number is held constant. It is believed that an angular step size of 3° and radial step sizes of 0.02231 for Pt = 1.25, 0.04055 for Pt = 1.50 and 0.05596 for Pt = 1.75 were fine enough to accurately calculate the drag coefficients.

Table 3. Computational Parameters Used and Drag Coefficients Calculated for Pt = 1.25.

R	Δz	Δx	M	N	r_∞	α	β	C_{DF}	C_{DP}	C_D
1.0	0.0223	0.0524	60	142	23.775	1.4	0.8	235.07	879.43	1114.50
0.8	0.0223	0.0524	60	142	23.775	1.4	0.9	293.99	1100.62	1394.61
0.8	0.0223	0.0582	54	137	21.265	1.6	0.9	294.00	1100.62	1394.62
0.8	0.0223	0.0655	48	132	19.020	1.5	0.9	293.97	1101.06	1395.03
0.5	0.0223	0.0524	60	142	23.775	1.4	0.9	470.63	1763.22	2233.85
0.5	0.0223	0.0582	54	137	21.265	1.6	0.9	470.64	1763.58	2234.22
0.5	0.0223	0.0655	48	132	19.020	1.4	0.9	470.63	1763.58	2234.21
0.1	0.0223	0.0524	60	142	23.775	1.4	0.9	2353.84	8822.78	11176.62
0.1	0.0223	0.0655	48	132	19.020	1.4	0.8	2353.91	8823.23	11177.14
0.1	0.0223	0.0873	36	119	15.911	1.4	0.9	2353.94	8823.58	11177.52

Table 4. Computational Parameters Used and Drag Coefficients Calculated for Pt = 1.50.

R	Δz	Δx	M	N	r_∞	α	β	C_{DF}	C_{DP}	C_D
1.0	0.0405	0.0524	60	82	27.794	1.4	1.25	93.79	209.92	303.71
1.0	0.0405	0.0655	48	77	22.694	1.4	1.2	93.90	210.55	304.45
1.0	0.0405	0.0873	36	70	17.086	1.2	0.8	93.99	211.22	305.21
0.8	0.0405	0.0524	60	82	27.794	1.6	0.9	117.43	263.47	380.90
0.8	0.0405	0.0655	48	77	22.694	1.6	0.9	117.50	263.93	381.43
0.8	0.0405	0.0873	36	70	17.086	1.6	0.9	117.58	264.45	382.03
0.5	0.0405	0.0524	60	82	27.794	1.6	0.8	188.18	423.25	611.43
0.5	0.0405	0.0655	48	77	22.694	1.6	0.8	188.22	423.51	611.73
0.5	0.0405	0.0873	36	70	17.086	1.6	0.8	188.27	423.83	612.10
0.1	0.0405	0.0524	60	82	27.794	1.6	0.8	941.77	2121.18	3062.95
0.1	0.0405	0.0655	48	77	22.694	1.6	0.8	941.76	2121.19	3062.95
0.1	0.0405	0.0873	36	70	17.086	1.6	0.8	941.76	2121.21	3062.97

Table 5. Computational Parameters Used and Drag Coefficients Calculated for Pt = 1.75.

R	Δz	Δx	M	N	r_∞	α	β	C_{DF}	C_{DP}	C_D
1.0	0.0560	0.0524	60	62	32.125	1.6	1.4	56.92	98.85	155.77
1.0	0.0560	0.0655	48	58	25.682	1.4	1.1	57.08	99.58	156.66
1.0	0.0560	0.0873	36	53	19.413	1.4	1.1	57.48	101.15	158.63
0.8	0.0560	0.0524	60	62	32.125	1.6	0.9	71.54	125.16	196.70
0.8	0.0560	0.0655	48	58	25.682	1.6	0.9	71.63	125.58	197.21
0.8	0.0560	0.0873	36	53	19.413	1.6	0.9	71.93	126.74	198.67
0.5	0.0560	0.0524	60	62	32.125	1.6	0.8	115.00	202.43	317.43
0.5	0.0560	0.0655	48	58	25.682	1.6	0.8	115.04	202.61	317.65
0.5	0.0560	0.0873	36	53	19.413	1.6	0.8	115.20	203.28	318.48
0.1	0.0560	0.0524	60	62	32.125	1.6	0.8	576.37	1017.74	1594.11
0.1	0.0560	0.0655	50	59	27.160	1.6	1.1	576.37	1017.77	1594.14
0.1	0.0560	0.0873	36	53	19.413	1.6	0.8	576.37	1017.80	1594.17

As seen from Tables 3-5, the drag coefficient decreases significantly as the opening ratio becomes larger. It is expected that the drag coefficient will reach that of a single cylinder in an infinite fluid as the opening ratio becomes infinite. At a Reynolds number of 1.0 the total drag coefficient of a single cylinder is 10.34.[10]

In previous studies on tube bank fluid flow, the drag coefficient is reported in terms of the friction factor f where $f = C_D/4Pt$. Table 6 compares the friction factors of the present study with those calculated by Ishihara[19] and with those determined experimentally at Delaware[20] for tube banks of in-line square tube layout.

A probable explanation of the differences between the compared friction factors is that the present study is based on a single row of tubes of infinite length in which there is an infinite number of tubes while those previous studies were based on multiple rows of tubes of finite length in which there are finite number of tubes.

Table 6. Friction Factors Calculated and Measured by Various Workers.

R	Pt	f			
		Present Study (1 row)	Ishihara[19] (2 rows)	(3 rows)	Delaware Projects[20] (10 rows)
1.0	1.25	222.90	229.21	227.14	240.00
1.0	1.50	50.62	51.12	50.28	54.00
1.0	1.75	22.25			
0.1	1.25	2235.32	2292.56	2271.87	
0.1	1.50	510.49	511.45	503.05	
0.1	1.75	227.73			

Surface Pressure Distribution

The pressure variation on a cylindrical surface is given in the form of the pressure coefficient C_p. Calculated results at R from 0.1 to 1.0 and Pt = 1.25, 1.50 and 1.75 are shown in Figures 6-9. It is noticed that small variations in pressure occur near both the front and rear stagnation points. The minimum pressure occurs in the rear portion of the cylinder. As the Reynolds number increases, the rear stagnation pressure rises. The pressure drops sharply when the opening ratio becomes smaller. The effect of the neighboring tubes on the pressure distribution is such that the maximum rate of pressure drop occurs around the point of minimum clearance between the cylinders i.e. 90° from the front stagnation point. As the opening ratio becomes smaller, the rate of pressure drop increases in this region.

Since only numerical data have been reported on the pressure distribution around cylinders in multiple rows at these low Reynolds numbers[19], the calculated results based on the pressure at the front stagnation point are plotted for comparison with these data in Figures 10-13. In the front stagnation region, the pressure of the second and third rows increases due to momentum recovery in the rear stagnation region of the preceding row. As seen from Figures 10-13, a similar type of pressure variation occurs in the rear portion of the third row as occurs in the present study. The difference is because turbulence appeared behind the tube in multiple rows.

Surface Vorticity Distribution

The vorticity distributions around the surface of a cylinder are shown in Figures 14 and 15 for Reynolds numbers of 0.1 and 1.0

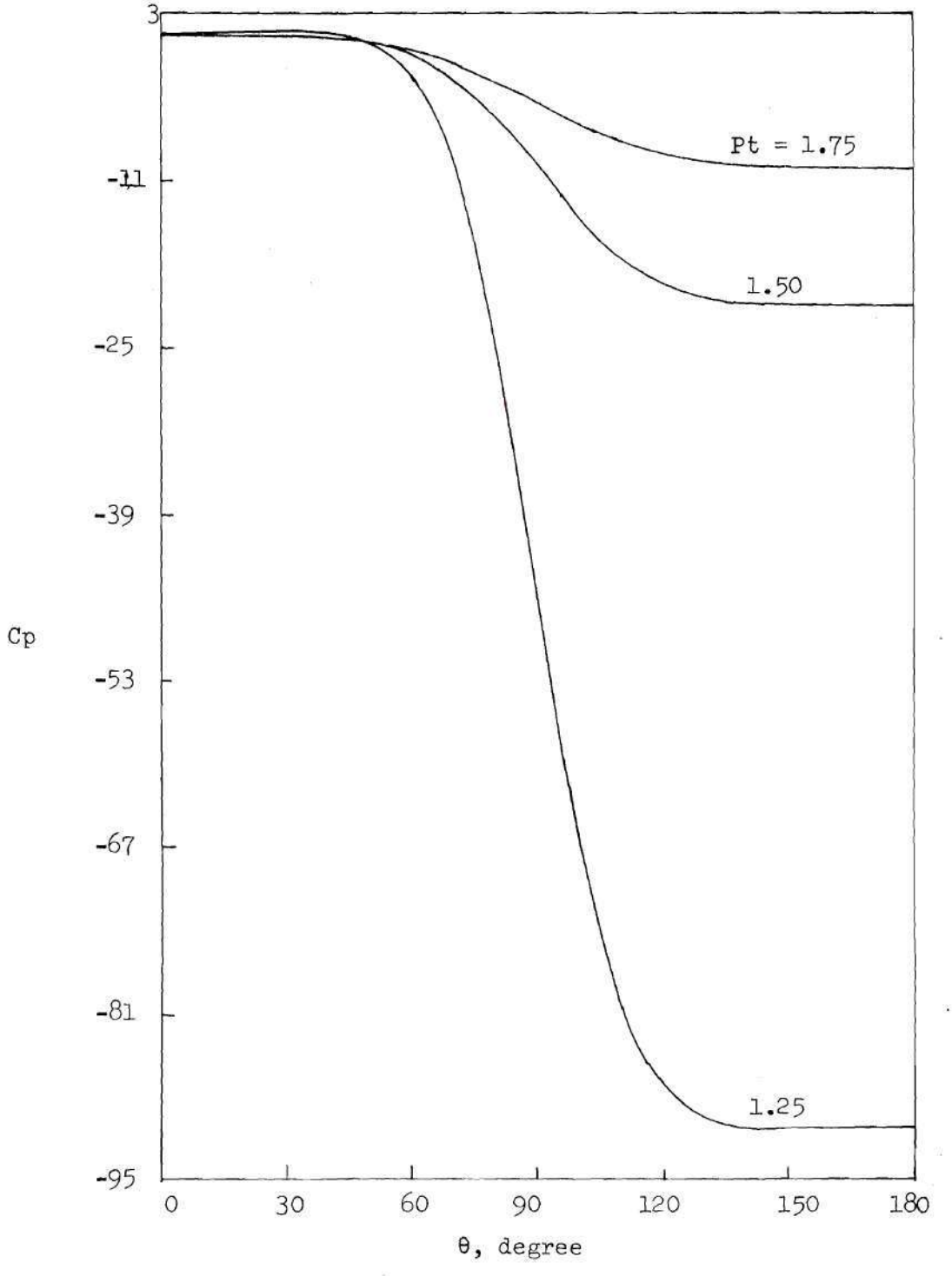

Figure 6. Surface Pressure Distribution (R=0.1)

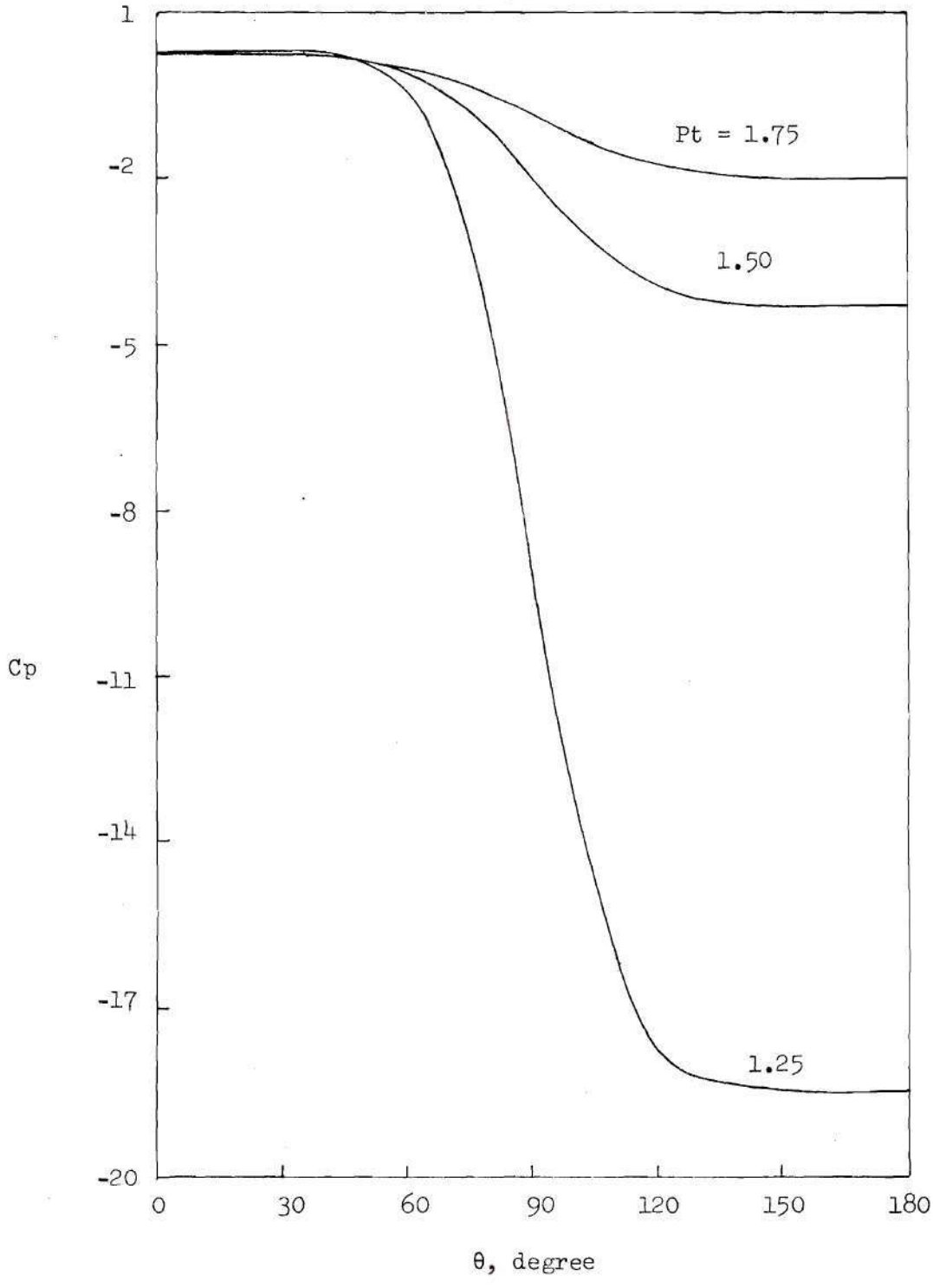

Figure 7. Surface Pressure Distribution (R = 0.5).

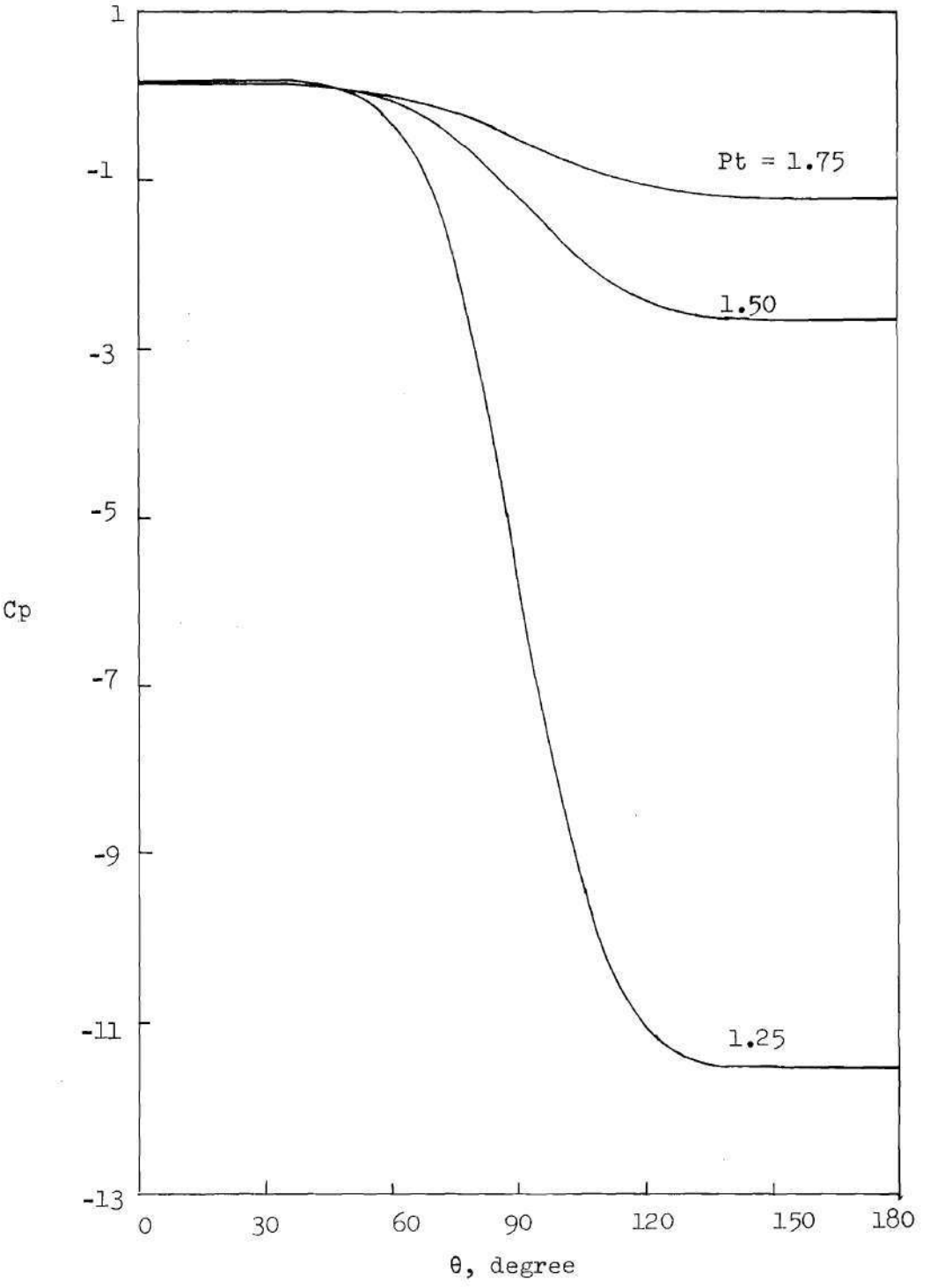

Figure 8. Surface Pressure Distribution (R = 0.8).

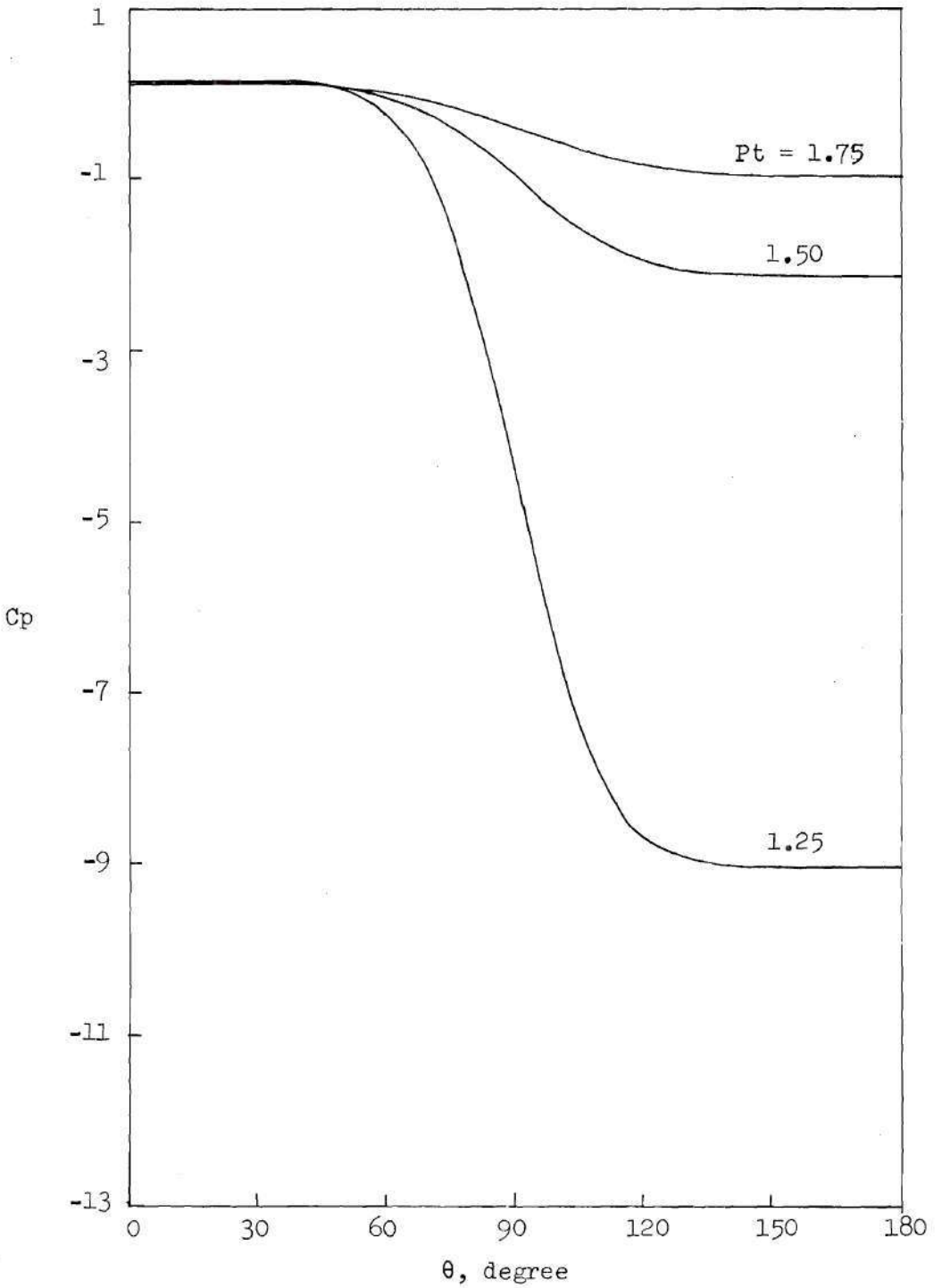

Figure 9. Surface Pressure Distribution (R = 1.0).

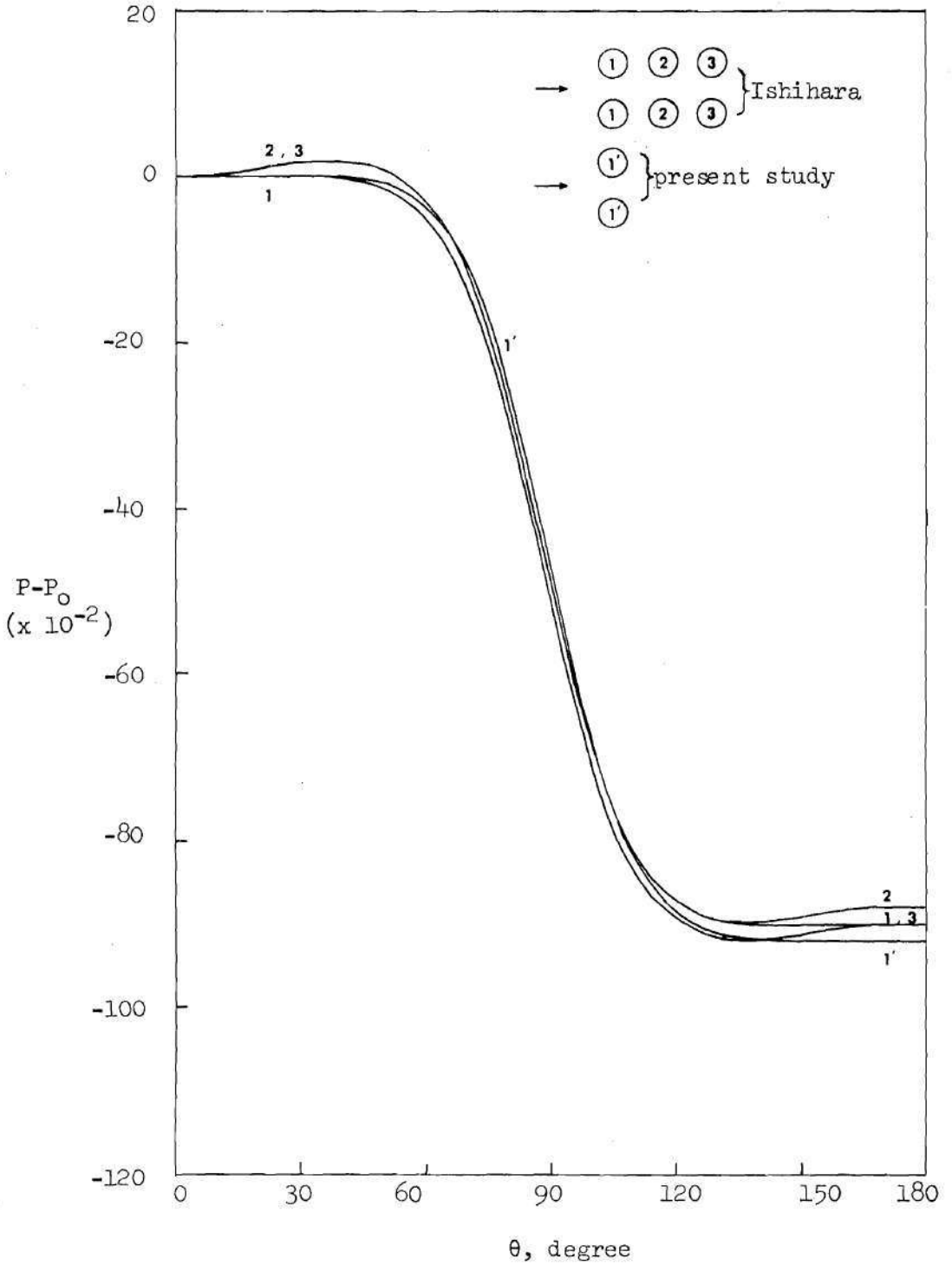

Figure 10. Comparison of Surface Pressure Distribution of 1-Row (Present Study) and 3-Row(19) Banks of Tubes (R = 0.1; Pt = 1.25). Numbers indicate the Orders of Rows.

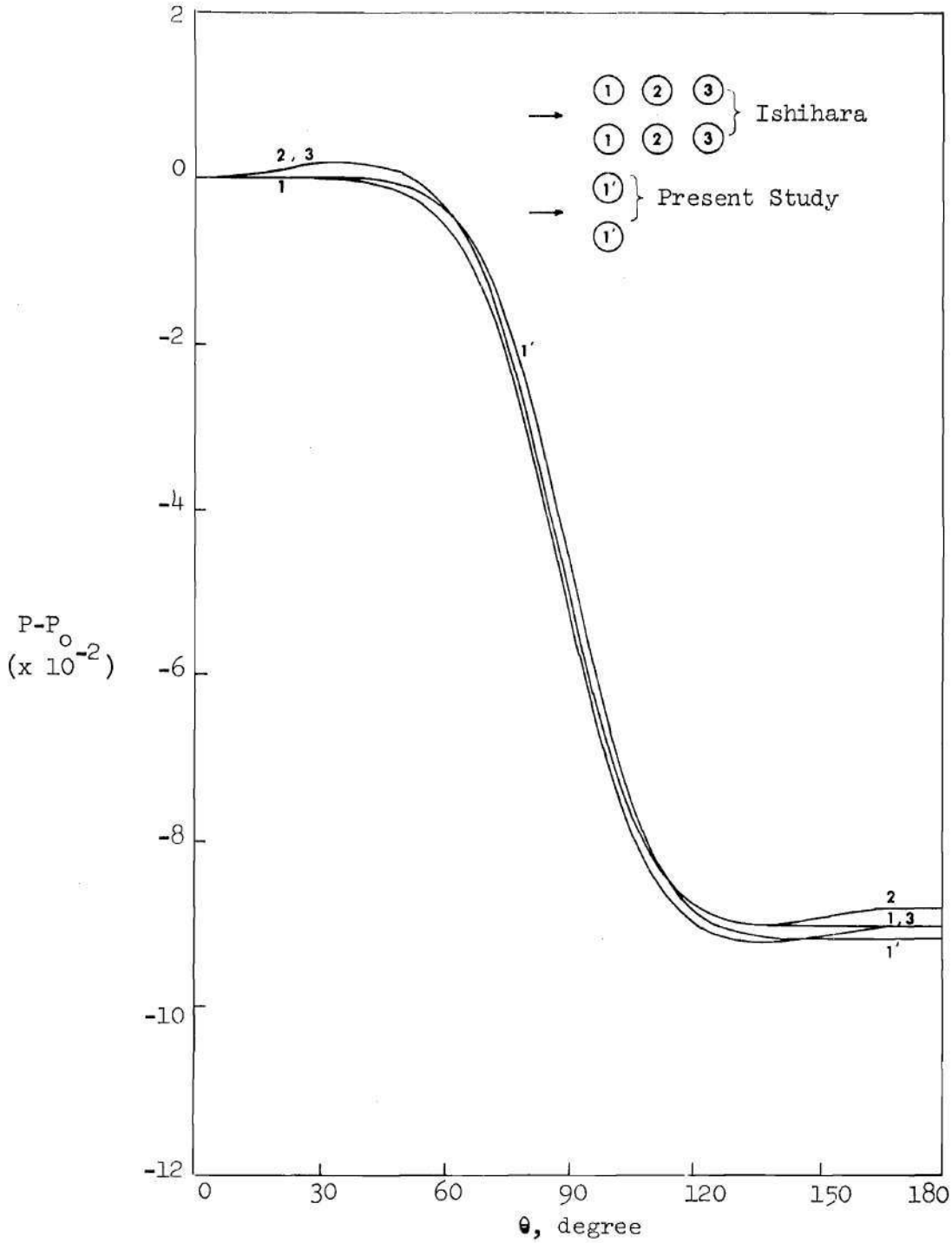

Figure 11. Comparison of Surface Pressure Distribution of 1-Row (Present Study) and 3-Row[19] Banks of Tubes (R=1.0; Pt = 1.25). Numbers Indicate the Orders of Rows.

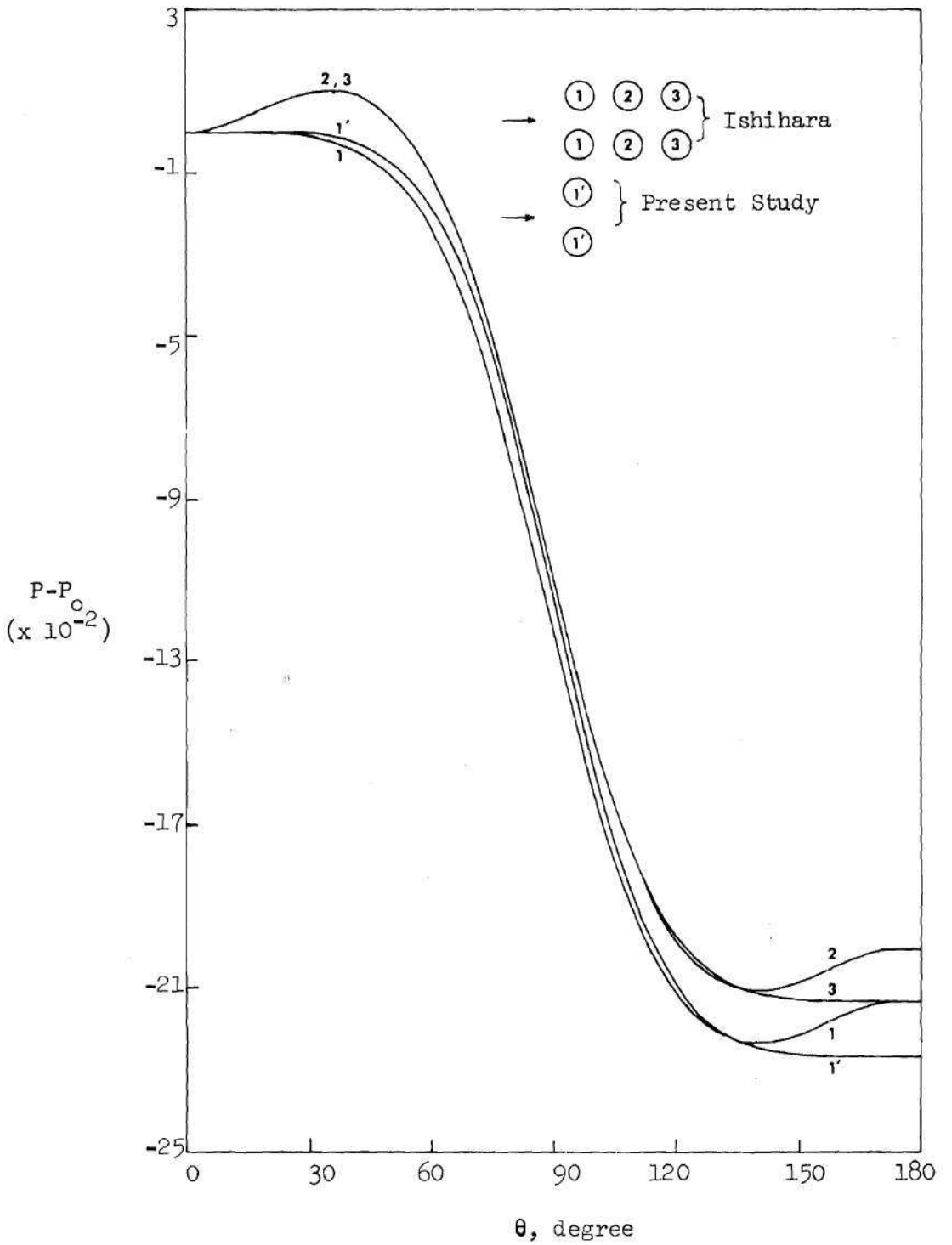

Figure 12. Comparison of Surface Pressure Distribution of 1-Row (Present Study) and 3-Row[19] Banks of Tubes (R=0.1; Pt = 1.50). Numbers Indicate the Orders of Rows.

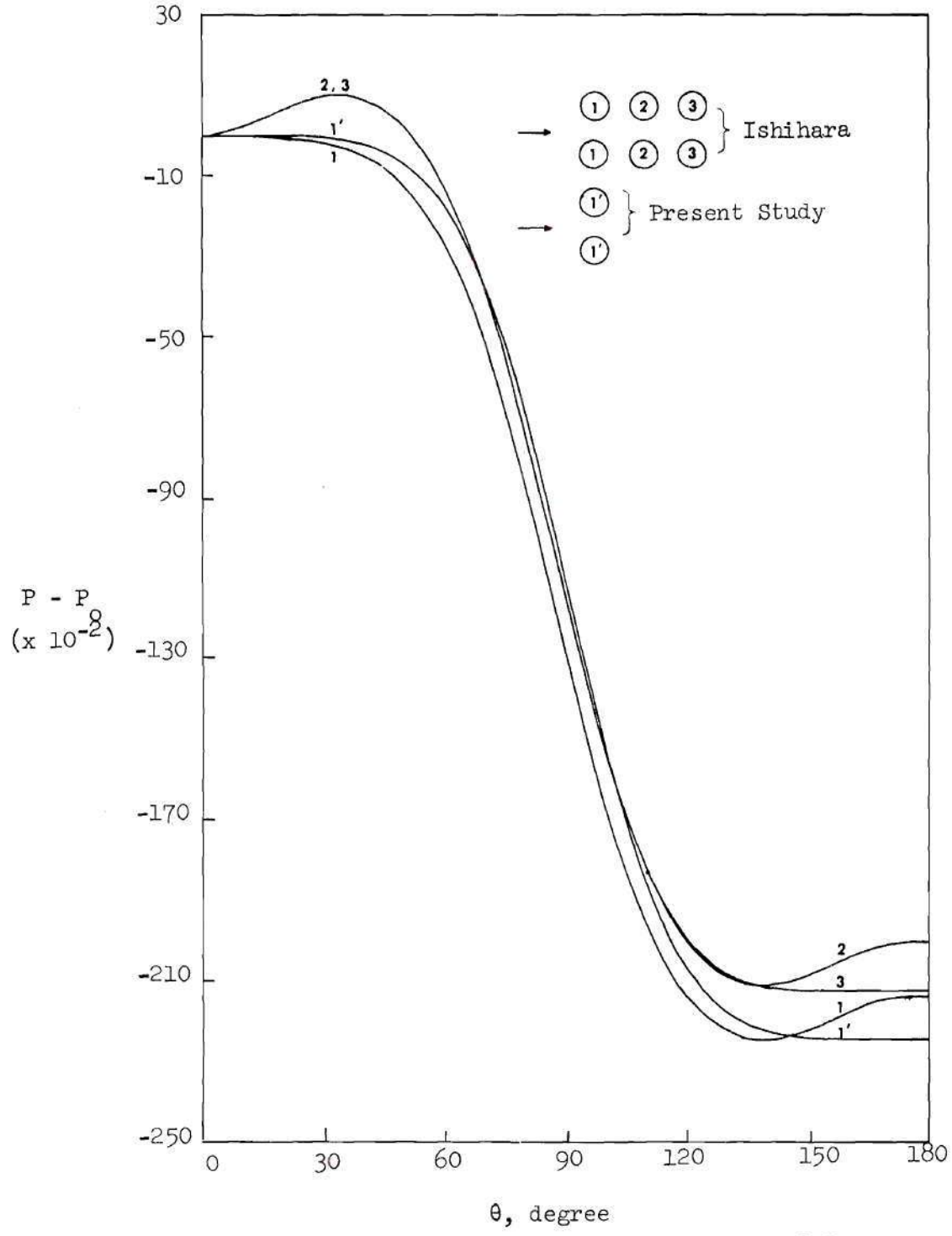

Figure 13. Comparison of Surface Pressure Distribution of 1-Row (Present Study and 3-Row[19] Banks of Tubes (R = 1.0; Pt = 1.50). Numbers Indicate the Orders of Rows.

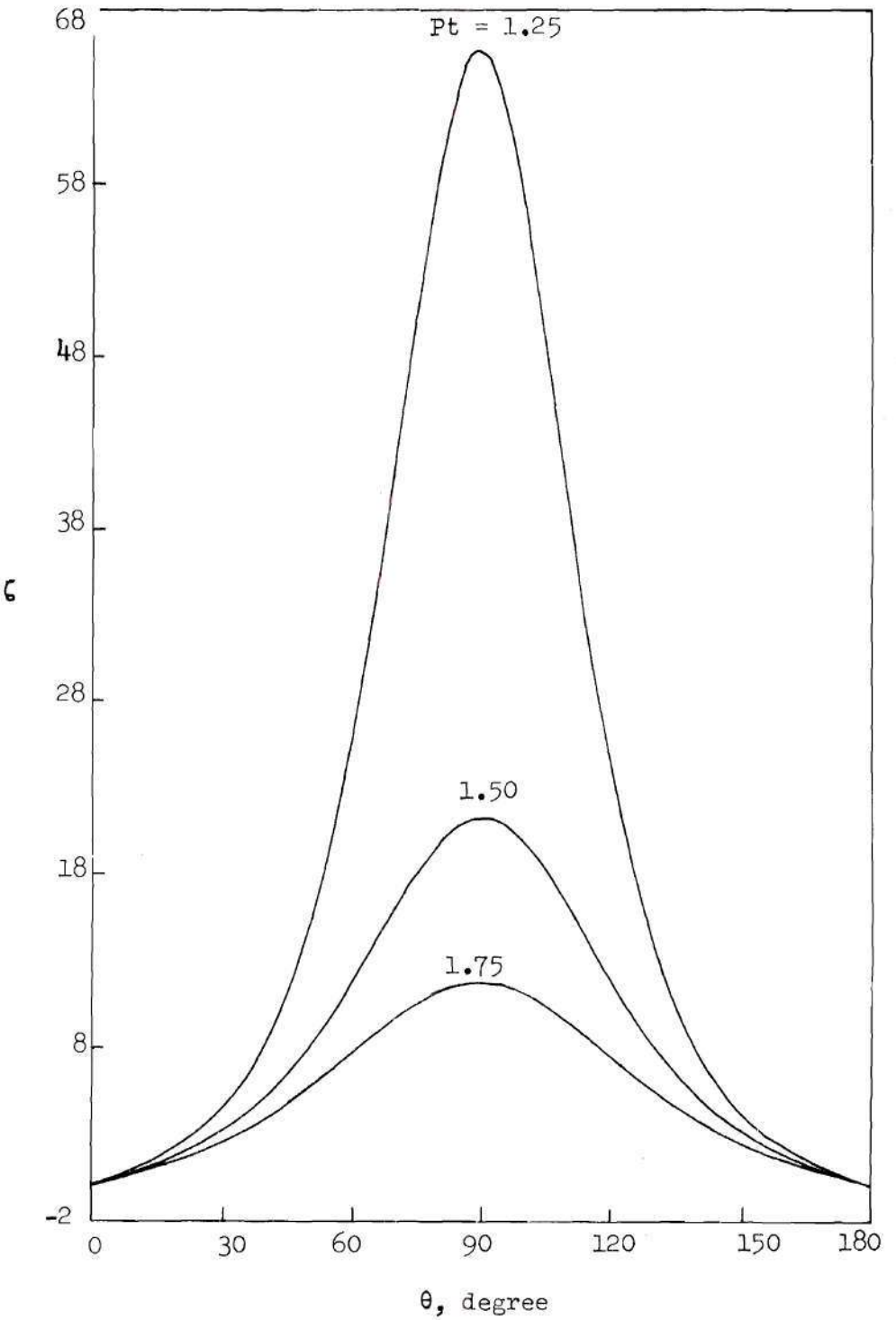

Figure 14. Surface Vorticity Distribution (R = 0.1).

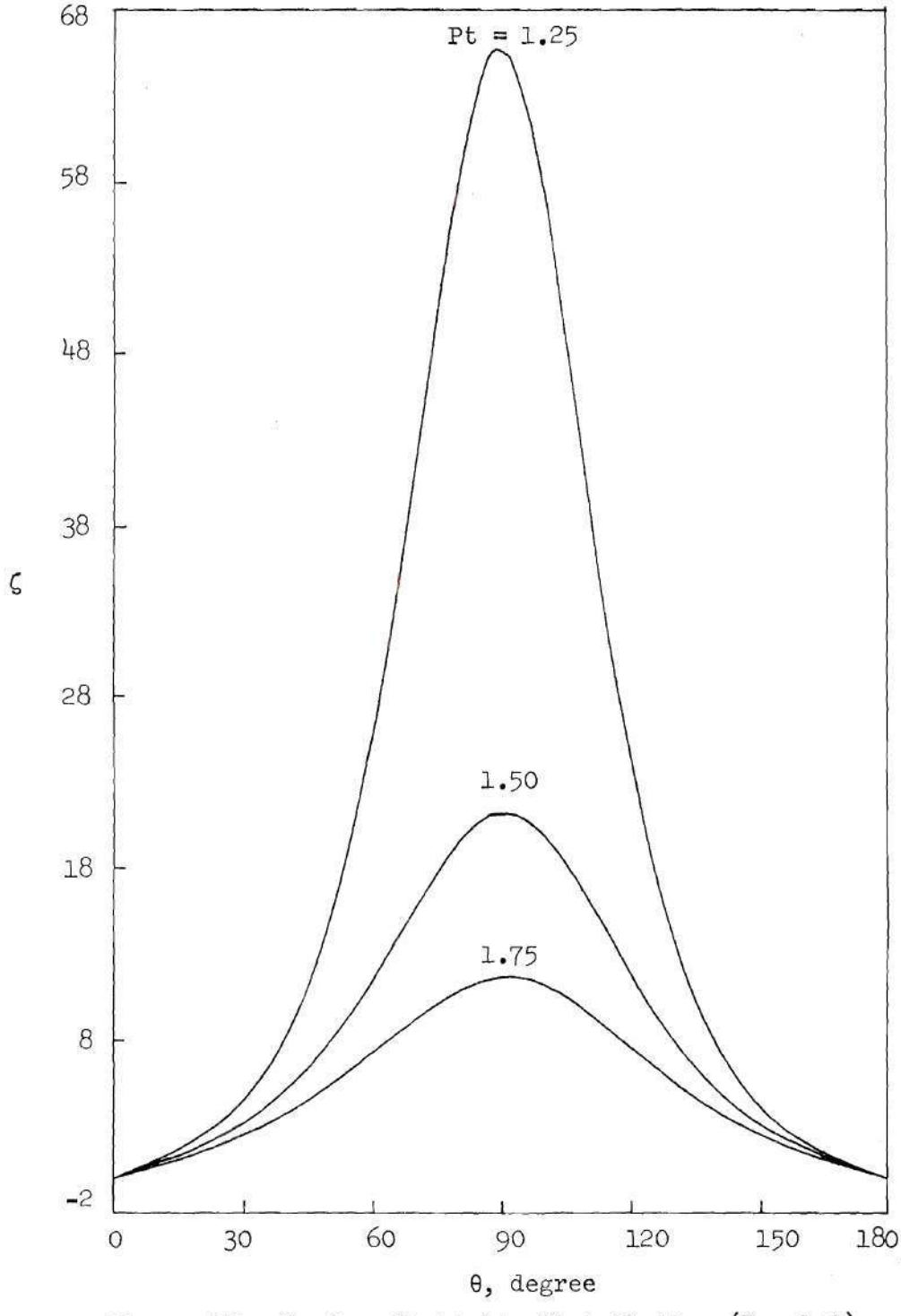

Figure 15. Surface Vorticity Distribution (R = 1.0).

and opening ratios of 1.25, 1.50 and 1.75. The effect of Reynolds numbers studied on the variation of surface vorticity is minimal. However, the surface vorticity increases sharply as the opening ratio becomes smaller and the point of maximum vorticity appears around the point of minimum clearance of the tube row. The results of the present study are compared with those of multiple rows of tubes in Figures 16-19. In the case of multiple rows, the surface vorticity variations in the front portion of the first row and in the rear portion of the third row are very similar to that of a single row. The negative vorticity which occurred in the first and second rows indicates the presence of eddies in the rear of the tubes.

Flow Patterns

Streamlines and their corresponding vorticity contours are shown in Figures 20-28 at Reynolds numbers of 0.1 to 1.0 and opening ratios of 1.25, 1.50 and 1.75. These contours were plotted using the GPCP (General Purpose Contouring Program) of California Computer Products. Figures 20 to 28 show that the flow patterns are almost symmetrical fore and aft at low Reynolds numbers. In the region far from a cylinder, the streamlines are not disturbed by the existence of the cylinder and are parallel to the upper and lower symmetry lines. As the Reynolds number increases, the vorticity distribution becomes more unsymmetrical.

Constant Radial Suction Mass Flux

Low Reynolds number flow past an infinite row of circular cylinders with constant radial suction mass flux was investigated

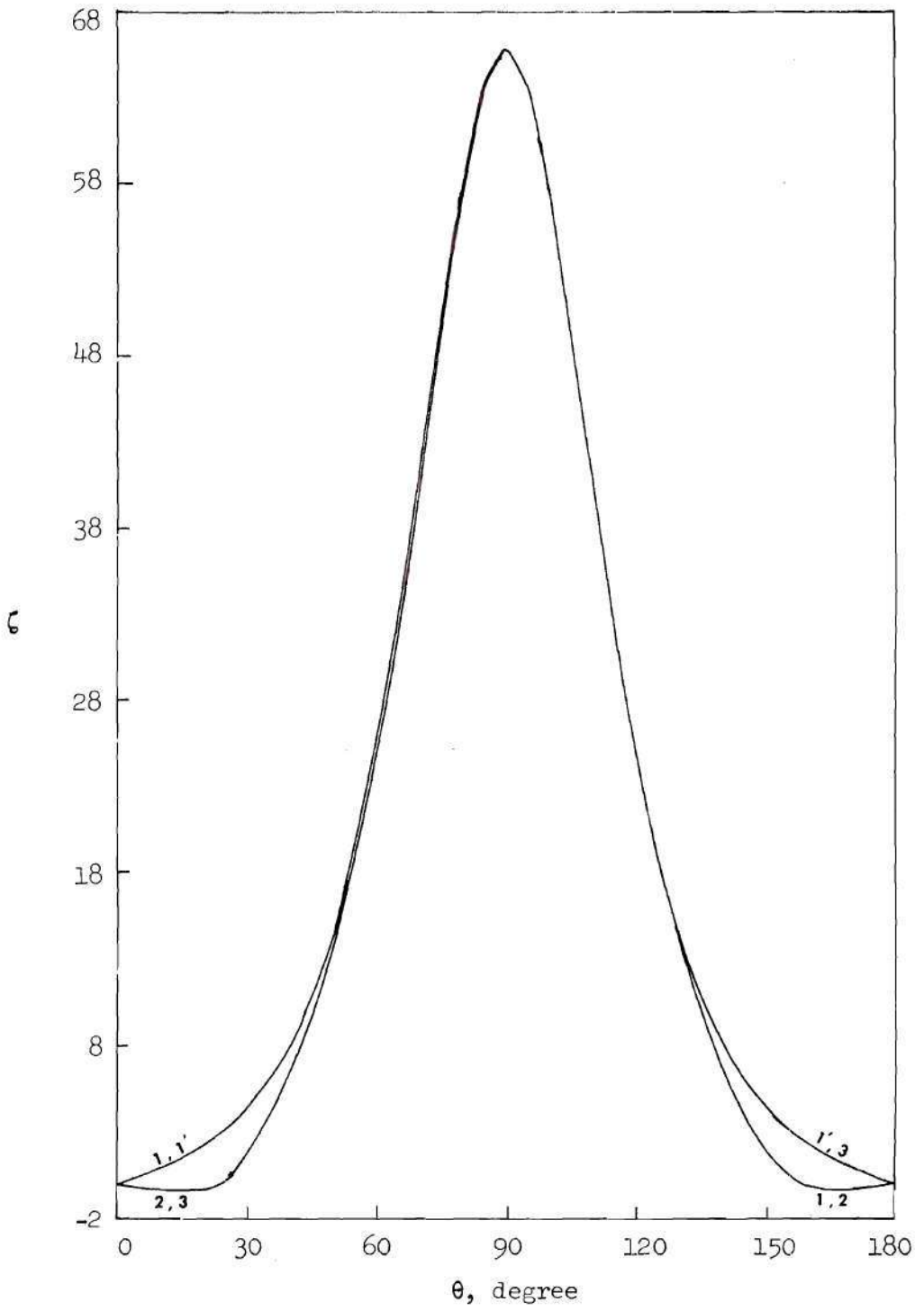

Figure 16. Comparison of Surface Vorticity Distribution of 1-Row (Present Study) and 3-Row[19] Banks of Tubes (R = 0.1; Pt = 1.25). (For legend see Figure 10).

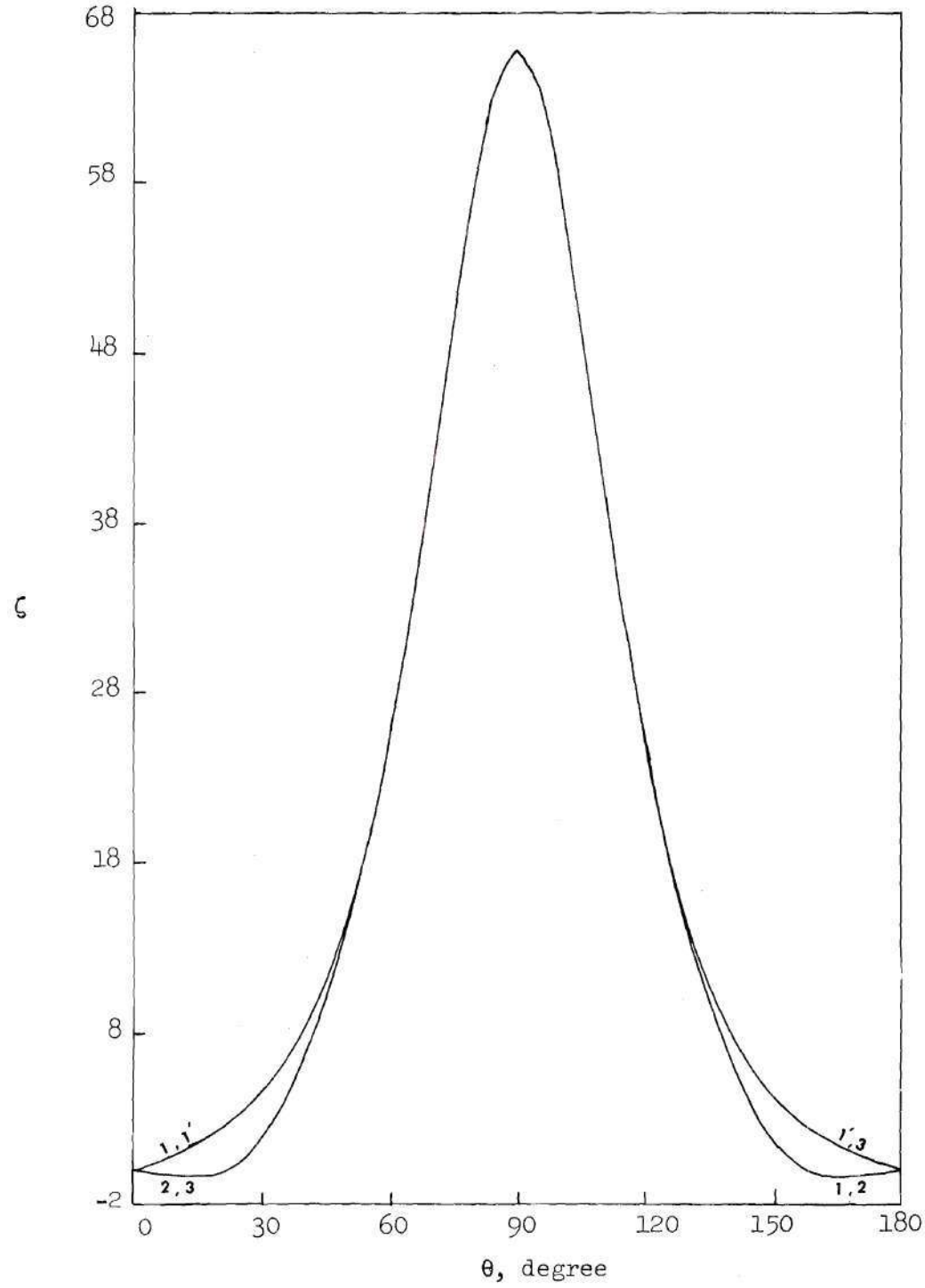

Figure 17. Comparison of Surface Vorticity Distribution of 1-Row (Present Study) and 3-Row[19] Banks of Tubes (R = 1.0; Pt = 1.25). (For Legend see Figure 10).

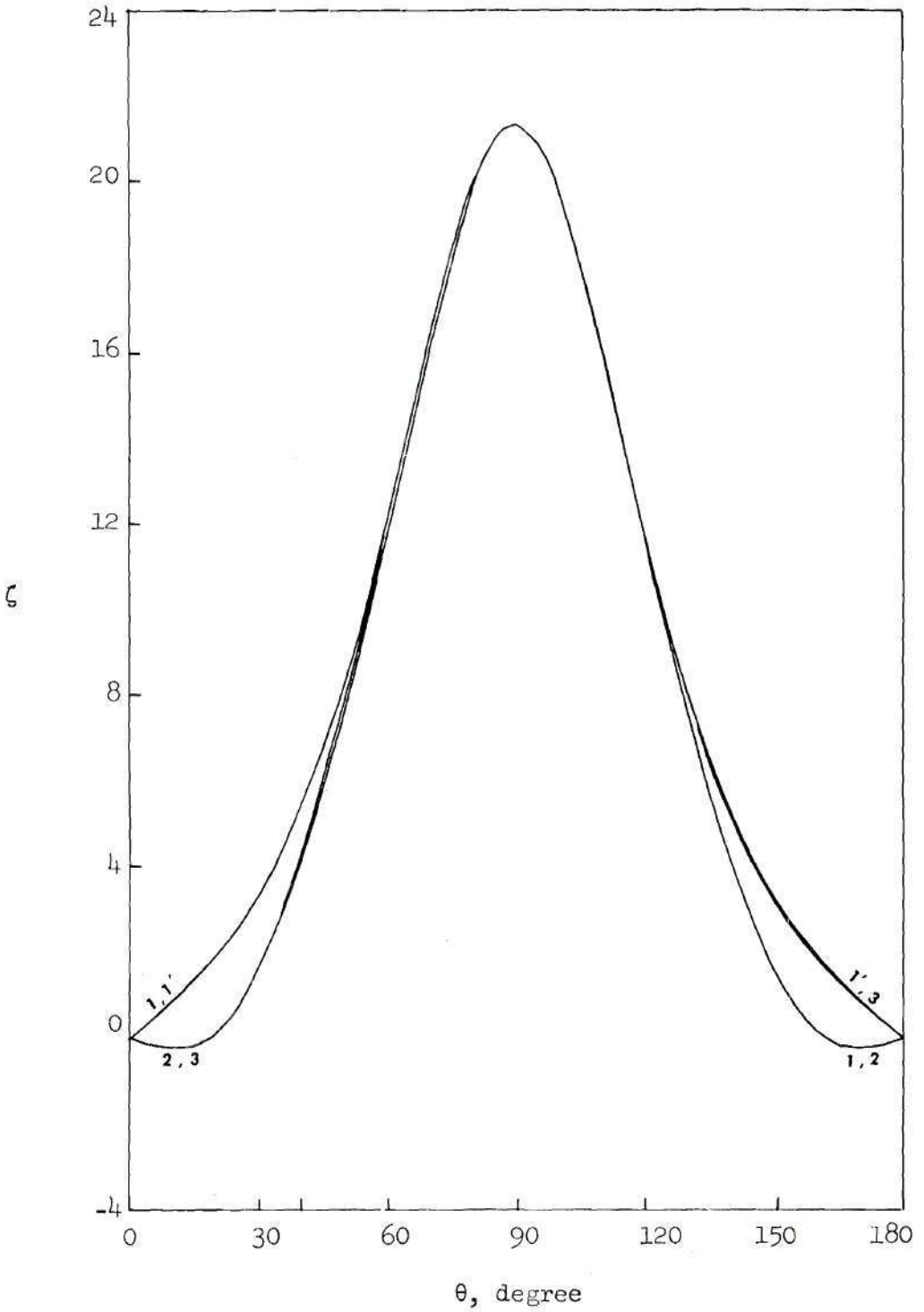

Figure 18. Comparison of Surface Vorticity Distribution of 1-Row (Present Study) and 3-Row[19] Banks of Tubes (R = 0.1; Pt = 1.50) (For legend see Figure 10).

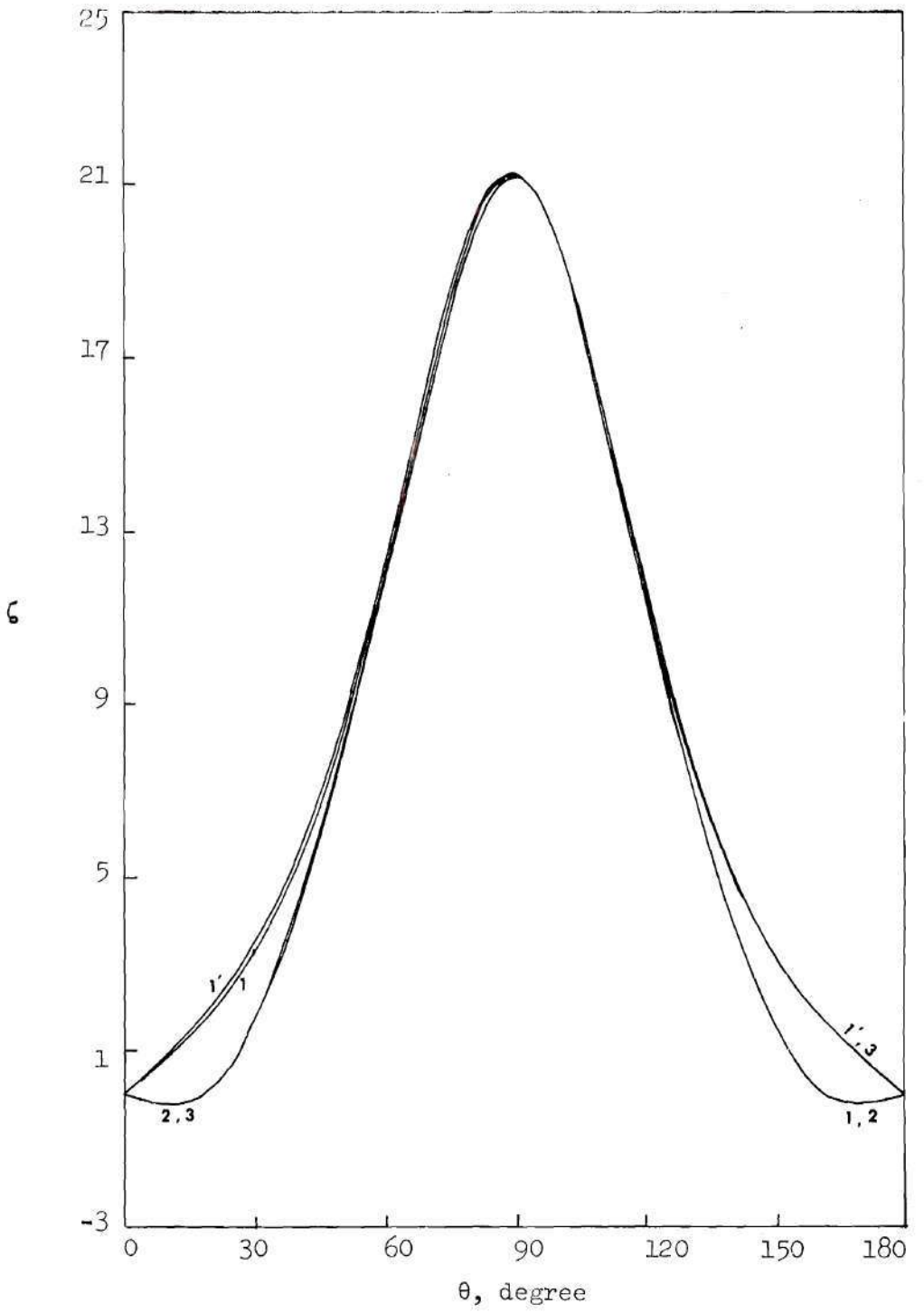

Figure 19. Comparison of Surface Vorticity Distribution of 1-Row (Present Study) and 3-Row[19] Banks of Tubes (R = 1.0; Pt = 1.50). (For legend see Figure 10).

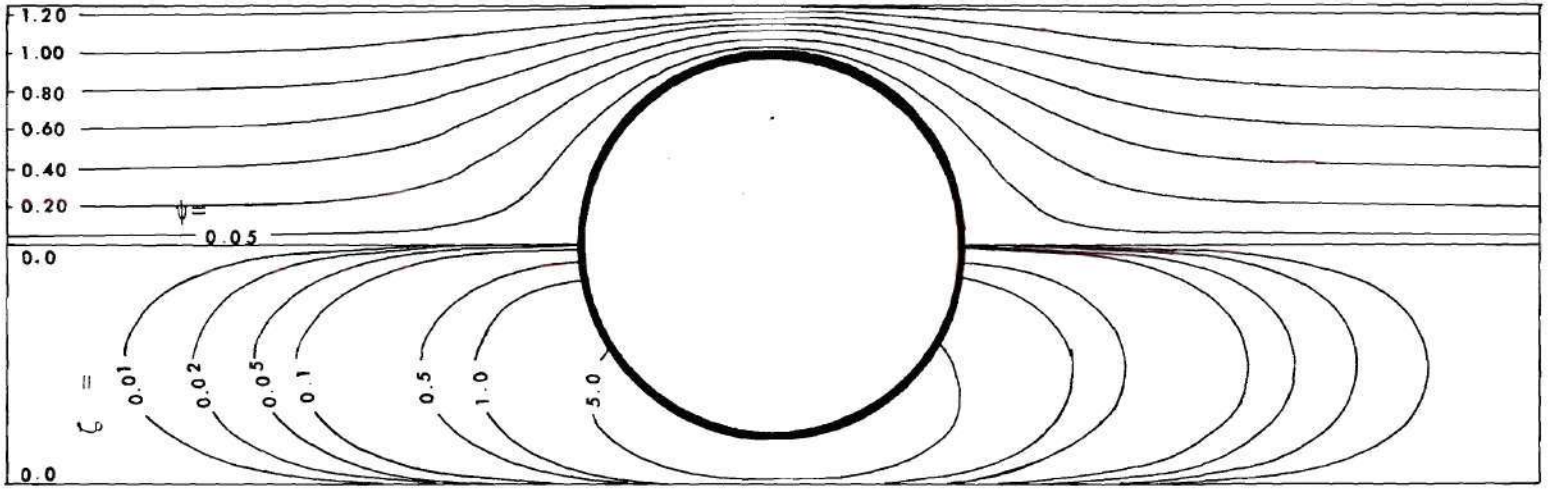

Figure 20. Contours of Stream Function (ψ) and Vorticity(ζ) (R = 0.1; Pt = 1.25).

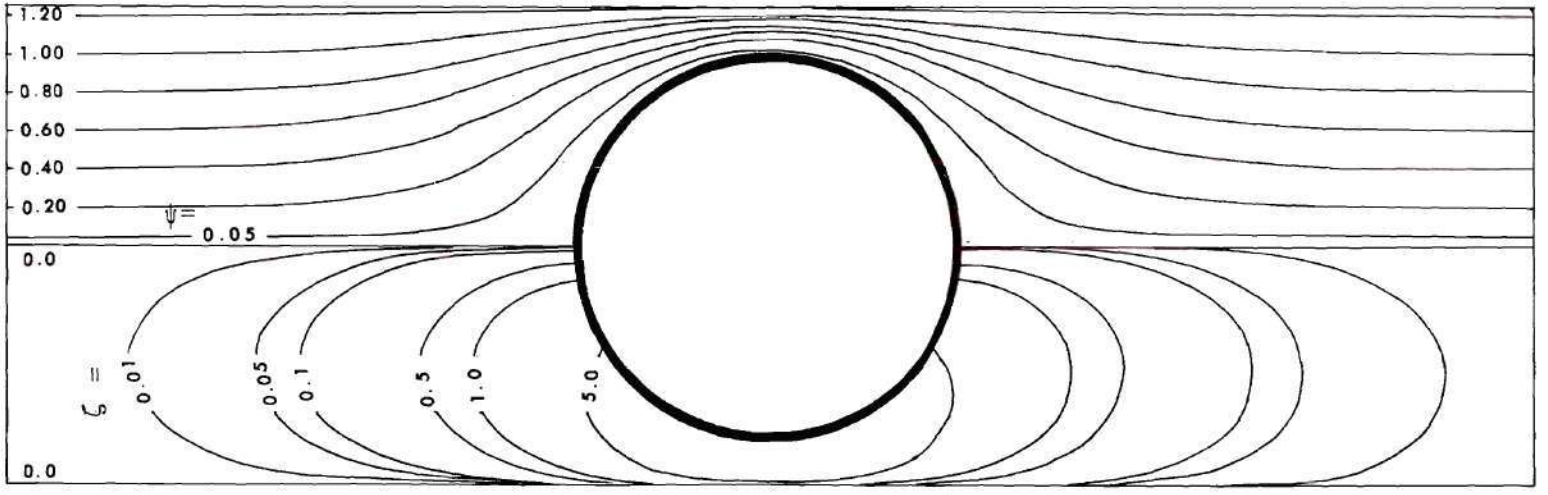

Figure 21. Contours of Stream Function (ψ) and Vorticity (ζ) (R = 0.5; Pt = 1.25).

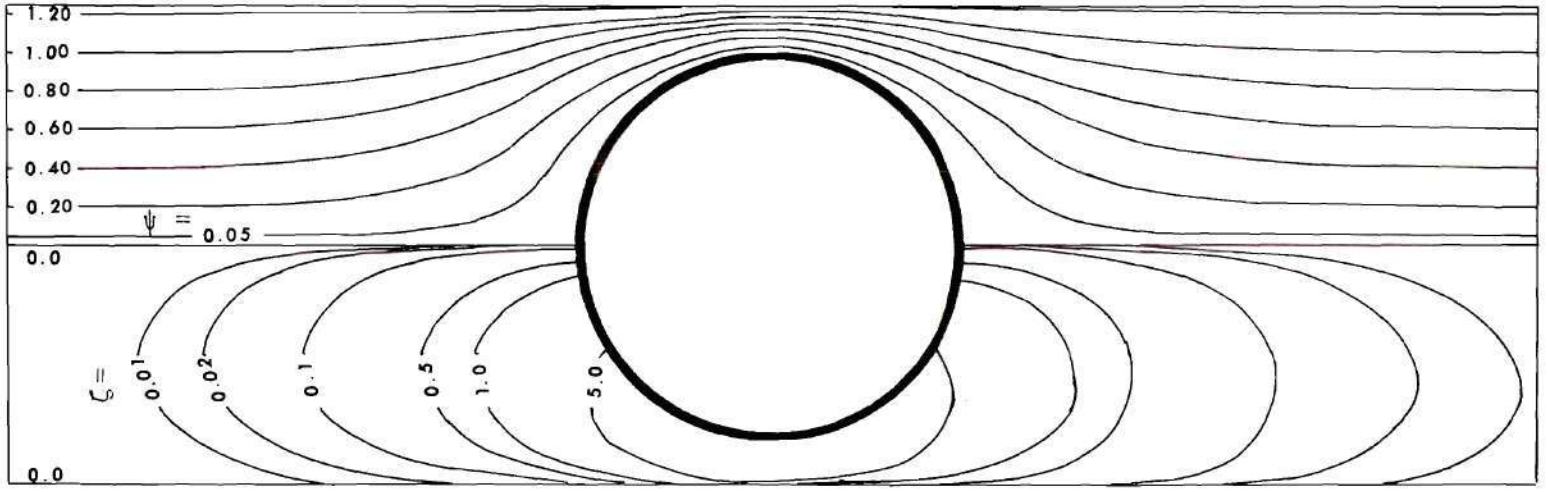

Figure 22. Contours of Stream Function (ψ) and Vorticity (ζ) (R = 1.0; Pt = 1.25).

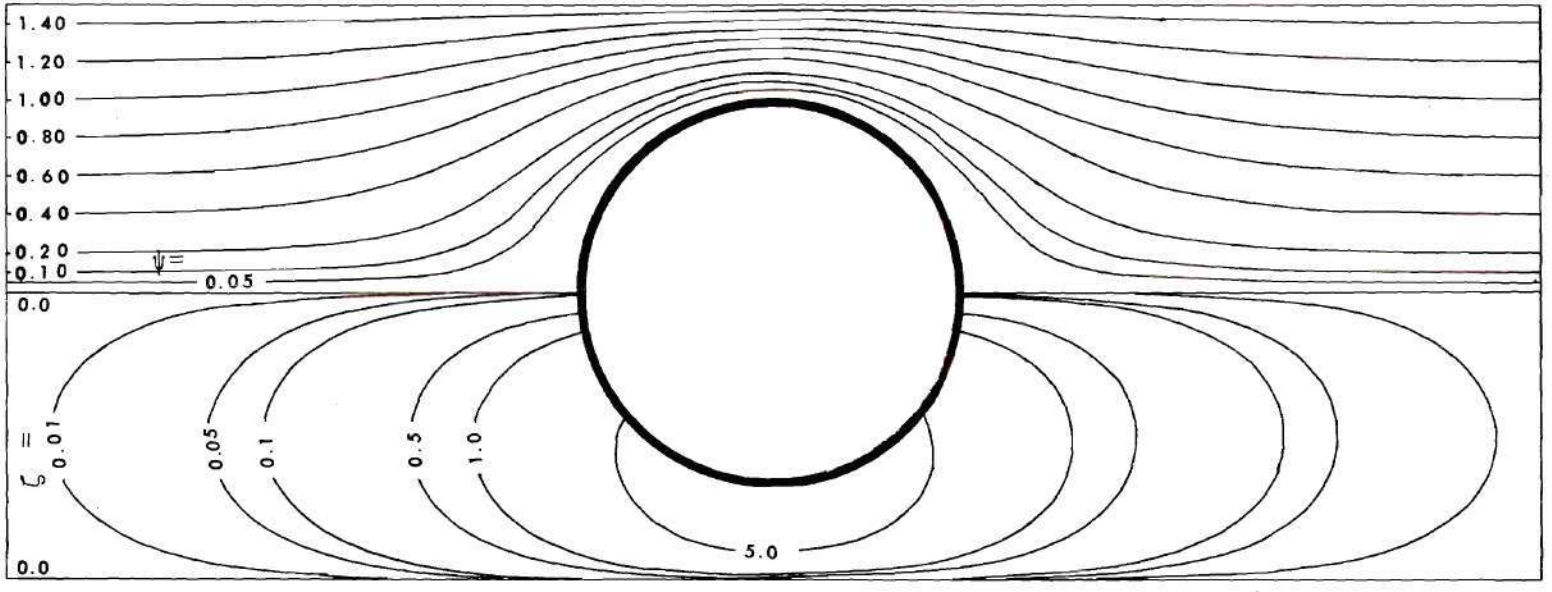

Figure 23. Contours of Stream Function (ψ) and Vorticity (ζ) (R = 0.1; Pt = 1.50).

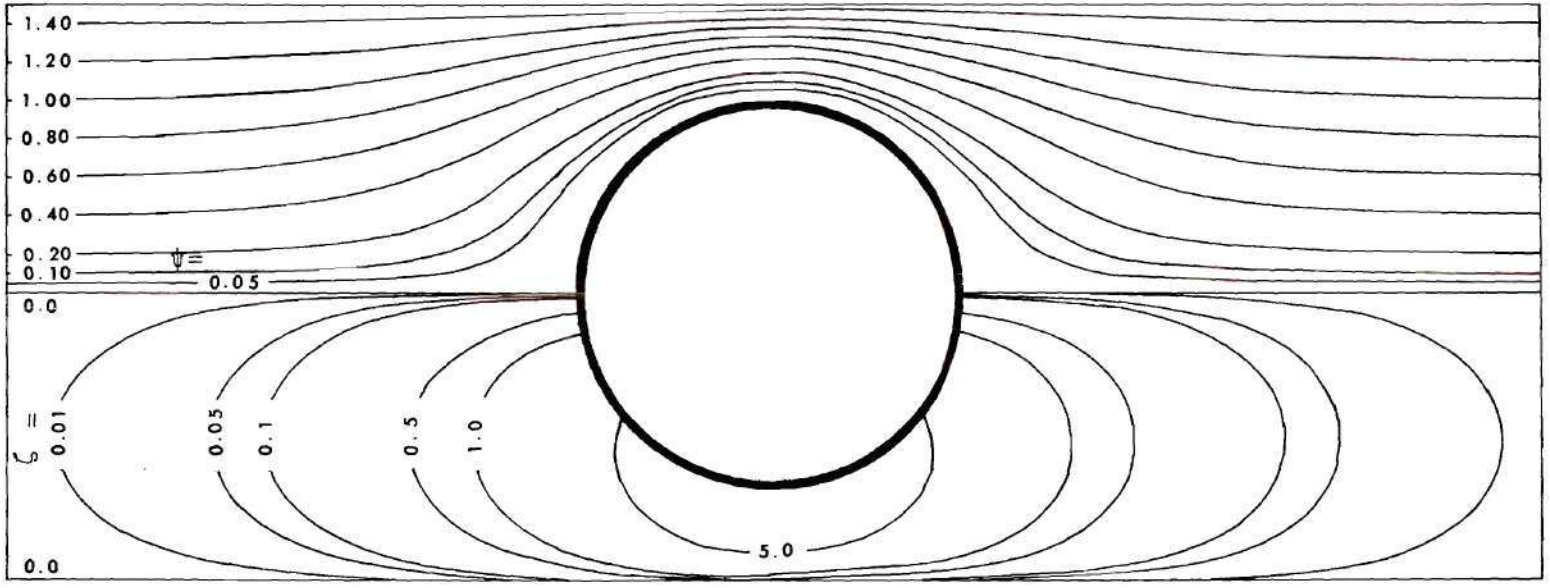

Figure 24. Contours of Stream Function (ψ) and Vorticity (ζ) (R = 0.5; Pt = 1.50).

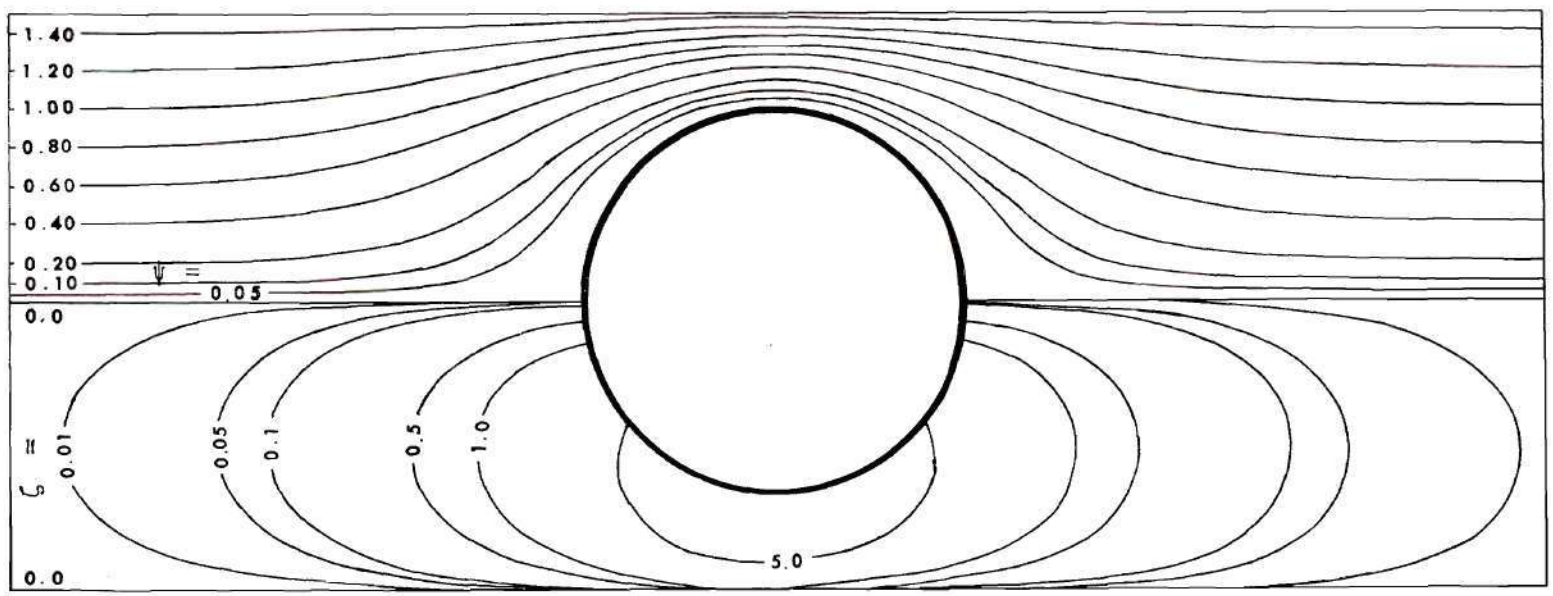

Figure 25. Contours of Stream Function (ψ) and Vorticity (ζ) (R = 1.0; Pt = 1.50).

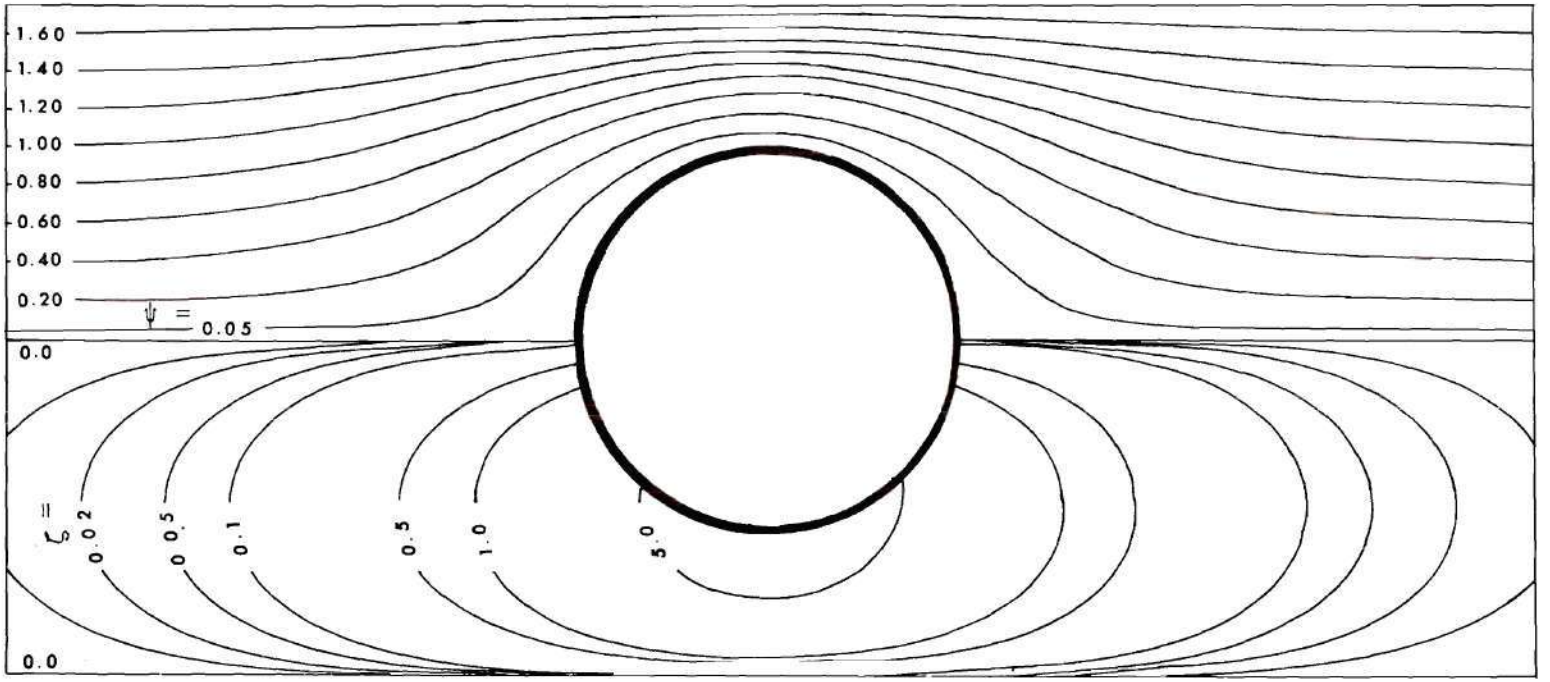

Figure 26. Contours of Stream Function (ψ) and Vorticity (ζ) (R = 0.1; Pt = 1.75).

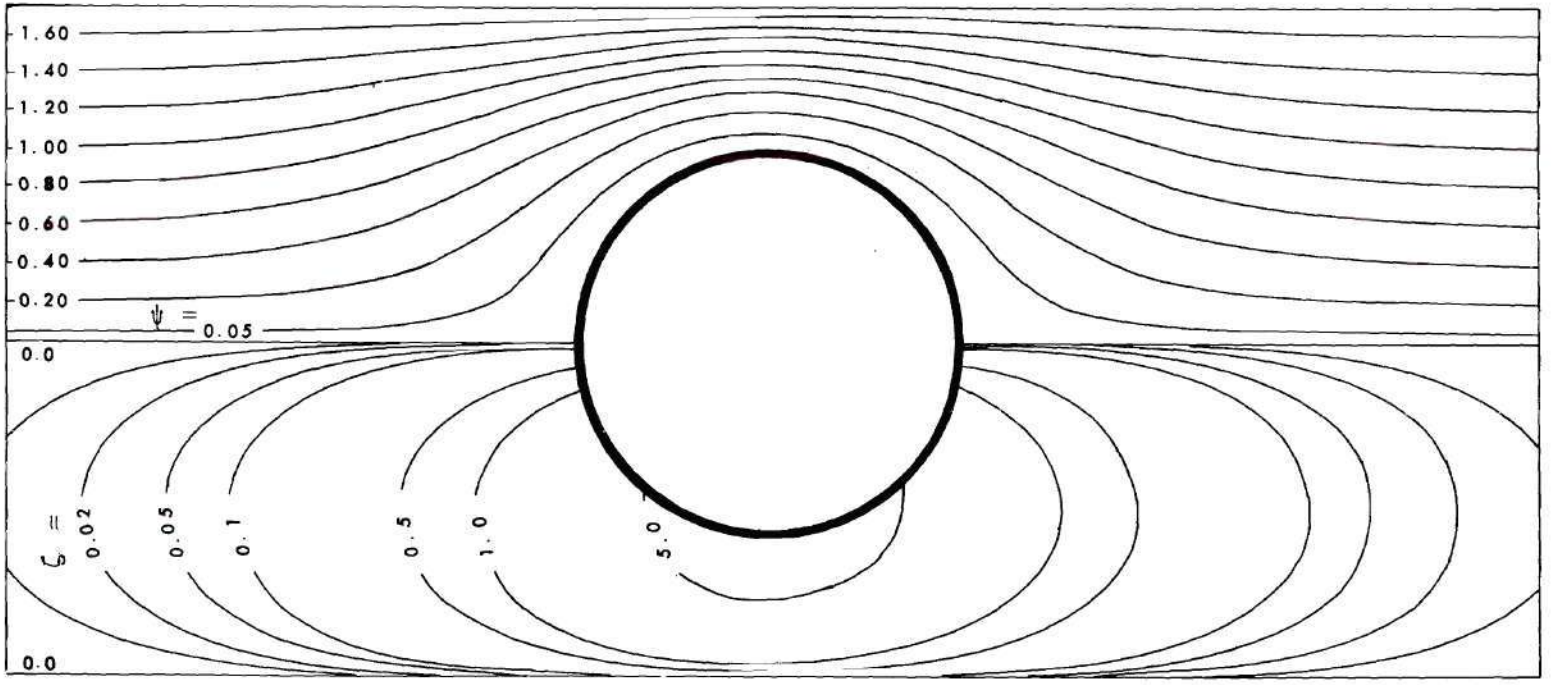

Figure 27. Contours of Stream Function (ψ) and Vorticity(ζ) (R = 0.5; Pt = 1.75).

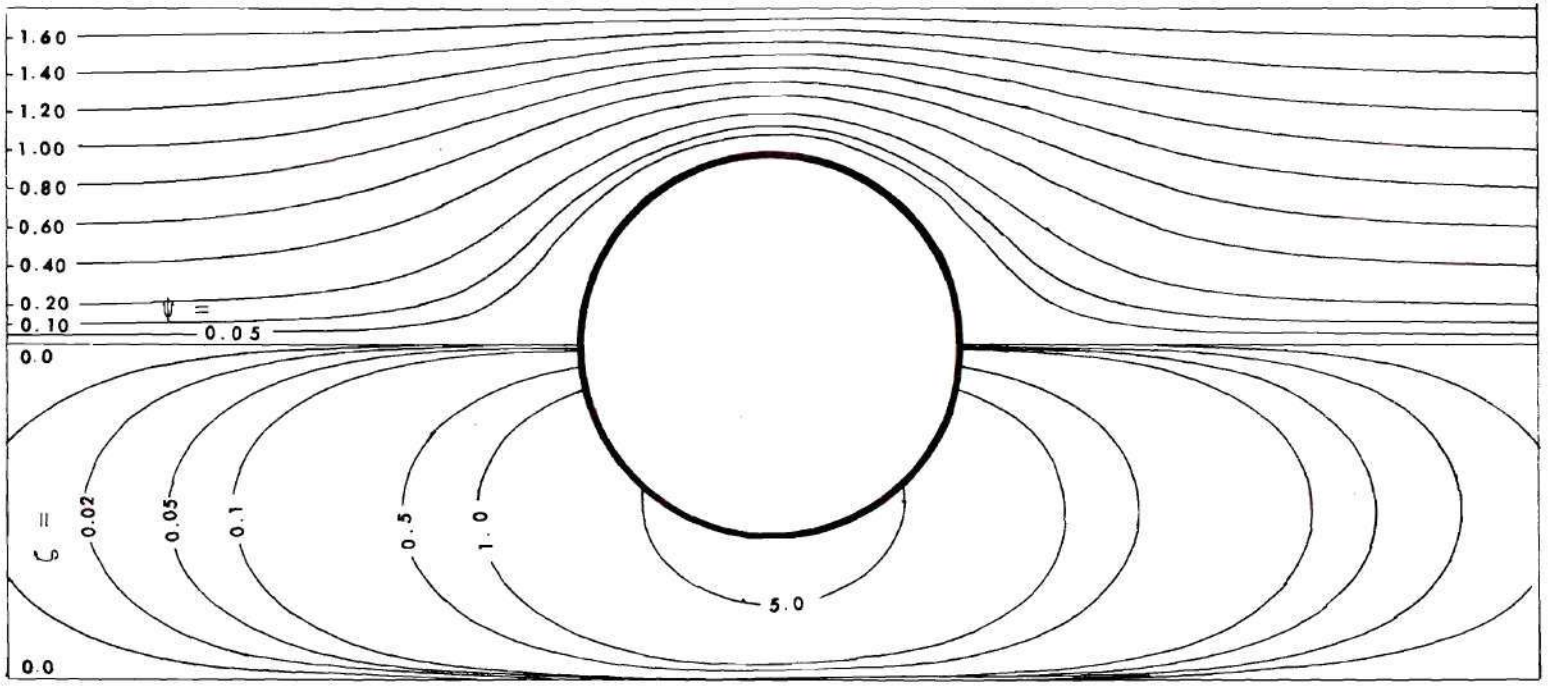

Figure 28. Contours of Stream Function (ψ) and Vorticity (ζ) (R = 1.0; Pt = 1.75).

for a pure fluid and for a binary solution. The radial suction flux (G) is expressed in gallons per square foot per day (gfd) as shown in Appendix B.

Pure Fluids

The computational parameters used and the drag coefficients calculated at radial suction fluxes of 3.82-11.45 gfd are summarized in Tables 7-9. The results indicate that the drag coefficients are not significantly affected by these radial suction fluxes. The effect of higher radial suction fluxes on the drag coefficients is shown in Table 10 for a Reynolds number of 1.0 and Pt = 1.50 and 1.75. The drag coefficient decreases as the radial suction mass flux is increased and this is mainly because of the decrease in the pressure drag coefficient.

In Figures 29-35, contours of the stream function with and without suction are plotted for comparison. It is seen that with suction the downstream streamlines move closer to the cylinder wall and display a distinct asymmetry. Since the stream function at the cylinder wall varies with the angular position (i.e. $\Psi = -V_o x$), the streamlines in the rear region of the cylinder are affected more significantly by suction than those in the front region. The extent of the asymmetry depends upon the magnitude of the radial suction mass flux.

The surface pressure coefficients in the direction of flow at a Reynolds number of 1.0 and opening ratios of 1.50 and 1.75 are listed in Table 11. Although the influence of the radial suction flux considered is small, the extent of the variation of the pressure coefficient

Table 7. Computational Parameters Used and Drag Coefficients Calculated at Various Radial Suction Mass Fluxes for Pt = 1.25.

R	Δz	Δx	M	N	α	β	G	$-V_o$	C_{DF}	C_{DP}	C_D
1.0	0.0223	0.0524	60	142	1.6	0.9	11.45	0.0012	235.07	879.28	1114.35
0.8	0.0223	0.0524	60	142	1.6	0.9	11.45	0.0015	293.99	1100.43	1394.42
0.8	0.0223	0.0524	60	142	1.6	0.9	7.63	0.0010	293.99	1100.49	1394.48
0.8	0.0223	0.0524	60	142	1.6	0.9	3.82	0.0005	293.99	1100.56	1394.55
0.5	0.0223	0.0524	60	142	1.6	0.9	11.45	0.0024	470.62	1762.93	2233.55
0.5	0.0223	0.0524	60	142	1.6	0.9	7.63	0.0016	470.62	1763.02	2233.64
0.5	0.0223	0.0524	60	142	1.6	0.9	3.82	0.0008	470.62	1763.12	2233.74
0.1	0.0223	0.0524	60	142	1.6	0.9	11.45	0.0120	2353.84	8821.36	11175.20
0.1	0.0223	0.0524	60	142	1.6	0.9	7.63	0.0080	2353.84	8821.84	11175.68
0.1	0.0223	0.0524	60	142	1.6	0.9	3.82	0.0040	2353.84	8822.31	11176.15

Table 8. Computational Parameters Used and Drag Coefficients Calculated at Various Radial Suction Mass Fluxes for Pt = 1.50.

R	Δz	Δx	M	N	α	β	G	$-V_o$	C_{DF}	C_{DP}	C_D
1.0	0.0405	0.0524	60	82	1.6	0.9	11.45	0.0012	93.79	209.86	303.65
1.0	0.0405	0.0524	60	82	1.6	0.9	7.63	0.0008	93.79	209.88	303.67
1.0	0.0405	0.0524	60	82	1.6	0.9	3.82	0.0004	93.79	209.90	303.69
0.8	0.0405	0.0524	60	82	1.6	0.9	11.45	0.0015	117.43	263.39	380.82
0.8	0.0405	0.0524	60	82	1.6	0.9	7.63	0.0010	117.43	263.42	380.85
0.8	0.0405	0.0524	60	82	1.6	0.9	3.82	0.0005	117.43	263.44	380.87
0.5	0.0405	0.0524	60	82	1.6	0.9	11.45	0.0024	188.18	423.13	611.31
0.5	0.0405	0.0524	60	82	1.6	0.9	7.63	0.0016	188.18	423.17	611.35
0.5	0.0425	0.0524	60	82	1.6	0.9	3.82	0.0008	188.18	423.21	611.39
0.1	0.0425	0.0524	60	82	1.6	0.9	11.45	0.0120	941.77	2120.60	3062.37
0.1	0.0425	0.0524	60	82	1.6	0.9	7.63	0.0080	941.77	2120.79	3062.56
0.1	0.0425	0.0524	60	82	1.6	0.9	3.82	0.0040	941.77	2120.99	3062.75

Table 9. Computational Parameters Used and Drag Coefficients Calculated at Various Radial Suction Mass Fluxes for Pt = 1.75.

R	Δz	Δx	M	N	α	β	G	$-V_o$	C_{DF}	C_{DP}	C_D
1.0	0.0560	0.0524	60	62	1.6	0.9	11.45	0.0012	56.92	98.81	155.73
1.0	0.0560	0.0524	60	62	1.6	0.9	7.63	0.0008	56.92	98.82	155.74
1.0	0.0560	0.0524	60	62	1.6	0.9	3.82	0.0004	56.92	98.84	155.76
0.8	0.0560	0.0524	60	62	1.6	0.9	11.45	0.0015	71.54	125.11	196.65
0.8	0.0560	0.0524	60	62	1.6	0.9	7.63	0.0010	71.54	125.13	196.67
0.8	0.0560	0.0524	60	62	1.6	0.9	3.82	0.0005	71.54	125.15	196.69
0.5	0.0560	0.0524	60	62	1.6	0.9	11.45	0.0024	115.00	202.35	317.35
0.5	0.0560	0.0524	60	62	1.6	0.9	7.63	0.0016	115.00	202.38	317.38
0.5	0.0560	0.0524	60	62	1.6	0.9	3.82	0.0008	115.00	202.40	317.40
0.1	0.0560	0.0524	60	62	1.6	0.9	11.45	0.0120	576.37	1017.39	1593.76
0.1	0.0560	0.0524	60	62	1.6	0.9	7.63	0.0080	576.37	1017.51	1593.88
0.1	0.0560	0.0524	60	62	1.6	0.9	3.82	0.0040	576.37	1017.63	1594.00

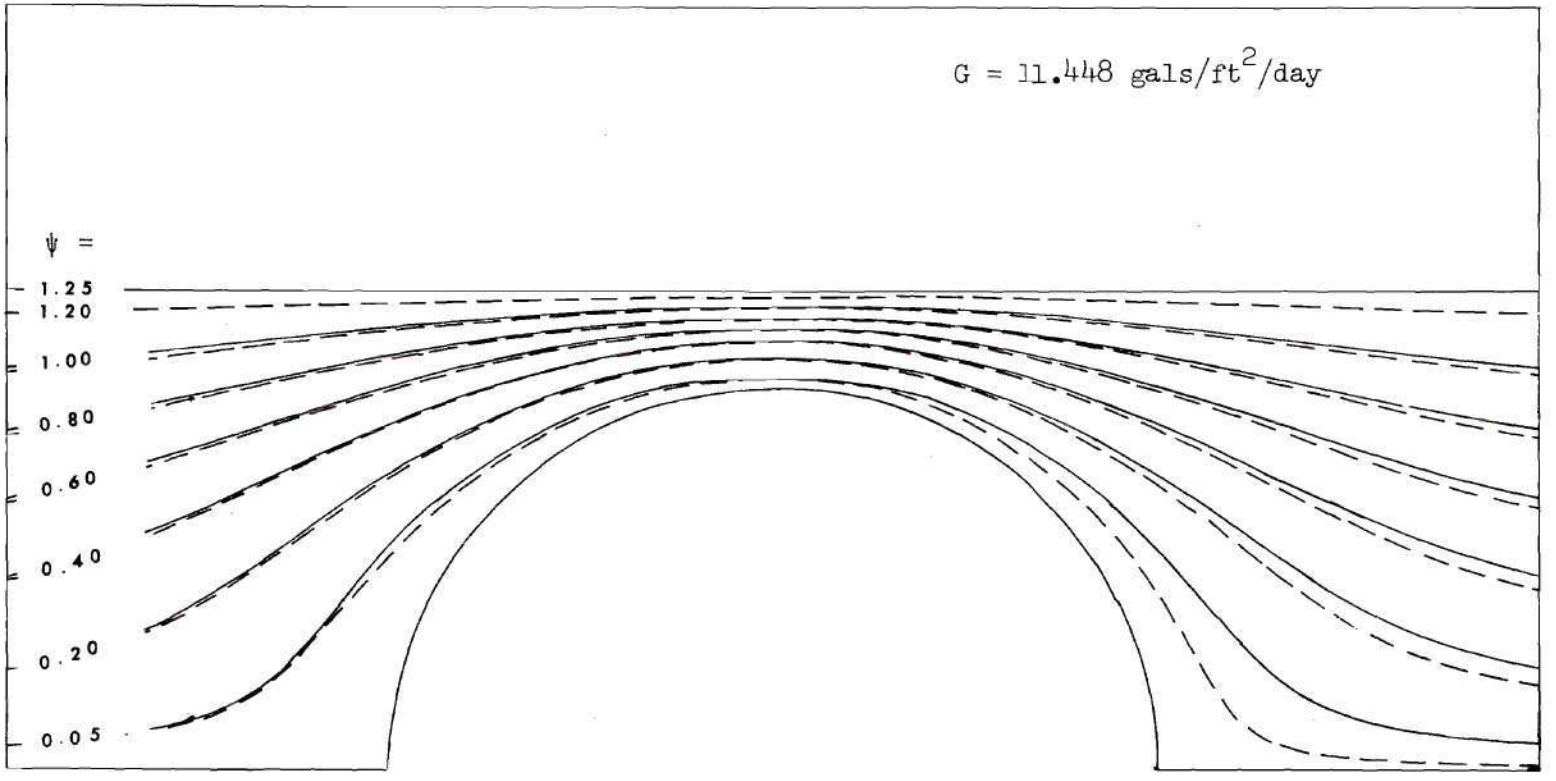

Figure 29. Contours of Stream Function with (---) and Without (-) Suction (R = 0.1; Pt = 1.25).

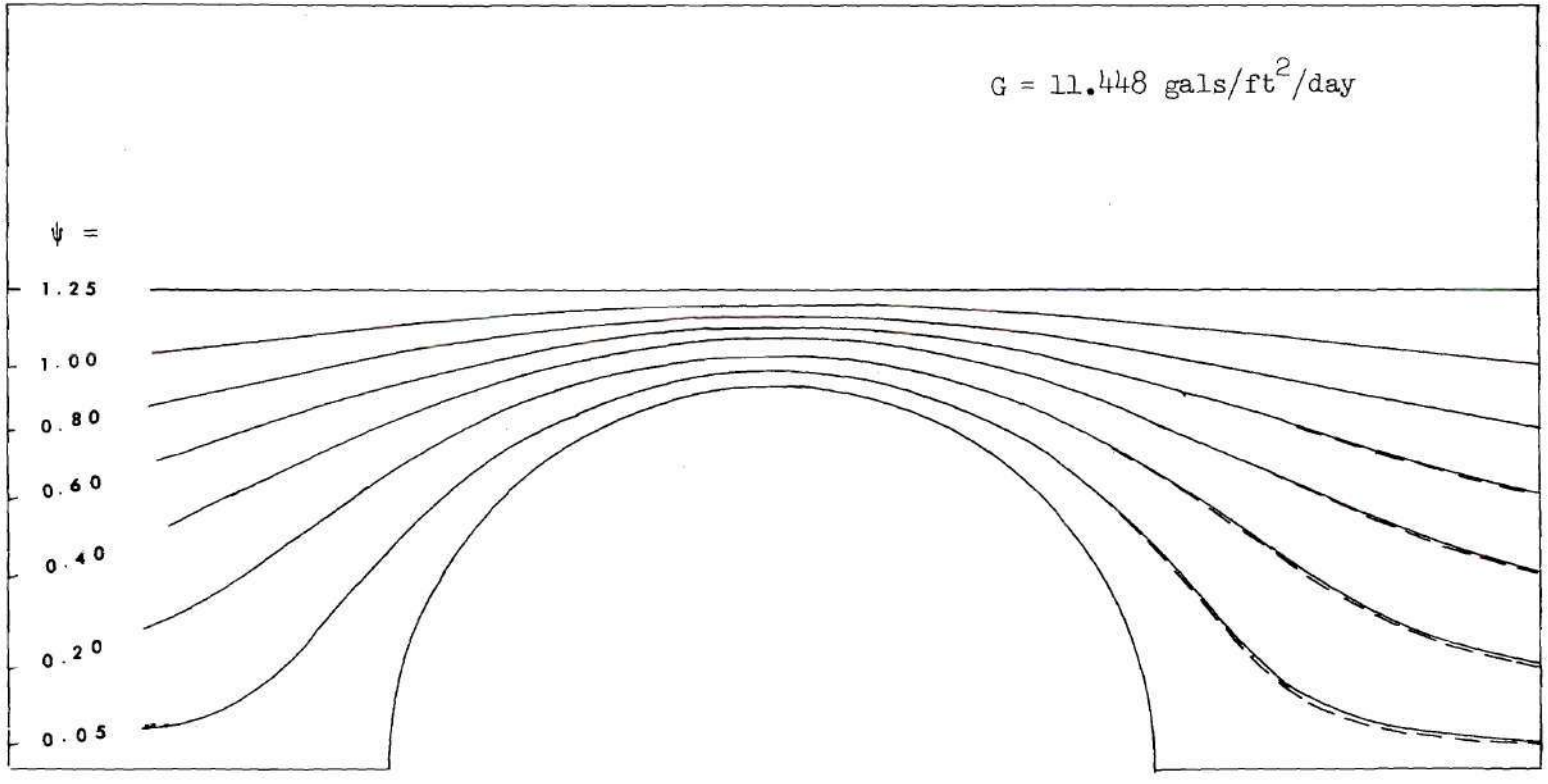

Figure 30. Contours of Stream Function with (---) and without (-) Suction (R = 1.0; Pt = 1.25).

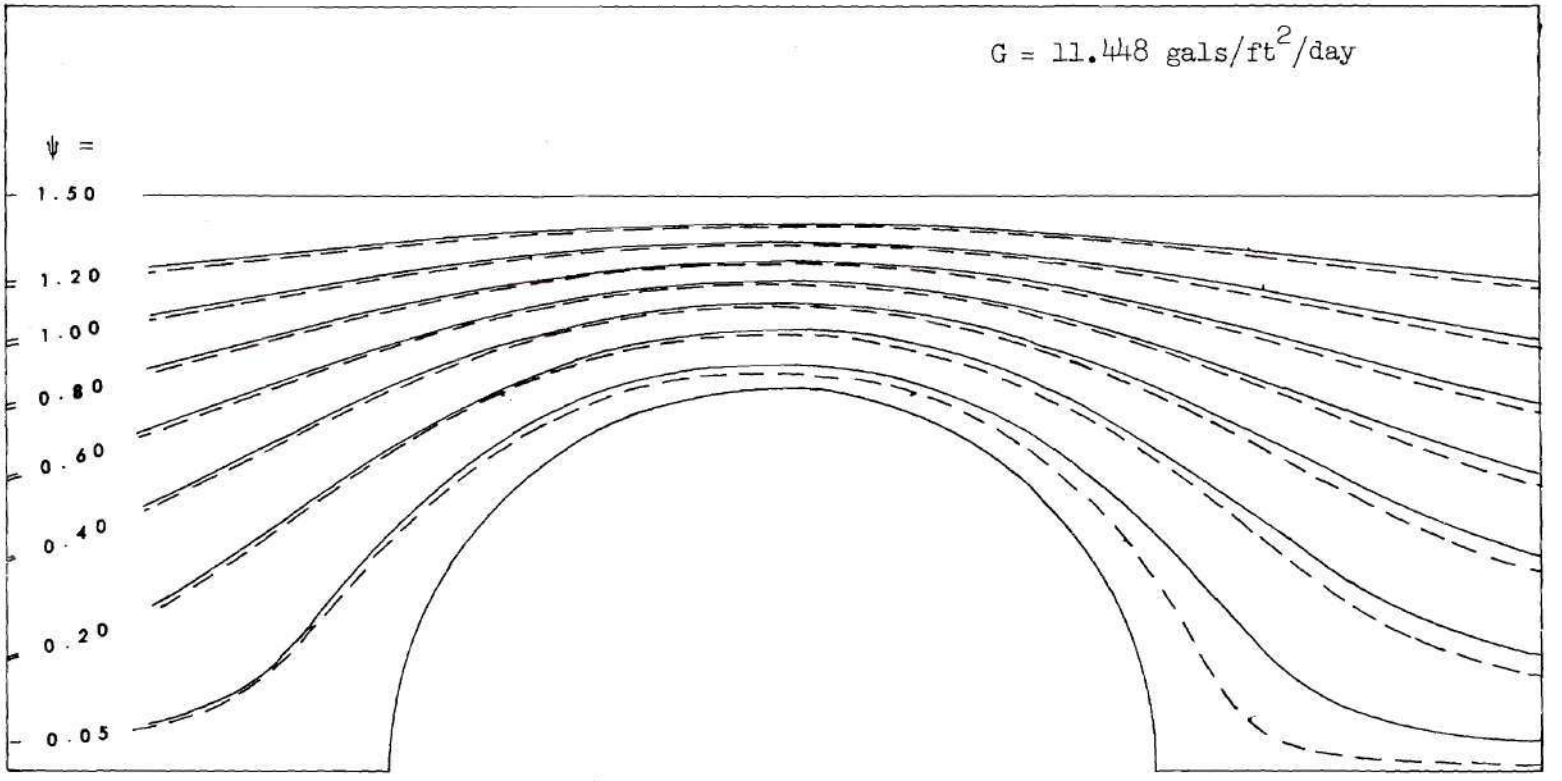

Figure 31. Contours of Stream Function With (---) and Without (-) Suction (R = 0.1; Pt = 1.50).

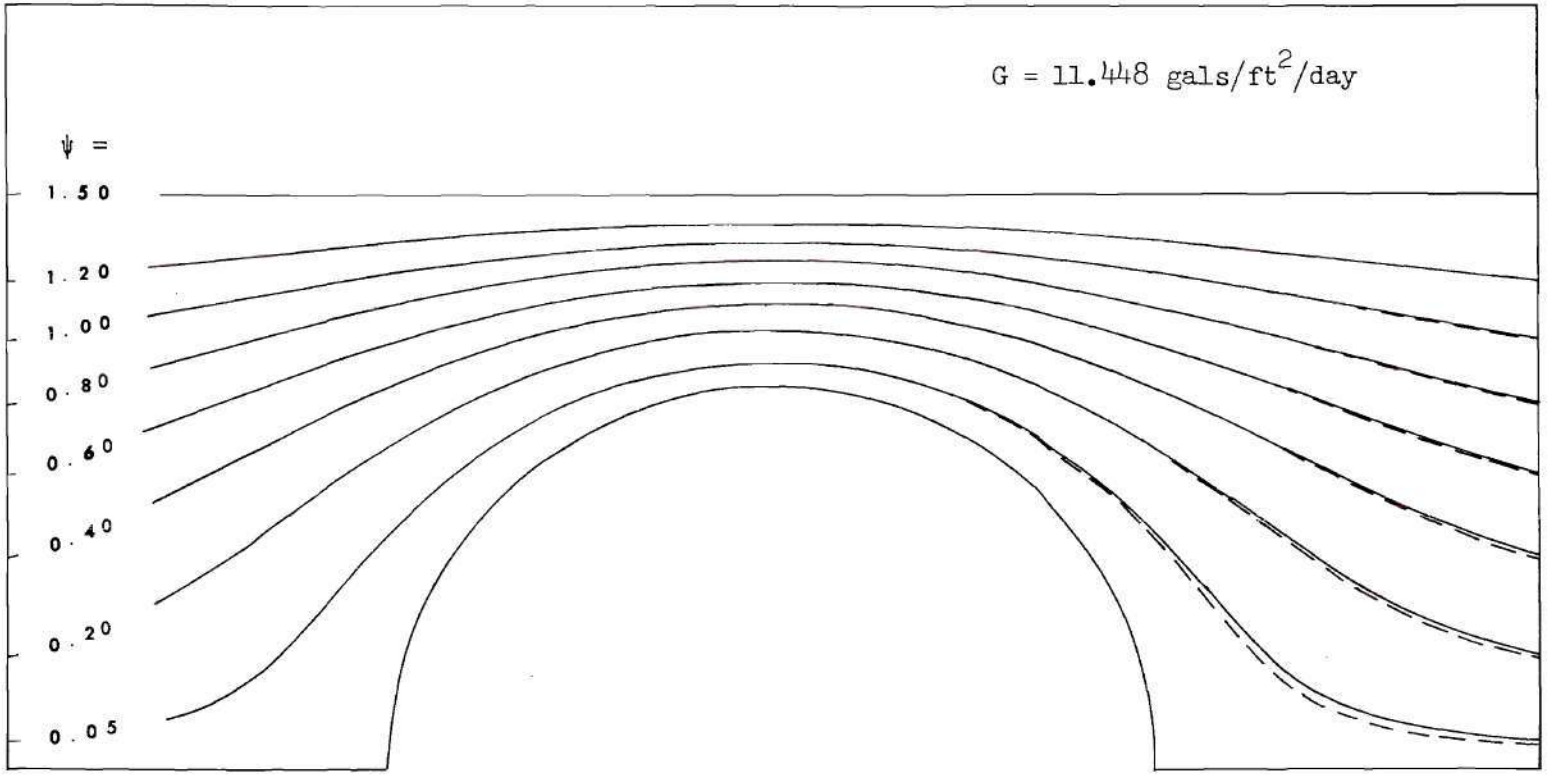

Figure 32. Contours of Stream Function With (---) and Without(-) Suction (R = 0.5; Pt = 1.50).

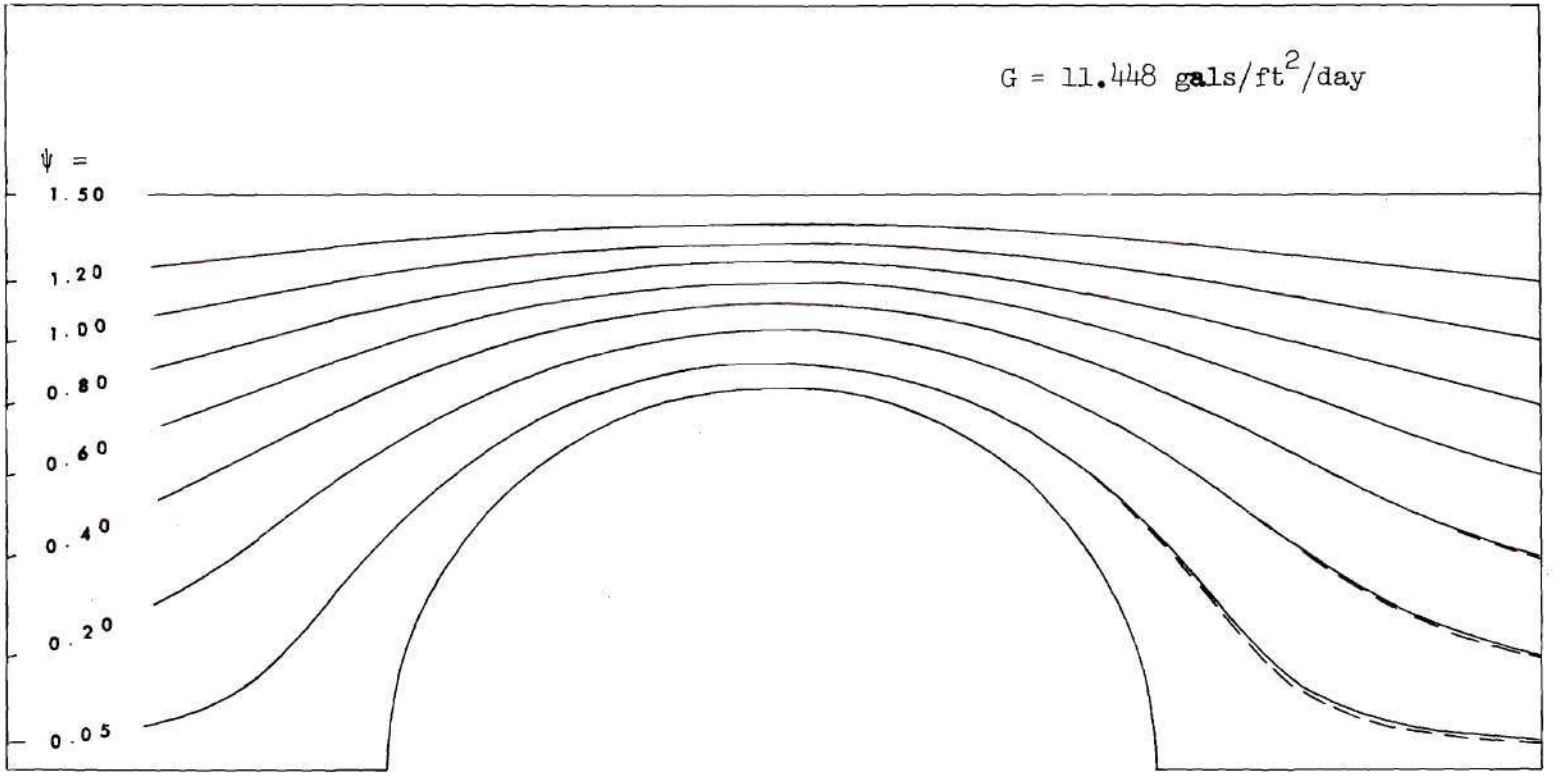

Figure 33. Contours of Stream Function With (---) and Without (-) Suction (R = 1.0; Pt = 1.50).

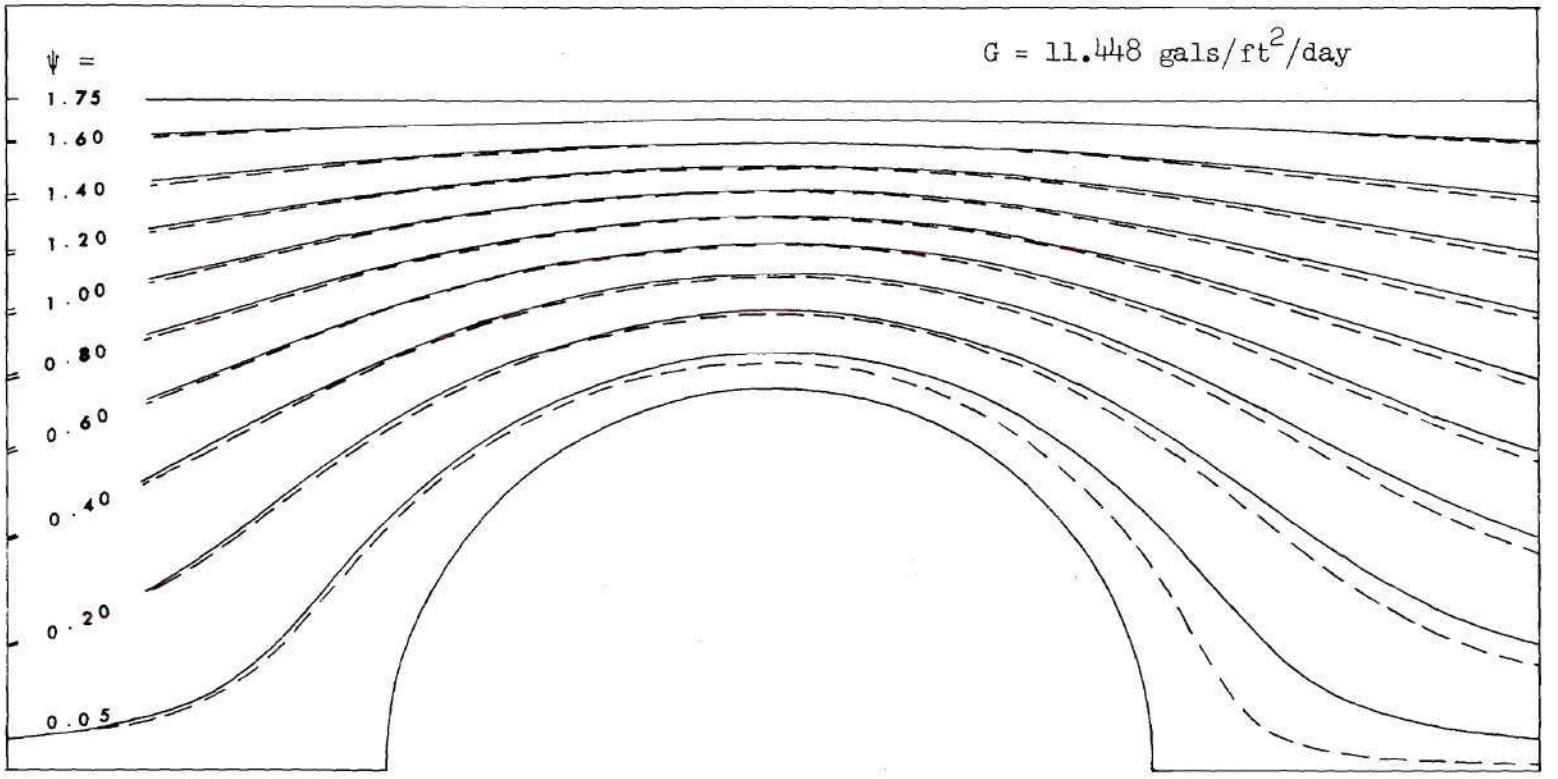

Figure 34. Contours of Stream Function With (---) and Without (-) Suction (R = 0.1; Pt = 1.75).

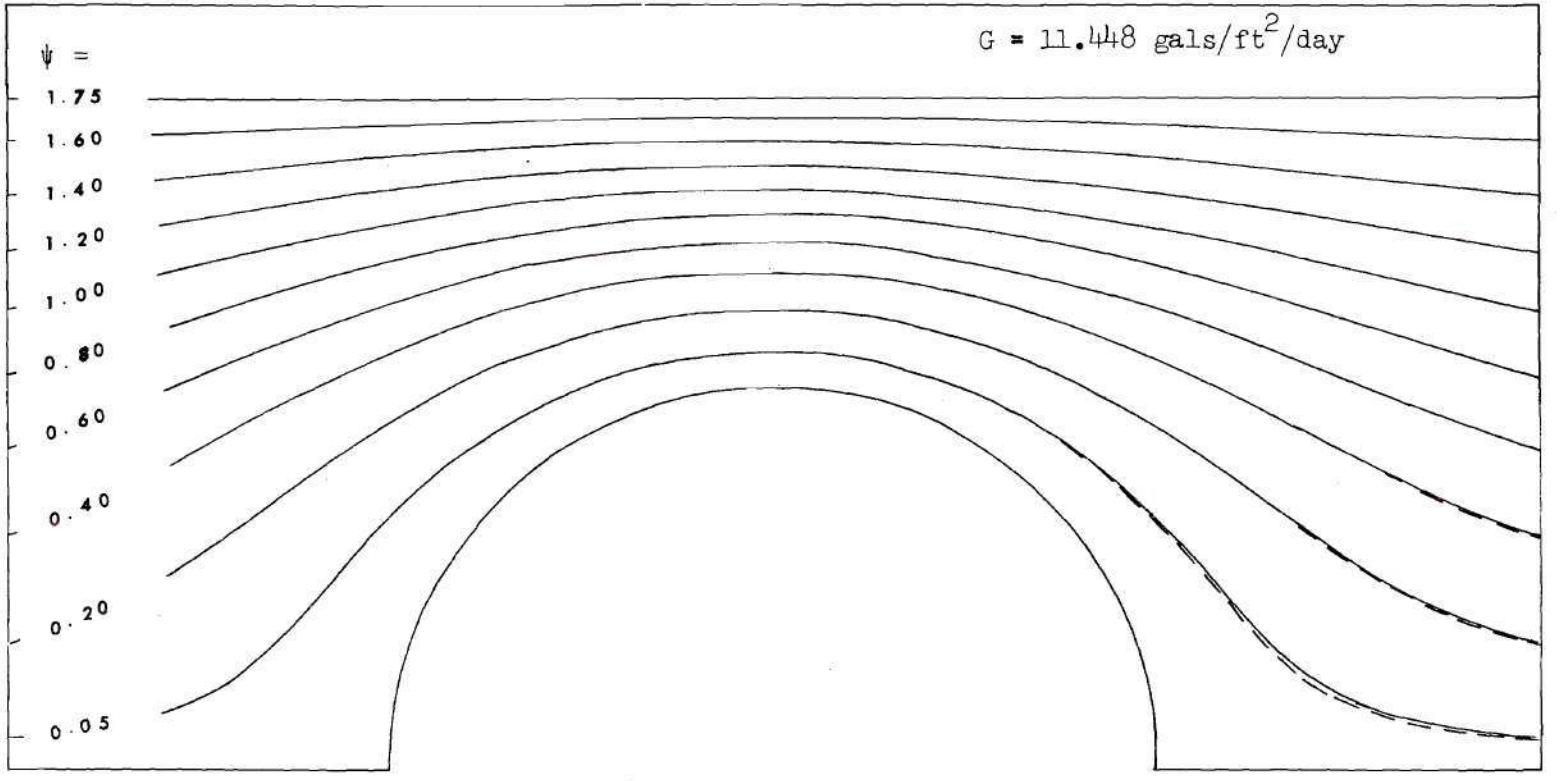

Figure 35. Contours of Stream Function With (---) and Without (-) Suction (R = 1.0; Pt = 1.75).

Table 10. Effect of Radial Suction Flux on Drag Coefficient-Pure Fluid (R = 1.0).

Pt	$-V_o$	G	C_{DF}	C_{DP}	C_D
1.75	0.0	0.0	56.92	98.85	155.77
1.75	0.0012	11.45	56.92	98.81	155.73
1.75	0.004	38.2	56.91	98.71	155.62
1.75	0.008	76.3	56.90	98.56	155.46
1.75	0.012	114.5	56.89	98.42	155.31
1.50	0.0	0.0	93.79	209.92	303.71
1.50	0.0012	11.45	93.79	209.86	303.65
1.50	0.004	38.2	93.79	209.71	303.50
1.50	0.008	76.3	93.78	209.50	303.28
1.50	0.012	114.5	93.78	209.29	303.07

Table 11. Effect of Radial Suction Flux on Surface Pressure Variation-Pure Fluid (R = 1.0).

Pt	$-V_o$	G	C_P				
			0°	45°	90°	135°	180°
1.75	0.0	0.0	11.043	7.680	-39.444	-93.280	-97.108
1.75	0.0012	11.45	11.049	7.684	-39.429	-93.234	-97.052
1.75	0.012	114.5	11.097	7.716	-39.286	-92.816	-96.548
1.50	0.0	0.0	12.209	8.464	-95.982	-208.500	-212.186
1.50	0.0012	11.45	12.217	8.468	-95.973	-208.433	-212.106
1.50	0.012	114.5	12.285	8.502	-95.889	-207.831	-211.386

can still be seen. The pressure in the front region of the cylinder is higher and then drops more slowly than it does in the case of no surface flux.

The surface vorticity distributions at a Reynolds number of 1.0 and opening ratios of 1.50 and 1.75 are listed in Table 12. The effect of the radial suction flux on the surface vorticity is smaller than that on the surface pressure. This accounts for the slight change in the friction drag coefficient.

Binary Solution

The local Nusselt numbers as functions of angular position around the surface at Reynolds numbers of 0.1 to 1.0 are shown in Figures 36-41. The local Nusselt number increases slowly with θ, reaches its maximum value at the minimum clearance and then drops sharply.

Overall Nusselt numbers are calculated by integrating the local Nusselt numbers along the stream and are shown in Figure 42. The linear relations between the value of $Nu_{overall}/Sc^{1/3}$ and $R^{1/3}$ are given for the different radial suction fluxes and opening ratios by

$$Nu_{overall}/Sc^{1/3} = 1.53\ R^{1/3} + k_1 \qquad (4\text{-}1)$$

for Pt = 1.75 and

$$Nu_{overall}/Sc^{1/3} = 1.68\ R^{1/3} + k_2 \qquad (4\text{-}2)$$

for Pt = 1.50, where k_1 = 0.57, 0.07, 0.06, and 0.04 and k_2=0.59, 0.11, 0.10, and 0.08 when the mass flux = 114.5, 11.45, 7.63, and 3.82 gfd respectively.

Table 12. Effect of Radial Suction Flux on Surface Vorticity Variation-Pure Fluid (R = 1.0).

Pt	$-V_o$	G	ζ						
			0°	30°	60°	90°	120°	150°	180°
1.75	0.0	0.0	0.0	2.503	7.219	11.665	7.751	2.609	0.0
1.75	0.0012	11.45	0.0	2.505	7.221	11.665	7.749	2.608	0.0
1.75	0.012	114.5	0.0	2.517	7.235	11.661	7.728	2.594	0.0
1.50	0.0	0.0	0.0	3.218	11.563	21.211	11.981	3.234	0.0
1.50	0.0012	11.45	0.0	3.220	11.567	21.211	11.977	3.232	0.0
1.50	0.012	114.5	0.0	3.241	11.602	21.209	11.937	3.211	0.0

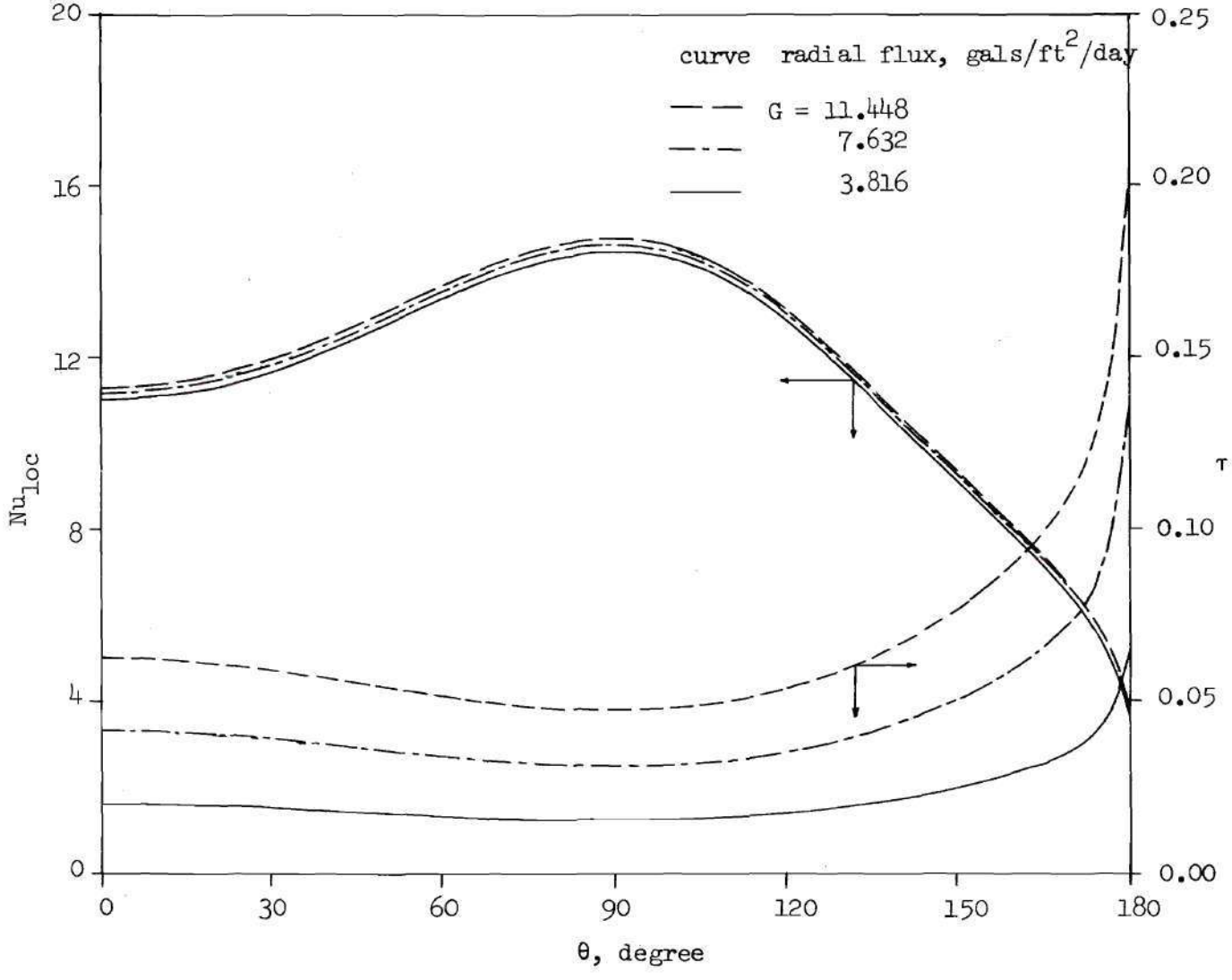

Figure 36. Distribution of Local Nusselt Number and Concentration Polarization Around the Cylindrical Surface (R = 0.5; Pt = 1.50).

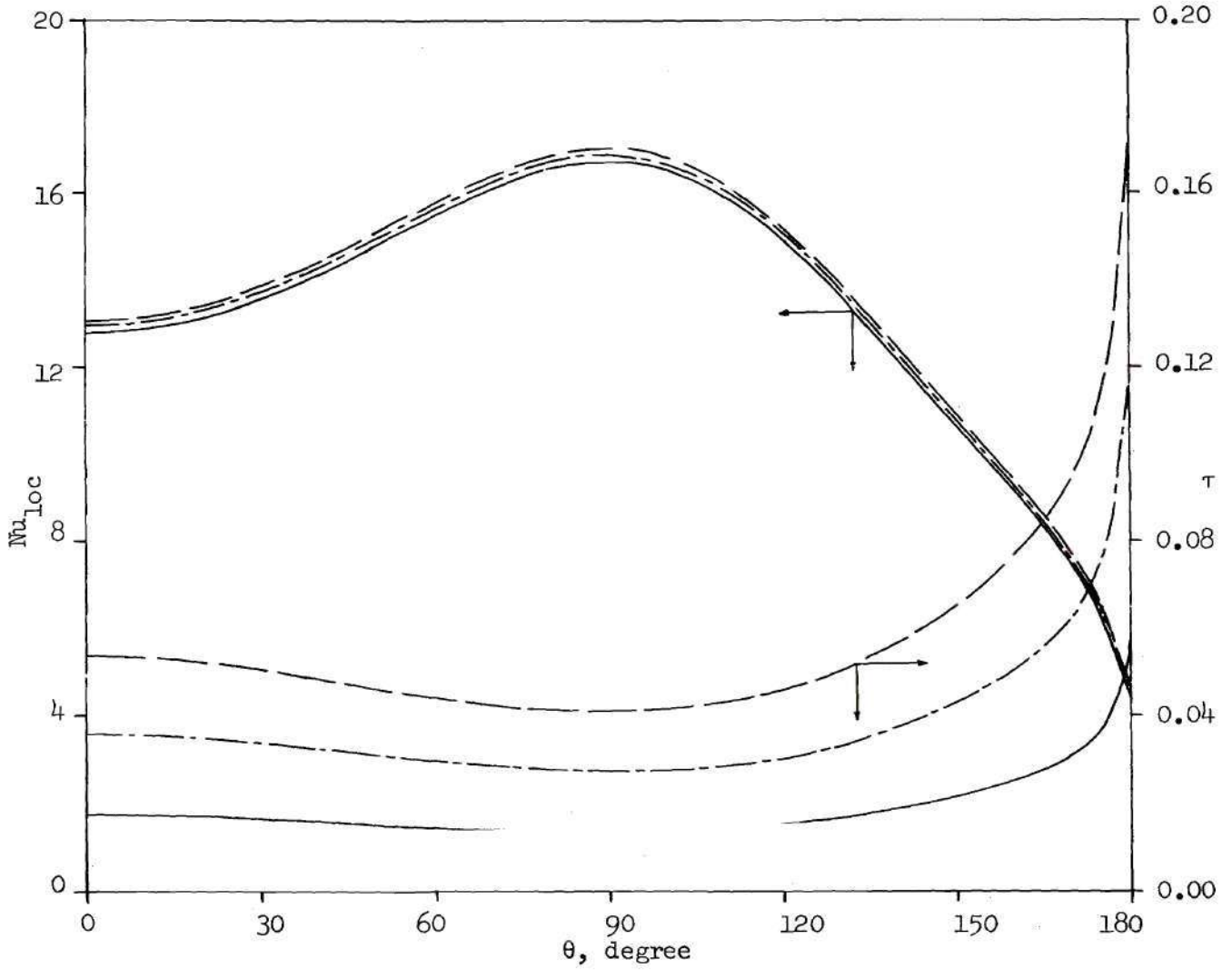

Figure 37. Distribution of Local Nusselt Number and Concentration Polarization Around the Cylindrical Surface (R = 0.8; Pt = 1.50). For legend see Figure 36.

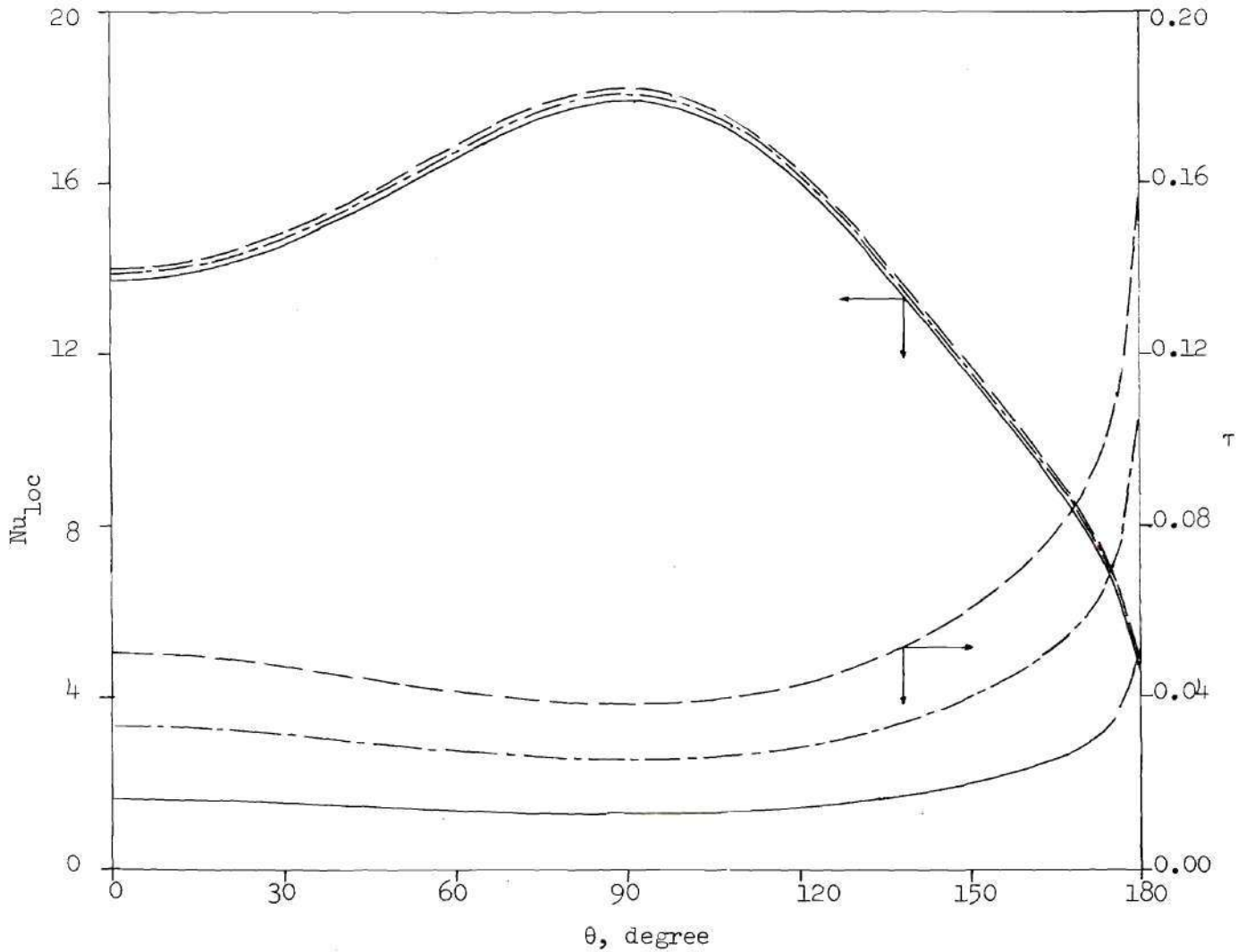

Figure 38. Distribution of Local Nusselt Number and Concentration Polarization Around the Cylindrical Surface (R = 1.0; Pt = 1.50). For legend see Figure 36.

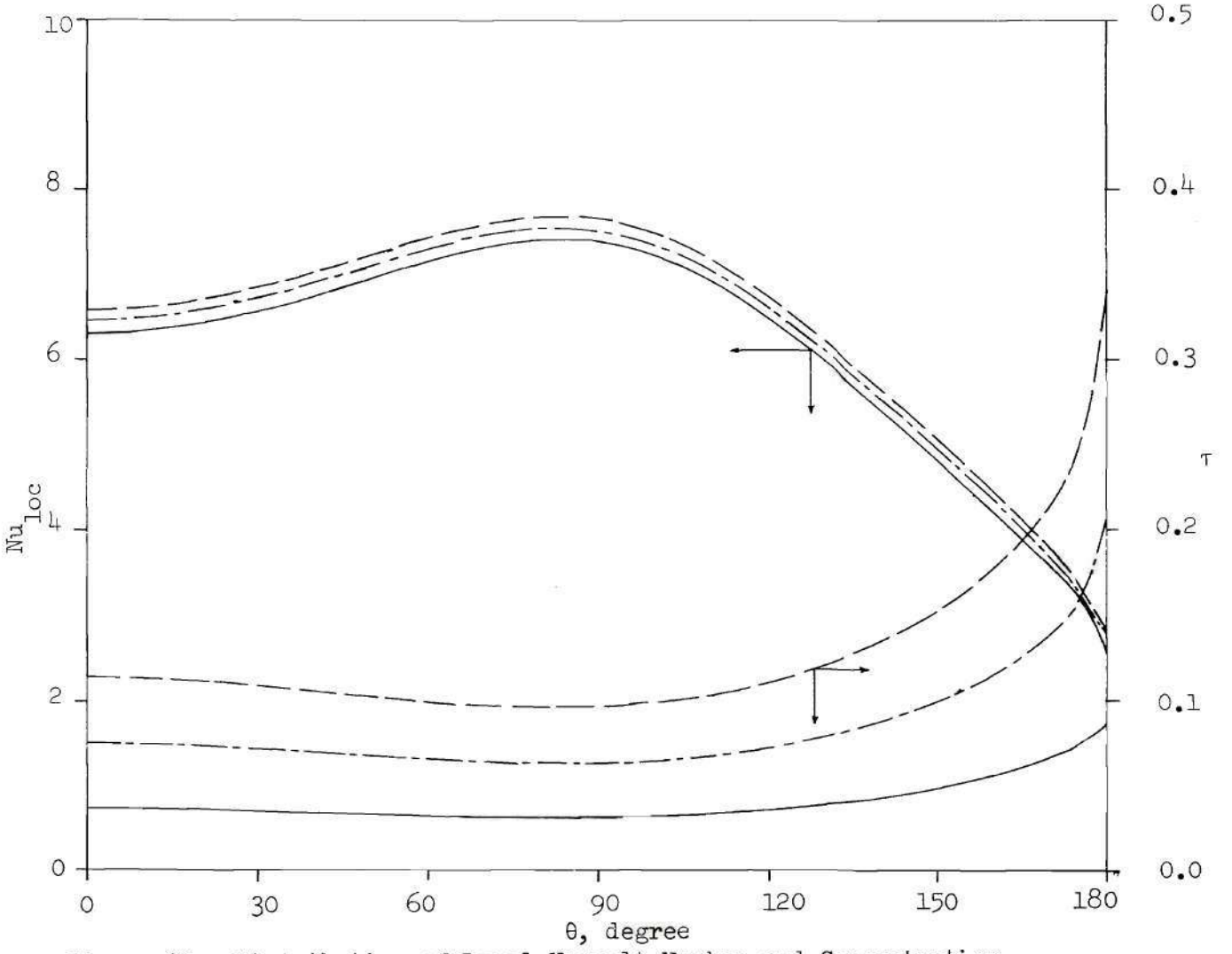

Figure 39. Distribution of Local Nusselt Number and Concentration Polarization Around the Cylindrical Surface (R = 0.1; Pt = 1.75). For legend see Figure 36.

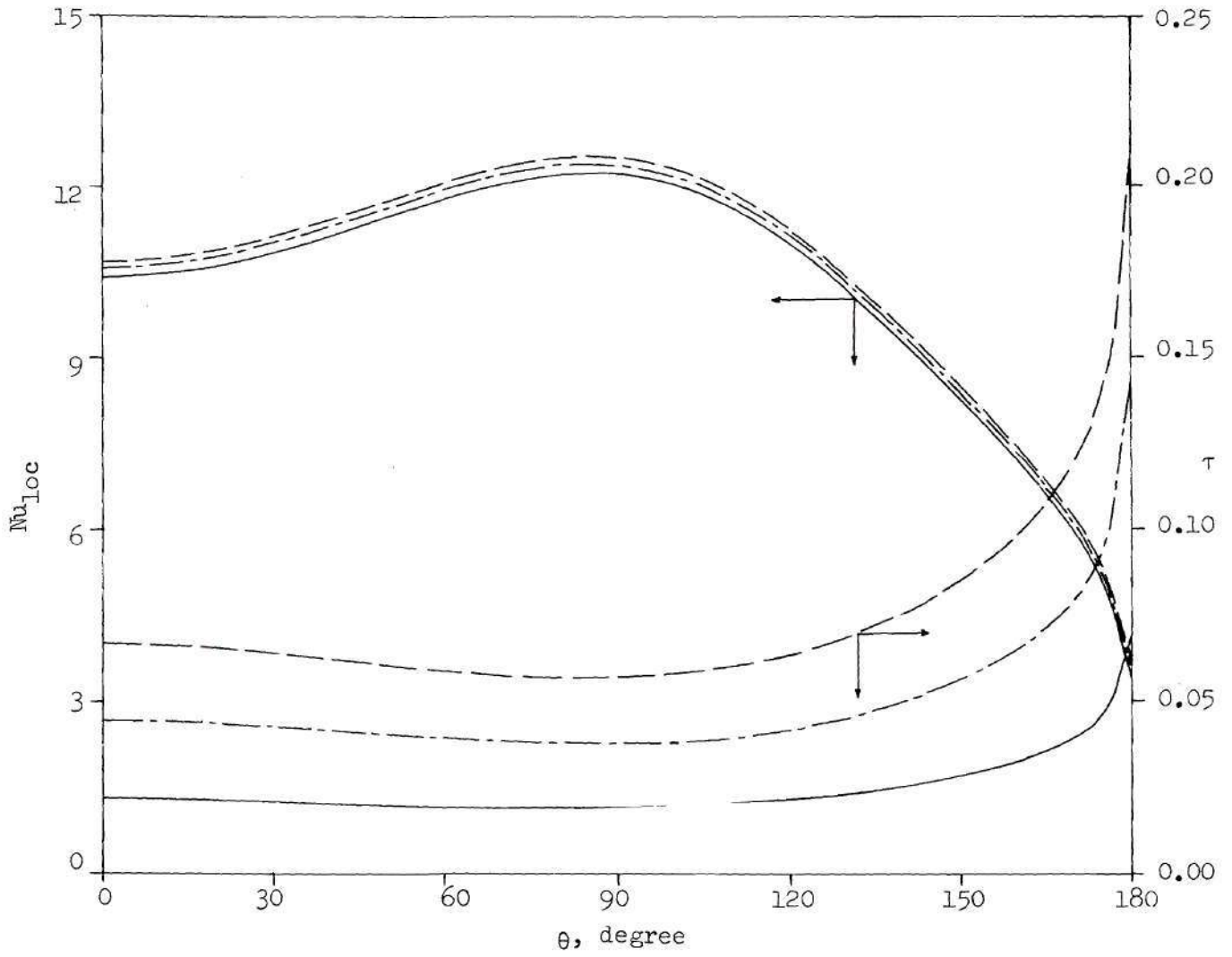

Figure 40. Distribution of Local Nusselt Number and Concentration Polarization Around the Cylindrical Surface (R = 0.5; Pt = 1.75). For legend see Figure 36.

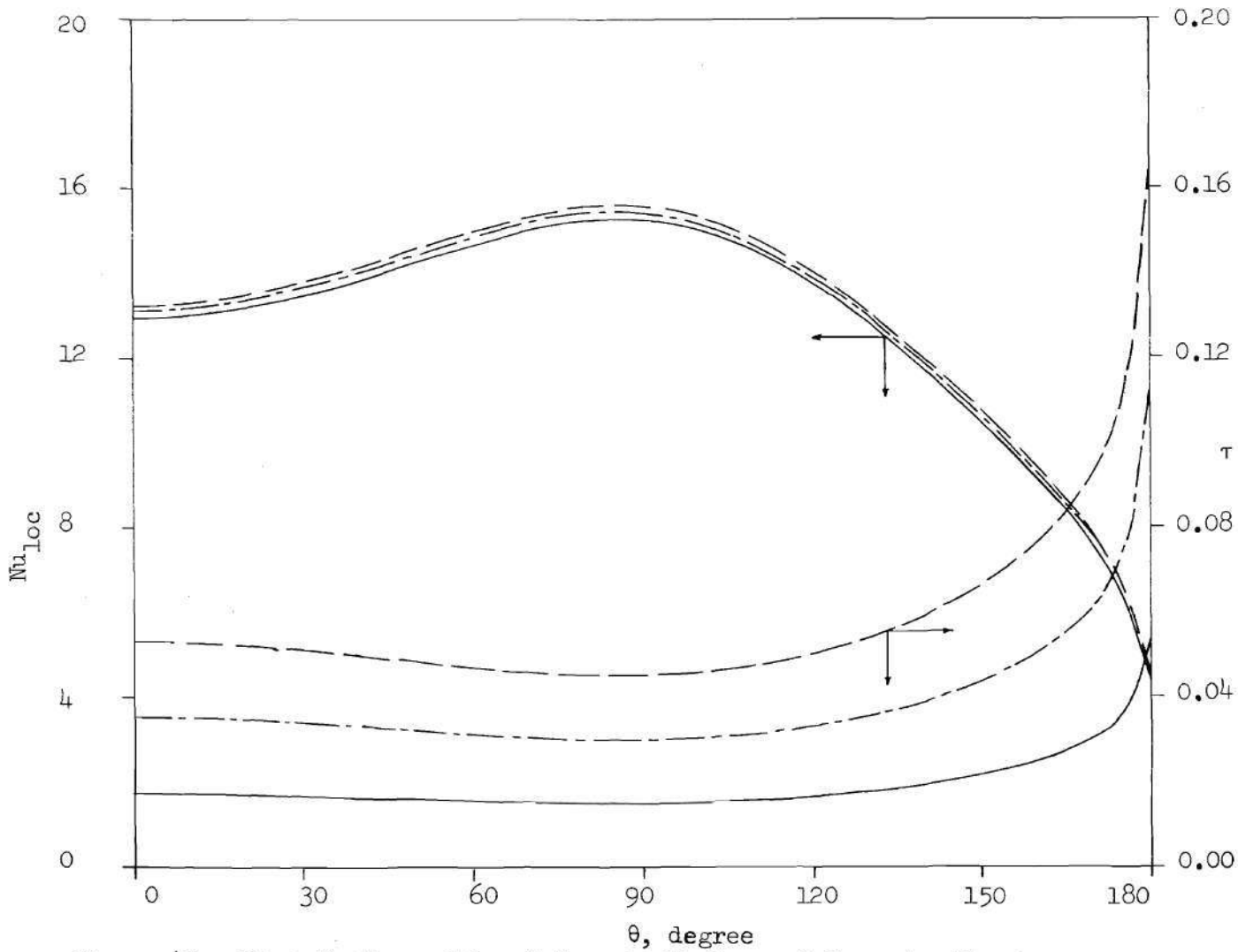

Figure 41. Distribution of Local Nusselt Number and Concentration Polarization Around the Cylindrical Surface (R = 1.0; Pt = 1.75). For legend see Figure 36.

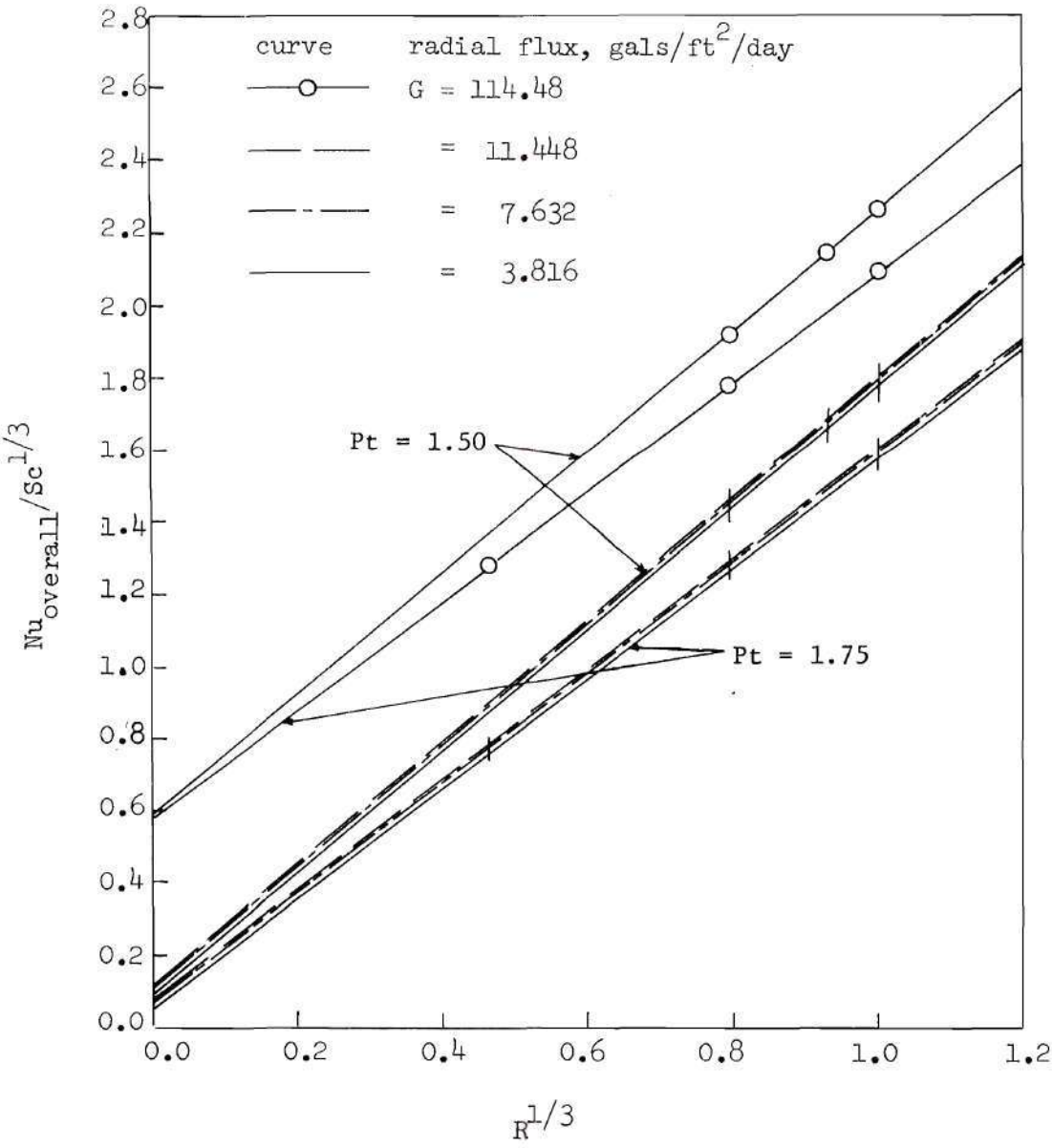

Figure 42. Nusselt Type Mass Transfer Representation.

As seen from Figure 42, the overall Nusselt number increases as the opening ratio becomes smaller.

Since the mass transfer has not been considered in previous studies on multiple cylinders, no data are available for comparison. However, by using the analogy between heat and mass transfer, the heat transfer data of Bergline[20] at Reynolds numbers of 2 to 40 can be used for comparison with the results of this study. The overall heat transfer coefficient (Nu_h) in a 10-row bank of in-line tubes can be expressed as[20]

$$Nu_h = 1.2\ R^{1/3}\ Pr^{1/3} \quad (Pt = 1.50)$$

where Pr is the Prandtl number. In the Delaware experiment the outermost tubes of the tube banks were half-way imbedded on the side walls to minimize the side wall effect. It is also known that the heat-transfer coefficient is 50% greater for a single row than for 10 rows; therefore $Nu_h = 1.8\ R^{1/3}\ Pr^{1/3}$ for a single row of tubes with Pt = 1.50. Using the analogy between heat and mass transfer, the above heat transfer equation can be written for mass transfer as

$$Nu_{overall} = 1.8\ R^{1/3}\ Sc^{1/3} \quad (Pt = 1.50)$$

The difference between this expression and Equation (4-2) can be explained by the different ranges of the Reynolds numbers and the different boundary conditions - constant wall temperature instead of constant heat flux.

Since the overall Nusselt number in mass transfer is a function of the suction mass flux, the coefficient at high mass transfer rates

should be calculated by multiplying the one at low mass transfer rates by a correction factor. In order to find the coefficient at zero mass flux through extrapolation, the overall Nusselt number is plotted versus the radial suction mass flux in Figures 43 and 44. Based on the extrapolations for Pt = 1.50 and 1.75, the correction factor is given as a linear function of the radial suction mass flux in Figures 43 and 44 for low mass-transfer rates and in Figure 45 for high mass-transfer rates.

The concentration buildup on the surface of the cylinder can be expressed by a dimensionless term (concentration polarization) defined by

$$\tau = \frac{\rho_{Ao} - \rho_{A\infty}}{\rho_{A\infty}}$$

The concentration polarization as a function of the angular position around the surface at Reynolds numbers of 0.1 to 1.0 is shown in Figures 36-41.

The concentration polarization decreases with increase in Reynolds number at constant mass flux. At each Reynolds number studied, the concentration polarization increases as the opening ratio or the suction mass flux becomes larger. Also note the sharp rise in the concentration polarization at the very rear portion of the cylinder, especially when the radial suction mass flux is large.

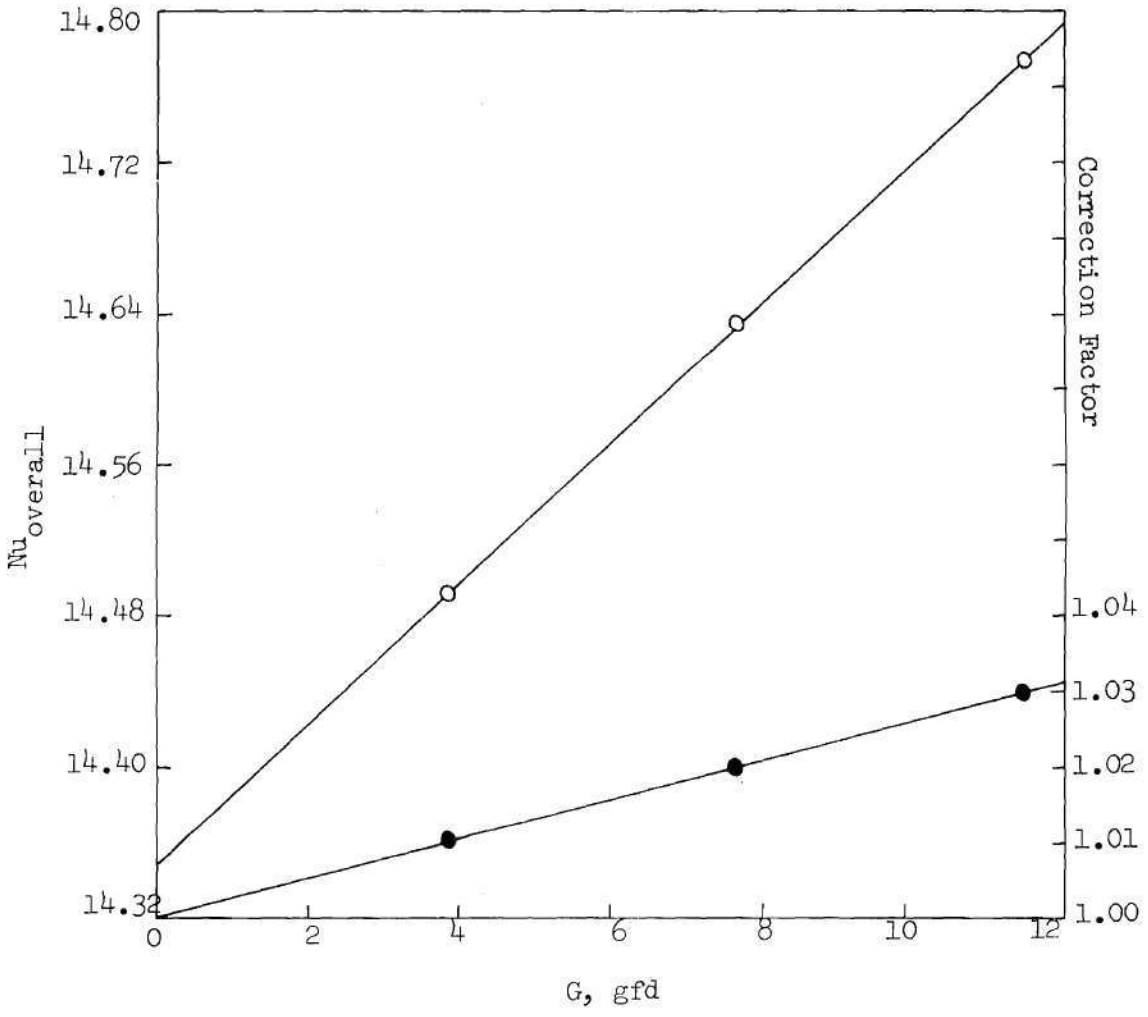

Figure 43. Variation of Overall Nusselt Number (o) and Correction Factor (●) with Radial Suction Mass Flux (R = 1.0; Pt = 1.50).

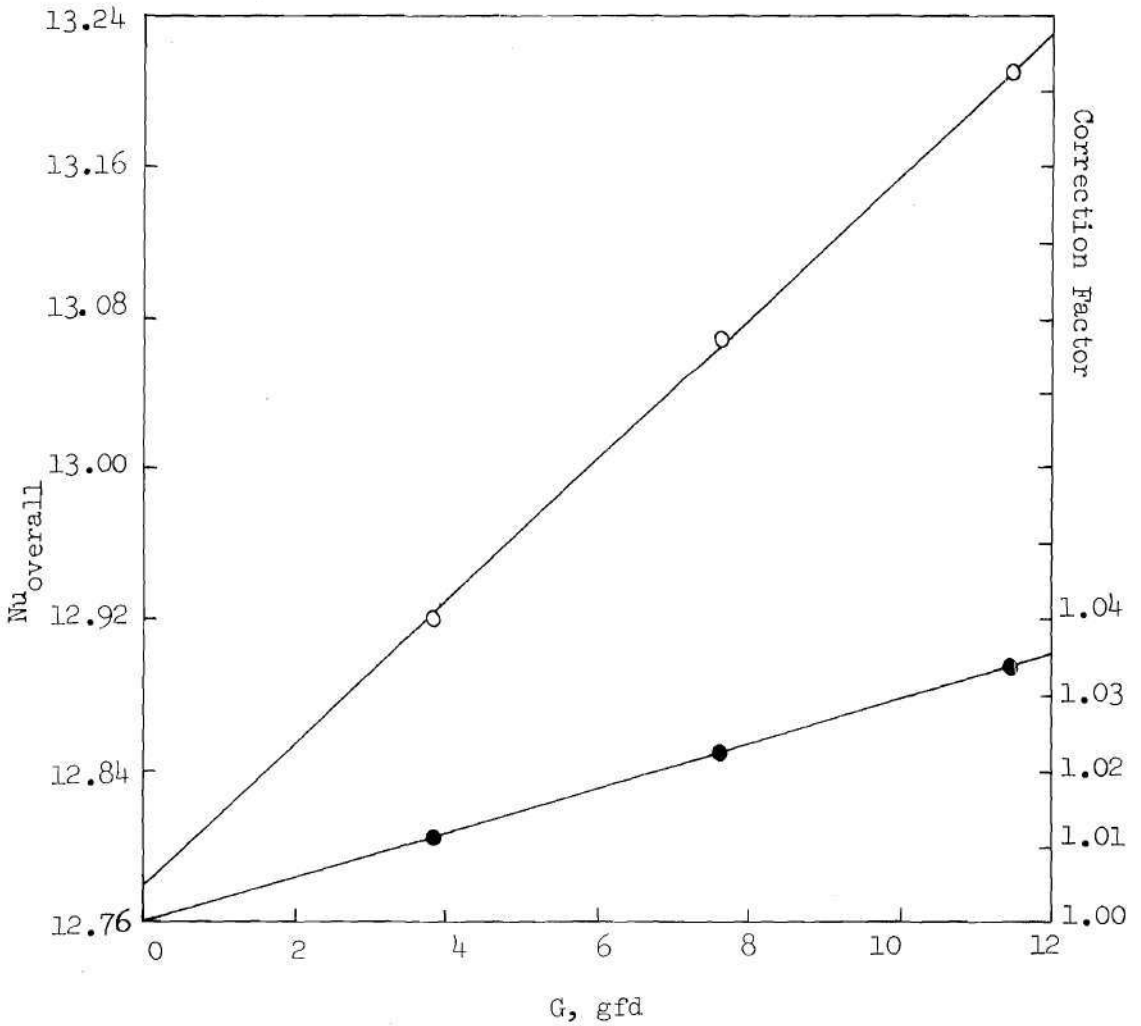

Figure 44. Variation of Overall Nusselt Number (o) and Correction Factor (●) with Radial Suction Mass Flux (R = 1.0; **Pt** = 1.75).

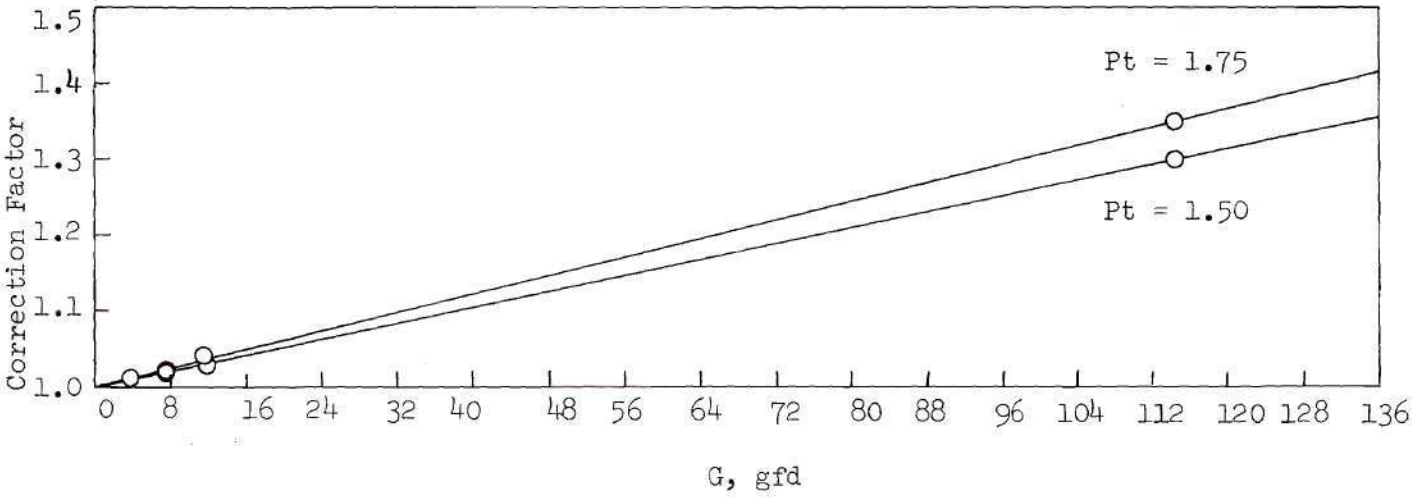

Figure 45. Variation of Correction Factor with Radial Suction Mass Flux.

CHAPTER V

CONCLUSIONS AND RECOMMENDATIONS

Viscous, incompressible flow at low Reynolds numbers past an infinite row of cylinders provides a severe test of numerical methods in dealing with this curved boundary problem. However, if the step sizes and the relaxation factors are chosen properly, computation time can be shortened and the flow characteristics can be determined accurately. The surface-interaction model and other boundary conditions proposed are considered to be adequate. The drag coefficient is large at low Reynolds numbers and the position of the outer boundary has little effect on the results of various flow properties. The opening ratio was found to be a major factor affecting many flow characteristics.

With mass transfer, the symmetrical flow pattern is reshaped into a distinct asymmetry downstream because of the effect of the suction mass flux at the cylinder wall. The local Nusselt number increases slowly from the front stagnation point and reaches its maximum at the minimum clearance between the cylinders and then drops sharply. Concentration polarization proceeds in the opposite direction to that of the local Nusselt number. The overall Nusselt number can be expressed as

$$Nu_{overall}/Sc^{1/3} = 1.53\ R^{1/3} + k_1 \quad (Pt = 1.75)$$

and

$$Nu_{overall}/Sc^{1/3} = 1.68\ R^{1/3} + k_2 \qquad (Pt = 1.50)$$

where k_1 and k_2 are determined by the magnitude of the radial suction mass flux.

Over the entire Reynolds number range studied, characteristic flow quantities such as the surface pressure and vorticity distributions and mass transfer coefficient agree well with available experimental data and numerical solutions.

Recommendations

Since the determination of the fluid flow and mass transport for higher Reynolds numbers would be of definite practical interest, the present method should be extended to higher Reynolds numbers when a computer with larger memory storage capacity and higher speed becomes available.

Another obvious extension of this study would be the case of flow past multiple rows of tubes arranged in various configurations such as staggered square, equilateral triangle and in-line square. Also the viscous incompressible flow past a single row or multiple rows of submerged bodies of other shapes such as spheres can be treated in a way similar to the present study.

This study can also be extended to include the case of flow past a row of cylinders with radial injection at the walls.

APPENDICES

APPENDIX A

COMPUTATIONAL ALGORITHM FOR THE METHOD OF THOMAS

Consider the system of equations

$$B_1 V_1 + C_1 V_2 = D_1$$

$$A_I V_{I-1} + B_I V_I + C_I V_{I+1} = D_I \quad (2 \leq I \leq N-3)$$

$$A_{N-2} V_{N-3} + B_{N-2} V_{N-2} + C_{N-2} V_{N-1} = D_{N-2}$$

$$E'_{N-1} V_{N-3} + A'_{N-1} V_{N-2} + B'_{N-1} V_{N-1} = D'_{N-1}$$

Eliminating the term E', the last two equations can be combined to give

$$A_{N-1} V_{N-2} + B_{N-1} V_{N-1} = D_{N-1}$$

where

$$A_{N-1} = A'_{N-1} A_{N-2} - E'_{N-1} B_{N-2}$$

$$B_{N-1} = B'_{N-1} A_{N-2} - E'_{N-1} C_{N-2}$$

$$D_{N-1} = D'_{N-1} A_{N-2} - E'_{N-1} D_{N-2}$$

The method of Thomas can be applied to solve the new system of simultaneous equations for which the matrix of coefficients A, B and C alone is called a tridiagonal matrix.

The complete algorithm for the solution of the tridiagonal system is

$$V_{N-1} = Y_{N-1}$$

$$V_I = Y_I - C_I V_{I+1}/\beta_I \quad (I = N-2, N-3, \ldots, 1)$$

where the β's and Y's are determined from the recursion formulas

$$\beta_1 = B_1$$

$$Y_1 = D_1/\beta_1$$

$$\beta_I = B_I - A_I C_{I-1}/\beta_{I-1}$$

$$Y_I = (D_I - A_I Y_{I-1})/\beta_I \quad (I = 2, 3, 4, \ldots, N-1)$$

APPENDIX B

CALCULATION OF RADIAL MASS FLUX

In order to calculate the radial mass flux (G), the general equation is given as follows:

$$G = V_o \chi \frac{\nu R}{2a}$$

where V_o is the radial surface velocity, ν is the kinematic viscosity of salt-water solution at $25^{\circ}C$, R is Reynolds number and a is the radius of the cylinder. A sample calculation is made by letting

$$V_o = 0.0012$$

$$\nu = 0.009 \text{ cm}^2/\text{sec}$$

$$R = 1.0$$

$$2a = 0.02 \text{ cm}$$

then

$$G = 0.0012 \chi \frac{0.009 \chi 1.0}{0.02} \text{ cm/sec}$$

or

$$= 11.448 \text{ gal/ft}^2/\text{day (gfd)}$$

The radial surface velocities at various Reynolds numbers and suction mass fluxes are shown in the following table:

Suction Mass Flux G (gfd)	Reynolds Number R	Radial Velocity $-V_o$
11.448	1.0	0.0012
11.448	0.8	0.0015
11.448	0.5	0.0024
11.448	0.1	0.0120
7.632	1.0	0.0008
7.632	0.8	0.0010
7.632	0.5	0.0016
7.632	0.1	0.0080
3.816	1.0	0.0004
3.816	0.8	0.0005
3.816	0.5	0.0008
3.816	0.1	0.0040

APPENDIX C

COMPUTER PROGRAMS

The computer programs are written in Fortran V language for a Univac-1108 electronic digital computer. According to the function of the programs, they are divided into three parts:

Part I - Solving the Navier Stokes equation for the important flow parameters.

Part II - Calculating the angular and radial velocity from the stream functions.

Part III - Solving the diffusion equation for the important mass transfer parameters.

In each part, the computer programs are preceded by the computer block diagrams to explain the functions of the subroutines and their relations with the main programs and other subroutines. Following are the definitions of the important variables appearing in the programs:

Program Symbol	Definition
Part I	
A, B	Matrices giving the fractional intercepts in the angular and radial directions.
ALPHA, BETA	Relaxation factors, α and β
DX, DZ	Step sizes in the angular and radial directions, Δx and Δz.

Program Symbol	Definition
EPSMAX, EPVMAX	Convergence conditions, 10^{-3} and 10^{-4}.
I, J	Grid-point subscripts, i and j.
IMAX, IMIN	Vectors such that IMAX(J) and IMIN(J) contain the column subscript I of the right-most and left-most grid points in row J.
IR, IL	Vectors such that IR(J) and IL(J) contain the highest and lowest column subscripts of a completely interior point in row J.
ITYPE	Matrix giving the type of each boundary point.
M, N	Total number of grid spacings in the angular and radial directions.
PT	Opening ratio.
PHI, PHIOLD	New and old values of the stream function, Ψ.
PHIBDR, VORBDR	Boundary values of the stream function and vorticity.
VORT, VOROLD	New and old values of the vorticity, ζ .
VORTZ1	Matrix giving the vorticity along the surface.
VZERO	Radial surface velocity.
CDF	Friction drag coefficient.
CDP	Pressure drag coefficient.
CD	Total drag coefficient.
FC	Friction factor.
NL	Number of step sizes into which the opening ratio is divided in the radial direction.

Program Symbol	Definition
Part II	
VX, XZ	Matrices giving the angular and radial velocity.
VXA, VSB	Matrices giving the angular velocity at the curved boundary.
VZA, VAB	Matrices giving the radial velocity at the curved boundary.
PHITPX, PHITPZ	Matrices giving the interpolating values of the stream function in the angular and radial directions.
Part III	
CBDR, CBOLD	New and old values of the concentration at the boundary.
CSTAR, CSOLD	New and old values of the concentration at the grid points.
CITPZ	Matrix giving the interpolating value of the concentration in the radial direction.
DCDZ	Matrix giving the concentration gradient in the radial direction at the surface.
FLOCNU	Local Nusselt number.
OVRLNU	Overall Nusselt number.
SCHMDT	Schmidt Number.
PE	Peclet number.

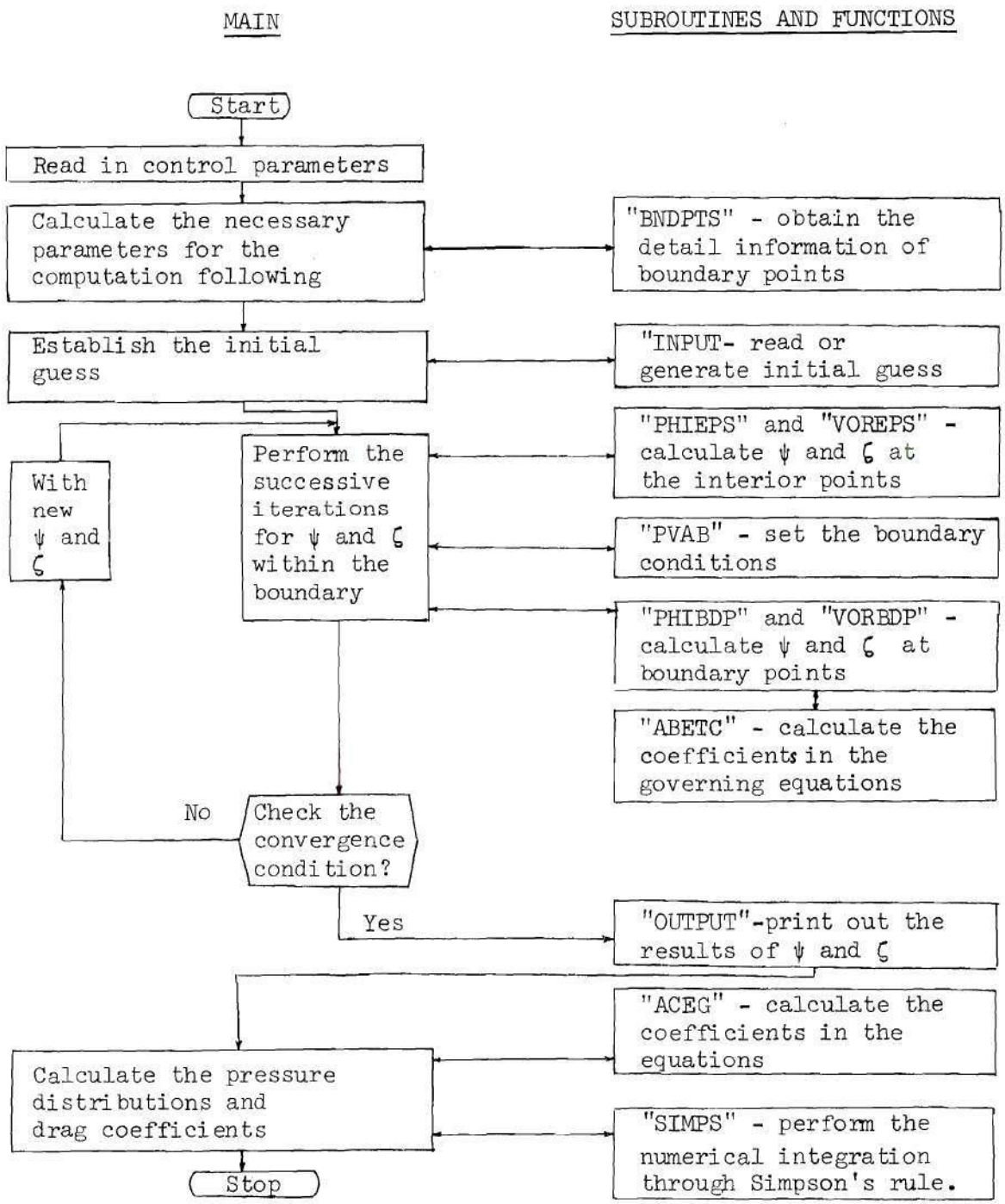

Figure C-1. Computer Block Diagram for Stream Function, Vorticity and Other Flow Parameters Calculation.

```
MAIN
  DIMENS   PROG
        COMMON DX,DZ,M,N,MP1,MP2,MHALF,N1,NP1,PT,VZERO,R,R1,R2
       1       ,PHIBDR,VORBDR,DXSQ,DXOVDZ,RATISQ,DX6,DX12,DZ6,
       2       DZ12,NL
        COMMON PHI(61,143),VORT(61,143),ITYPE(61,143),A(61,143
       1       ),B(61,143),IR(143),IL(143),IMAX(143),IMIN(143)
       2       ,EZ(143),ETWOZ(143),DXSQEZ(143)
   END
C       LOW REYNOLDS NUMBER FLOW PAST A SINGLE ROW OF
C       CYLINDERS WITH SURFACE MASS TRANSFER
C       AUTHOR: TA-YEH J. FANG, SCHOOL OF CHEMICAL ENGINEERING
C               , GEORGIA TECH, ATLANTA, GEORGIA 30332
C               JULY,1973
        INCLUDE DIMENS,LIST
        DIMENSION PI(61),PJ(61),P(61),DVDX(143),DVDZ(61),Y(61)
       1         ,VORTZ1(61)
        READ (5,102) M,NL,PT,R,ALPHA,BETA,VZERO,EPSMAX,EPVMAX
        PAI = 3.1415926536
        DX = PAI/M
        MHALF = M/2 + 1
        MP1 = M + 1
        MP2 = M + 2
        PHIBDR = PT - VZERO*(MHALF - 1)*DX
        ZX = ALOG(PT)
        DZ = ZX/NL
        N1 = NL + 1
        DX6 = 6.0*DX
        DZ6 = 6.0*DZ
        DX12 = 12.0*DX
        DZ12 = 12.0*DZ
        DXSQ = DX*DX
        DZSQ = DZ*DZ
        RATISQ = DXSQ/DZSQ
        DXOVDZ = DX/DZ
        R1 = 2.0*(1.0 + RATISQ)
        R2 = R*DX*DZ/8.0
C       ..... DETERMINE THE NUMBER OF GRID SPACING IN RADIAL
C             DIRECTION AND THE BOUNDARY POINTS OF BOTH LEFT
C             AND RIGHT HALF AND THEIR ASSOCIATED INTERCEPTS
        CALL BNDPTS
        WRITE (6,230) DZ,DX,R,M,N,PT,ALPHA,BETA,EPSMAX,EPVMAX,
       1              NL,VZERO,PHIBDR
        DO 12 J = 1,NP1,1
        EZ(J) = EXP((J-1)*DZ)
        ETWOZ(J) = EXP(2.0*(J-1)*DZ)
   12   DXSQEZ(J) = DXSQ*ETWOZ(J)
        REZ = 1.0/EZ(NP1)
        RETWOZ = 1.0/ETWOZ(NP1)
```

```
      RMAX = PI/SIN(DX)
      RR = 1.0/RMAX
      SQR = RMAX**2
      RSQ = 1.0/SQR
      DZSQ2 = 2*DZSQ
C     ..... ASSIGN THE INITIAL VALUES OF PHI, VORT .....
      CALL INPUT (1)
      ITERA = 0
   17 ITERA = ITERA + 1
      IF (EPS .GT. 10000.0) STOP
      EPS = 0.0
C     ..... CALCULATE THE STREAM FUNCTIONS .....
C     ..... THE LOWER DOMAIN .....
      DO 18 J = 2,NL,1
      DO 18 I = 2,M,1
      CALL PHIEPS (I,J,EPS,ALPHA)
   18 CONTINUE
C     ..... THE LEFT CURVE BOUNDARY POINTS .....
      DO 24 J = N1,N,1
      IRJ = IR(J)
      ILOW = IRJ + 1
      IHIGH = IMAX(J)
      DO 23 I = IHIGH,ILOW,-1
      CALL PVAB (I,J,PHIA,PHIB,VORTA,VORTB,0,1,$23)
      CALL PHIBDP (I,J,EPS,PHIA,PHIB,1,1,ALPHA)
   23 CONTINUE
      IF (IRJ .LT. 2) GO TO 20
C     ..... THE UPPER LEFT HALF CURVE DOMAIN .....
      DO 19 I = IRJ,2,-1
      CALL PHIEPS (I,J,EPS,ALPHA)
   19 CONTINUE
C     ..... THE RIGHT CURVE BOUNDARY POINTS .....
   20 ILJ = IL(J)
      IHIGH = ILJ - 1
      ILOW = IMIN(J)
      DO 27 I = ILOW,IHIGH,1
      CALL PVAB (I,J,PHIA,PHIB,VORTA,VORTB,0,-1,$27)
      CALL PHIBDP (I,J,EPS,PHIA,PHIB,-1,2,ALPHA)
   27 CONTINUE
      IF (ILJ .GT. M) GO TO 24
C     ..... THE UPPER RIGHT HALF CURVE DOMAIN .....
      DO 28 I = ILJ,M,1
      CALL PHIEPS (I,J,EPS,ALPHA)
   28 CONTINUE
   24 CONTINUE
      IF ((ITERA/200)*200 .NE. ITERA) GO TO 29
      WRITE (6, 205) ITERA
      WRITE (6,207)
      CALL OUTPUT (PHI)
```

```
   29 IF (EPS .GE. EPSMAX) GO TO 17
      WRITE (6,206)
      WRITE (6,205) ITERA
      WRITE (6,207)
      CALL OUTPUT (PHI)
      DO 30 I = 1,MP1
      IF (VZERO - 0.0) 300,291,300
  300 VORT(I,1) = (8.0*PHI(I,2) - PHI(I,3) - 7.0*PHI(I,1))
     1            /DZSQ2
      GO TO 30
  291 VORT(I,1) = (8.0*PHI(I,2) - PHI(I,3))/DZSQ2
   30 CONTINUE
      WRITE (6,208)
      WRITE (6,209) (I, VORT(I,1), I=1,MP1)
      VORBDR = 0.0
      ICOUNT =
      II = 0
   99 ICOUNT = ICOUNT + 1
C     ..... CHECK THE RATE OF CONVERGENCE .....
      IF ((ICOUNT/10)*10 .NE. ICOUNT) GO TO 33
      WRITE (6,210) ICOUNT
   33 EPS = 0.0
      EPSV = 0.0
C     ..... CALCULATE THE VORTICITY .....
C     ..... THE LOWER DOMAIN .....
      DO 31 J = 2,NL,1
      DO 31 I = 2,M,1
      CALL VOREPS (I,J,EPSV,BETA)
   31 CONTINUE
C     ..... THE LEFT CURVE BOUNDARY POINTS .....
      DO 42 J = N1,N,1
      IRJ = IR(J)
      ILOW = IRJ + 1
      IHIGH = IMAX(J)
      DO 36 I = IHIGH,ILOW,-1
      CALL PVAB (I,J,PHIA,PHIB,VORTA,VORTB,1,1,$36)
      CALL VORDOP (I,J,EPSV,PHIA,PHIB,VORTA,VORTB,1,0,BETA)
   36 CONTINUE
      IF (IRJ .LT. 2) GO TO 37
C     ..... THE UPPER LEFT HALF CURVE DOMAIN .....
      DO 32 I = IRJ,2,-1
      CALL VOREPS (I,J,EPSV,BETA)
   32 CONTINUE
C     ..... THE RIGHT CURVE BOUNDARY POINTS .....
   37 ILJ = IL(J)
      IHIGH = ILJ - 1
      ILOW = IMIN(J)
      DO 40 I = ILOW,IHIGH,1
      CALL PVAB (I,J,PHIA,PHIB,VORTA,VORTB,1,-1,$40)
```

```
      CALL VORBOP (I,J,EPSV,PHIA,PHIB,VORTA,VORTB,-1,0,BETA)
   40 CONTINUE
      IF (ILJ .GT. M) GO TO 42
C     ..... THE UPPER RIGHT HALF CURVE DOMAIN .....
      DO 41 I = ILJ,M,1
      CALL VOREPS (I,J,EPSV,BETA)
   41 CONTINUE
   42 CONTINUE
      IF ((ICOUNT/500)*500 .NE. ICOUNT) GO TO 43
      WRITE (6,210) ICOUNT
      WRITE (6,211)
      CALL OUTPUT (VORT)
   43 IF (ICOUNT .GT. 3000) GO TO 97
C     ... RECALCULATE THE MOST ACCURATE VALUES OF PHI ...
C     ..... THE LOWER DOMAIN .....
      DO 47 J = 2,NL,1
      DO 47 I = 2,M,1
      CALL PHIEPS (I,J,EPS,ALPHA)
   47 CONTINUE
C     ..... THE LEFT CURVE BOUNDARY POINTS .....
      DO 59 J = N1,N,1
      IRJ = IR(J)
      ILOW = IRJ + 1
      IHIGH = IMAX(J)
      DO 53 I = IHIGH,ILOW,-1
      CALL PVAB (I,J,PHIA,PHIB,VORTA,VORTB,0,1,$53)
      CALL PHIBOP (I,J,EPS,PHIA,PHIB,1,3,ALPHA)
   53 CONTINUE
      IF (IRJ .LT. 2) GO TO 49
C     ..... THE UPPER LEFT HALF CURVE DOMAIN .....
      DO 48 I = IRJ,2,-1
      CALL PHIEPS (I,J,EPS,ALPHA)
   48 CONTINUE
   49 ILJ = IL(J)
      IHIGH = ILJ - 1
      ILOW = IMIN(J)
C     ..... THE RIGHT CURVE BOUNDARY POINTS .....
      DO 57 I = ILOW,IHIGH,1
      CALL PVAB (I,J,PHIA,PHIB,VORTA,VORTB,0,-1,$57)
      CALL PHIBOP (I,J,EPS,PHIA,PHIB,-1,4,ALPHA)
   57 CONTINUE
      IF (ILJ .GT. M) GO TO 59
C     ..... THE UPPER RIGHT HALF CURVE DOMAIN .....
      DO 58 I = ILJ,M,1
      CALL PHIEPS (I,J,EPS,ALPHA)
   58 CONTINUE
   59 CONTINUE
      IF ((ICOUNT/500)*500 .NE. ICOUNT) GO TO 44
      WRITE (6,207)
```

```
      CALL OUTPUT (PHI)
   44 DO 45 I = 1,MP1,1
      IF (VZERO - 0.0) 440,441,440
  440 VORT(I,1) = (8.0*PHI(I,2) - PHI(I,3) - 7.0*PHI(I,1))
     1          /DZSQ2
      GO TO 45
  441 VORT(I,1) = (8.0*PHI(I,2) - PHI(I,3))/DZSQ2
   45 CONTINUE
      IF ((ICOUNT/500)*500 .NE. ICOUNT) GO TO 46
      WRITE (6,208)
      WRITE (6,209) (I, VORT(I,1), I=1,MP1)
   46 IF ((ICOUNT/100)*100 .NE. ICOUNT) GO TO 50
      WRITE (6,240) EPS,EPSV
   50 IF (EPS .GE. EPVMAX .OR. EPSV .GE. EPVMAX) GO TO 99
      WRITE (6,206)
      WRITE (6,240) EPS,EPSV
      WRITE (6,210) ICOUNT
      WRITE (6,207)
      CALL OUTPUT (PHI)
      WRITE (6,211)
      CALL OUTPUT (VORT)
      WRITE (6,208)
      WRITE (6,209) (I, VORT(I,1), I=1,MP1)
      IF (II .NE. 0) GO TO 99
      MO2 = M/2
      DO 66 J = 1,NP1,1
      DO 66 I = 1,MO2,1
      L1 = 2*(I - 1) + 1
      L2 = 2*I
      WRITE (10,104) (K,J,PHI(K,J), K=L1,L2,1)
   66 WRITE (11,104) (K,J,VORT(K,J), K=L1,L2,1)
      DO 67 J = 1,NP1,1
      WRITE (10,108) (MP1,J,PHI(MP1,J))
   67 WRITE (11,108) (MP1,J,VORT(MP1,J))
      DO 68 I = 1,MP1,1
   68 WRITE (12,109) I,VORT(I,1)
C     ..... CALCULATE THE PRESSURE DISTRIBUTION AND THE DRAG
C           COEFFICIENTS .....
      DO 501 J = 1,NP1,1
      IF (J .LT. N1) GO TO 504
      IHIGH = IMAX(J)
      IF (IHIGH - 3) 502,503,504
  502 CALL ACEG (IHIGH,J,A1,A2,C1,C2,E1,E2,G1,ACX,ACEX)
      DVDX(J) = (C2*VORT(IHIGH,J) - A1*(2.0 + A1)*VORT(IHIGH
     1          -1,J) - VORBDR)/ACX
      GO TO 501
  503 CALL ACEG (IHIGH,J,A1,A2,C1,C2,E1,E2,G1,ACX,ACEX)
      DVDX(J) = (4.0*VORBDR - E2*C1*VORT(IHIGH,J) + 4.0*A1*
     1          E2*VORT(IHIGH-1,J) - A1*C1*(8.0 + 3.0*A1)*
```

```
     2              VORT(IHIGH-2,J))/DCEX
      GO TO 501
  504 DVDX(J) = (-11.0*VORT(1,J) + 18.0*VORT(2,J) - 9.0*VORT
     1              (3,J) + 2.0*VORT(4,J))/DX6
  501 CONTINUE
      VZROSQ = VZERO**2
      PZERO = 1.0 - VZROSQ + 4.0*SIMPS(DVDX,DZ,1,MP1)/R
      WRITE (6,290) PZERO
      DO 505 I = 1,MP1,1
      DVDZ(I) = (-11.0*VORT(I,1) + 18.0*VORT(I,2) - 9.0*VORT
     1              (I,3) + 2.0*VORT(I,4))/DZ6
      VORTZ1(I) = VORT(I,1)
      PI(I) = 2.0*SIMPS(DVDZ,DX,1,I)/R - VZERO*SIMPS(VORTZ1,
     1          DX,1,I)
      P(I) = PZERO + 2.0*PI(I)
  505 PJ(I) = PI(I)*COS((I-1)*DX)
      WRITE (6,295)
      WRITE (6,209) (I,P(I), I=1,MP1)
      DO 506 I = 1,MP1,1
      WRITE (10,110) I,P(I),PI(I)
      IF (I .GT. MHALF) GO TO 500
      Y(I) = VORT(I,1)*SIN((I-1)*DX)
      GO TO 506
  500 Y(I) = VORT(I,1)*SIN((MP2-I-1)*DX)
  506 CONTINUE
      CDF = 4.0*SIMPS(Y,DX,1,MP1)/R
      WRITE (6,292) CDF
      CDP = 2.0*SIMPS(PJ,DX,1,MP1)
      WRITE (6,293) CDP
      CD = CDF + CDP
      WRITE (6,294) CD
      FC = CD/(4.0*PI)*((PI-1.0)/PI)
      WRITE (6,296) FC
      II = 1
      GO TO 99
   98 ICOUNT = ICOUNT - 1
   97 WRITE (6,217) DZ,DX,R,M,N,PI,ALPHA,BETA,EPSMAX,EPVMAX,
     1              NL,ITERA,ICOUNT,VZERO,PHIBOR,VORBOR,CDF
     2              ,CDP,CD,FC
      WRITE (6,213) N,EZ(1)
      WRITE (6,212) MP1,EZ(MP1),REZ,ETWOZ(MP1),RETWOZ
      WRITE (6,214) RMAX,RR,SQR,RSQ
  102 FORMAT ()
  104 FORMAT (2(2I3,E15.7))
  108 FORMAT (2I3,E15.7)
  109 FORMAT (I3,E15.7)
  110 FORMAT (I3,2E15.7)
  205 FORMAT (2HO                    ITERA = ,I3)
  206 FORMAT (1H1,24X, 'CONVERGENCE CONDITION HAS BEEN',
```

```
     1          1X, 'REACHED AFTER A NUMBER OF ITERATIONS')
207 FORMAT (1H0,25X, 'STREAM FUNCTION DISTRIBUTION AT',
     1          1X, 'ALL GRID POINTS'/)
208 FORMAT (1H0,13X, 'VORTICITY DISTRIBUTION ON THE',
     1          ' SURFACE OF THE CYLINDER'/)
209 FORMAT (5(I3,F12.6))
210 FORMAT (24H0                    ICOUNT = , I4)
211 FORMAT (1H0,23X, 'VORTICITY DISTRIBUTION AT ALL',
     1          1X, 'GRID POINTS')
212 FORMAT (//5X'EZ(NP1=',I3,')=',F10.4,2X,'REZ =',
     1          F12.8,2X,'ETWOZ =',F10.5,2X,'RETWOZ =',F12.9)
213 FORMAT (//5X'EZ(N=',I3,')=',F10.4)
214 FORMAT (//5X'RMAX = ',F12.7,2X,'RR =',F12.7,2X,'SQR ='
     1          'F12.7,2X,'RSQ =',F12.7)
217 FORMAT (1H1,4X,'DZ = ',F8.6,8X,'DX = ',F8.6,8X,'R = ',
     1          F5.1,8X,'M = ',I3,8X,'N = ',I3,8X,'PT = ',F4.2
     2          ,//,5X,'ALPHA = ',F6.3,7X,'BETA = ',F9.6,5X,
     3          'EPSMAX = ',1PE7.0,5X,'EPVMAX = ',1PE7.0,10X,
     4          'NL =',I3,//,5X,'ITERA = ',I3,10X,'ICOUNT = '
     5          'I4,8X,'VZERO = ',0PF9.6,4X,'PHIBDR = ',
     6          F10.7,7X,'VORBDR = ',F3.1,//,5X,'CDF = ',
     7          F14.6,1X,'CDP = ',F14.6,1X,'CD = ',F14.6,
     8          //,5X,'F = ',E14.6)
230 FORMAT (1H1,4X,'DZ = ',F8.6,8X,'DX = ',F8.6,8X,'R = ',
     1          F5.1,8X,'M = ',I3,8X,'N = ',I3,8X,'PT = ',F4.2
     2          ,//,5X,'ALPHA = ',F6.3,7X,'BETA = ',F9.6,5X,
     3          'EPSMAX = ', 1PE7.0, 5X, 'EPVMAX = ', 1PE7.0,
     4          10X,'NL = ',I2,//,5X,'VZERO = ',0PF9.6,4X,
     5          'PHIBDR = ',F9.6)
240 FORMAT ('    EPS =',E15.7,'    EPSV =',E15.7)
290 FORMAT (1H0,30X,'PZERO = ',F9.5)
292 FORMAT (1H0,22X,'DRAG COEFFICIENT CDF = ',F10.5)
293 FORMAT (1H0,22X,'DRAG COEFFICIENT CDP = ',F10.5)
294 FORMAT (1H0,10X,'TOTAL DRAG COEFFICIENT CD = CDF + ',
     1          'CDP = ',F10.5)
295 FORMAT (1H0,13X,'PRESSURE DISTRIBUTION ON THE SURFACE'
     1          ' OF THE CYLINDER'//)
296 FORMAT (1H0,10X,'FRICTION FACTOR FC = ',F10.5)
      STOP
      END
      SUBROUTINE BNDPTS
      INCLUDE DIMENS,LIST
      DIMENSION D(4),E(4),F(4)
      DATA D(1),D(2),D(4)/'(6H ','I=   ',','I2)'/
      DATA E(1),E(2),E(4)/'(3H ','J=,I3,',','I2)'/
      DATA F(1),F(2),F(4)/'(/6H ','I=   ',',I2)'/
      EPS = 0.000001
      WRITE (6,224)
      DO 5 J = 1,151,1
```

```
      FJM1 = J - 1
      PTOVR = PT/EXP(FJM1*DZ)
      XOVRDX = ASIN(PTOVR)/DX
      IM1 = XOVRDX + EPS
      IF(IM1 .LT. 1) GO TO 6
      FIM1 = IM1
      I = IM1 + 1
      IMAX(J)= I
      IM = MP2 - I
      IMIN(J) = IM
      ZOVRDZ = (ALOG(PT/SIN(FIM1*DX)))/DZ
      A(I,J) = XOVRDX - FIM1
      A(IM,J) = A(I,J)
      B(I,J) = ZOVRDZ - FJM1
      B(IM,J) = B(I,J)
      IF (ABS(B(I,J)) .LT. EPS) GO TO 2
      IF (ABS(B(I,J)) .GE. EPS) GO TO 3
    2 ITYPE(I,J) = 4
      ITYPE(IM,J) = 4
      B(I,J) = 0.0
      B(IM,J) = 0.0
      WRITE (6,223) (I,J,ITYPE(I,J),A(I,J),B(I,J),IM,J,
     1                ITYPE(IM,J),A(IM,J),B(IM,J))
      GO TO 5
    3 IF (B(I,J) .LE. 1.0) GO TO 4
      ITYPE(I,J) = 3
      ITYPE(IM,J) = 3
      B(I,J) = 1.0
      B(IM,J) = 1.0
      WRITE (6,223) (I,J,ITYPE(I,J),A(I,J),B(I,J),IM,J,
     1                ITYPE(IM,J),A(IM,J),B(IM,J))
      GO TO 5
    4 ITYPE(I,J) = 1
      ITYPE(IM,J) = 1
      WRITE (6,223) (I,J,ITYPE(I,J),A(I,J),B(I,J),IM,J,
     1                ITYPE(IM,J),A(IM,J),B(IM,J))
    5 CONTINUE
    6 NP1 = J - 1
C     ..... LOCATE BOUNDARY POINTS OF TYPE 2 ....
      N = NP1 - 1
      DO 9 J = 1,N,1
      FJM1 = J - 1
      I = IMAX(J) - 1
    7 IF (IMAX(J+1) .GE. I) GO TO 9
      IM = MP2 - I
      FIM1 = I - 1
      B(I,J) = (ALOG(PT/SIN(FIM1*DX)))/DZ - FJM1
      B(IM,J) = B(I,J)
      ITYPE(I,J) = 2
```

```
      ITYPE(IM,J) = 2
      A(1,J) = 1.0
      A(IM,J) = 1.0
      WRITE (6,223) (I,J,ITYPE(I,J),A(I,J),B(I,J),IM,J,
     1                 ITYPE(IM,J),A(IM,J),B(IM,J))
      I = I - 1
      GO TO 7
    8 CONTINUE
      IR(J) = 1
      IM = MP2 - I
      IL(J) = IM
    9 CONTINUE
      WRITE (6,221)
      L(3) = MP1
      WRITE (6,201) (I, I=1,MP1)
      E(3) = MP1
      WRITE (6,202) (J,(ITYPE(I,J), I=1,MP1), J=N,N1,-1)
      F(3) = MP1
      WRITE (6,203) (I, I=1,MP1)
      WRITE (6,222)
      WRITE (6,204)
      WRITE (6,218) ((J, IMAX(J), IMIN(J), J=NP1,NP1), (J,
     1IR(J), IMAX(J), IMIN(J), IL(J), J=N,N1,-1))
      WRITE (6,220)
  201 FORMAT (6H I=    ,61I2/)
  202 FORMAT (3H J=,I3,61I2)
  203 FORMAT (/6H I=    ,61I2)
  204 FORMAT (4X,'J',6X,'IR',6X,'IMAX',6X,'IMIN',6X,'IL')
  218 FORMAT (I4,1X,I3,15X,I2,8X,I2/(2X,I3,6X,I2,7X,I2,8X,
     1I2,7X,I2))
  220 FORMAT (/4X,'J',6X,'IR',6X,'IMAX',6X,'IMIN',6X,'IL')
  221 FORMAT (1H1, 'THE LOCATIONS OF THE BOUNDARY POINTS '
     1'AND THEIR TYPES'/)
  222 FORMAT (1H1, 'THE LOCATIONS OF THE INNER POINTS (IR '
     1'AND IL) AND THE BOUNDARY POINTS'/)
  223 FORMAT (3I3,2F10.6,15X,3I3,2F10.6/)
  224 FORMAT (1H1,2H I,3H  J,6H ITYPE,4X,1HA,9X,1HB,18X,
     12HIM,3H  J,6H ITYPE,4X,1HA,9X,1HB//)
      RETURN
      END
      SUBROUTINE INPUT (KP)
      INCLUDE DIMENS,LIST
      PAI = 3.1415926536
      IF (KP .NE. 0) GO TO 5
      DO 3 I = 2,M,1
      DO 3 J = 2,NP1,1
      IF (I .GT. MHALF) GO TO 2
      PHI(I,J) = E7(J)*SIN((I-1)*DX) - VZERO*(I-1)*DY
      GO TO 3
```

```
      2 PHI(I,J) = F7(J)*SIN((MP2-I-1)*DX) - VZERO*(I-1)*DX
      3 CONTINUE
        DO 4 I = 1,MP1,1
        DO 4 J = 2,MP1,1
      4 VORT(I,J) = 0.0
        GO TO 9
      6 MD2 = M/2
        DO 11 J =1,MP1,1
        DO 11 I = 1,MD2,1
        L1 = 2*(I-1) + 1
        L2 = 2*I
     11 READ (5,104) (IQ,JQ,PHI(K,J), K=L1,L2,1)
        DO 12 J = 1,MP1,1
     12 READ (5,108) IQ,JQ,PHI(MP1,J)
        DO 7 J = 1,MP1,1
        DO 7 I = 1,MD2,1
        L1 = 2*(I-1) + 1
        L2 = 2*I
      7 READ (5,104) (IQ,JQ,VORT(K,J), K=L1,L2,1)
        DO 8 J = 1,MP1,1
      8 READ (5,108) IQ,JQ,VORT(MP1,J)
      9 DO 10 J = 1,MP1,1
        PHI(1,J) = 0.0
     10 PHI(MP1,J) = -VZERO*PAI
        DO 13 I = 1,MP1,1
     13 PHI(I,1) = -VZERO*(I-1)*DX
    104 FORMAT (2(2I3,E15.7))
    108 FORMAT (2I3,F15.7)
        RETURN
        END
        SUBROUTINE PHIEPS (I,J,EPS ,ALPHA)
        INCLUDE DIMENS,LIST
        PHIOLD = PHI(I,J)
        PHI(I,J) = PHI(I,J) + ALPHA*( -VORT(I,J)*DXSQF7(J)
       1          + PHI(I+1,J) + PHI(I-1,J) + (PHI(I,J+1)
       2          + PHI(I,J-1))*RATISQ - R1*PHI(I,J))/R1
        EPS = EPS + ABS(PHI(I,J) - PHIOLD)
        RETURN
        END
        SUBROUTINE PVAB (I,J,PHIA,PHIB,VORTA,VORTB,IV,K,$)
        INCLUDE DIMENS,LIST
        IF (ITYPE(I,J)-3) 5,3,1
      1 PHI(I,J) = PHIBDR
        IF (IV .EQ. 0) GO TO 2
        VORT(I,J) = VORBDR
      2 RETURN 9
      3 PHIA = PHIBDR
        PHIB = PHI(I,J+1)
        IF (IV .EQ. 0) GO TO 3
```

```
      VORTA = VORBDR
      VORTB = VORT(I,J+1)
      GO TO 8
    5 IF (ITYPE(I,J) .EQ. 1) GO TO 7
      PHIA = PHI(I+K,J)
      PHIB = PHIBDR
      IF (IV .EQ. 0) GO TO 8
      VORTA = VORT(I+K,J)
      VORTB = VORBDR
      GO TO 8
    7 PHIA = PHIBDR
      PHIB = PHIBDR
      IF (IV .EQ. 0) GO TO 8
      VORTA = VORBDR
      VORTB = VORBDR
    8 RETURN
      END
      SUBROUTINE PHIBDP (I,J,EPS,PHIA,PHIB,K,KP,ALPHA)
      INCLUDE DIMENS,LIST
      CALL ABETC (I,J,KP,A1,B1,C,D,E,F,G,H,P,Q)
      PHIOLD = PHI(I,J)
      PHIIJ = (E*PHIA + C*PHI(I-K,J) + (F*PHIB + D*PHI(I,
     1            J-1))*RATISQ - 0.5*DXSQ*ETWOZ(J)*VORT(I,J)
     2           )/(RATISQ/B1 + 1.0/A1)
      PHI(I,J) = PHI(I,J) + ALPHA*(PHIIJ - PHI(I,J))
      EPS = EPS + ABS (PHI(I,J) - PHIOLD)
      RETURN
      END
      SUBROUTINE VOREPS (I,J,EPSV ,BETA)
      INCLUDE DIMENS,LIST
      VOROLD = VORT(I,J)
      VORT(I,J) = VORT(I,J) + BETA*(VORT(I+1,J) + VORT(I-1,J
     1            ) + (VORT(I,J+1) + VORT(I,J-1))*RATISQ -
     2            R1*VORT(I,J) + R2*((PHI(I+1,J) - PHI(I-1,J
     3            ))*(VORT(I,J+1) - VORT(I,J-1)) - (PHI(I,
     4            J+1) - PHI(I,J-1))*(VORT(I+1,J) - VORT
     5            (I-1,J))))/R1
      EPSV = EPSV + ABS(VORT(I,J) - VOROLD)
      RETURN
      END
      SUBROUTINE VORBDP (I,J,EPSV,PHIA,PHIB,VORTA,VORTB,K,
     1                   KP,BETA)
      INCLUDE DIMENS,LIST
      CALL ABETC (I,J,KP,A1,B1,C,D,E,F,G,H,P,Q)
      VOROLD = VORT(I,J)
      VORTIJ = ((E*VORTA + C*VORT(I-K,J))/RATISQ + F*
     1            VORTB + D*VORT(I,J-1) + K*R*((F*VORTB -
     2            H*VORT(I,J-1))*(E*PHIA - G*PHI(I-K,J) -
     3            P*PHI(I,J)) - (E*VORTA - G*VORT(I-K,J))*
```

```
     4                (F*PHI3 - H*PHI(I,J-1) - Q*PHI(I,J)))
     5                /(4.0*DX0VDZ))/(1.0/(A1*RATIS0) + 1.0/B1
     6               + K*R*(Q*(E*PHIA - G*PHI(I-K,J) - P*PHI(I,
     7               J)) - P*(F*PHIB - H*PHI(I,J-1) - Q*PHI(I,
     8               J)))/(4.0*DX0VDZ))
      VORT(I,J) = VORT(I,J) + BETA*(VORTIJ - VORT(I,J))
      EPSV = EPSV + ABS(VORT(I,J) - VOROLD)
      RETURN
      END
      SUBROUTINE ACEG (L,J,A1,A2,C1,C2,E1,E2,G1,ACX,ACEX)
      INCLUDE DIMENS,LIST
      A1 = A(L,J)
      C1 = 1.0 + A(L,J)
      E1 = 2.0 + A(L,J)
      G1 = 1.0 + 2.0*A(L,J)
      A2 = A1**2
      C2 = C1**2
      ACX = A1*C1*DX
      IF (L .LT. 3) GO TO 1
      E2 = E1**2
      ACEX = 2.0*A1*C1*E1*DX
    1 RETURN
      END
      SUBROUTINE ABETC (I,J,KP,A1,B1,C,D,E,F,G,H,P,Q)
      INCLUDE DIMENS,LIST
      A1 = A(I,J)
      B1 = B(I,J)
      C = 1.0/(1.0 + A1)
      D = 1.0/(1.0 + B1)
      E = 1.0/(A1*(1.0 + A1))
      F = 1.0/(B1*(1.0 + B1))
      IF (KP .NE. 0) GO TO 1
      G = 1.0/E
      H = 1.0/F
      P = (1.0 - A1)/A1
      Q = (1.0 - B1)/B1
    1 RETURN
      END
      SUBROUTINE OUTPUT (OUT)
      INCLUDE DIMENS,LIST
      DIMENSION OUT(61,143)
      DO 1 J = MP1,N1,-1
      IHIGH = IMAX(J)
      ILOW = IMIN(J)
      WRITE (6,225)  (J, (I,OUT(I,J), I=1,IHIGH))
      WRITE (6,226) (IM,OUT(IM,J), IM=MP1,ILOW,-1)
    1 CONTINUE
      DO 2 J= NL,1,-1
      WRITE (6,225)  (J, (I,OUT(I,J), I=1,MP1))
```

```
  2 CONTINUE
225 FORMAT ('    J =', I3/(10(I3,F9.6)))
226 FORMAT (1X,(I3,F9.6))
    RETURN
    END
    FUNCTION SIMPS (F,H,IA,IB)
    DIMENSION F(1)
    L = (IB - IA)/2
    IF (IB-IA-1) 1,2,3
  1 SIMPS = 0.0
    RETURN
  2 SIMPS = (F(IA) + F(IB))*H/2.0
    RETURN
  3 SUM = F(IA)
    LM1 = L - 1
    IF (LM1 .LT. 1) GO TO 5
    DO 4 I = 1,LM1
  4 SUM = SUM + 4.0*F(IA+2*I-1) + 2.0*F(IA+2*I)
  5 IF ((IB - IA) .NE. (2*L)) GO TO 6
    SUM = SUM + 4.0*F(IA+2*L-1) + F(IA+2*L)
    SIMPS = H*SUM/3.0
    RETURN
  6 SUM = SUM + 4.0*F(IA+2*L-1) + 2.5*F(IA+2*L)
    SIMPS = H*(SUM/3.0 + F(IB)/2.0)
    RETURN
    END
```

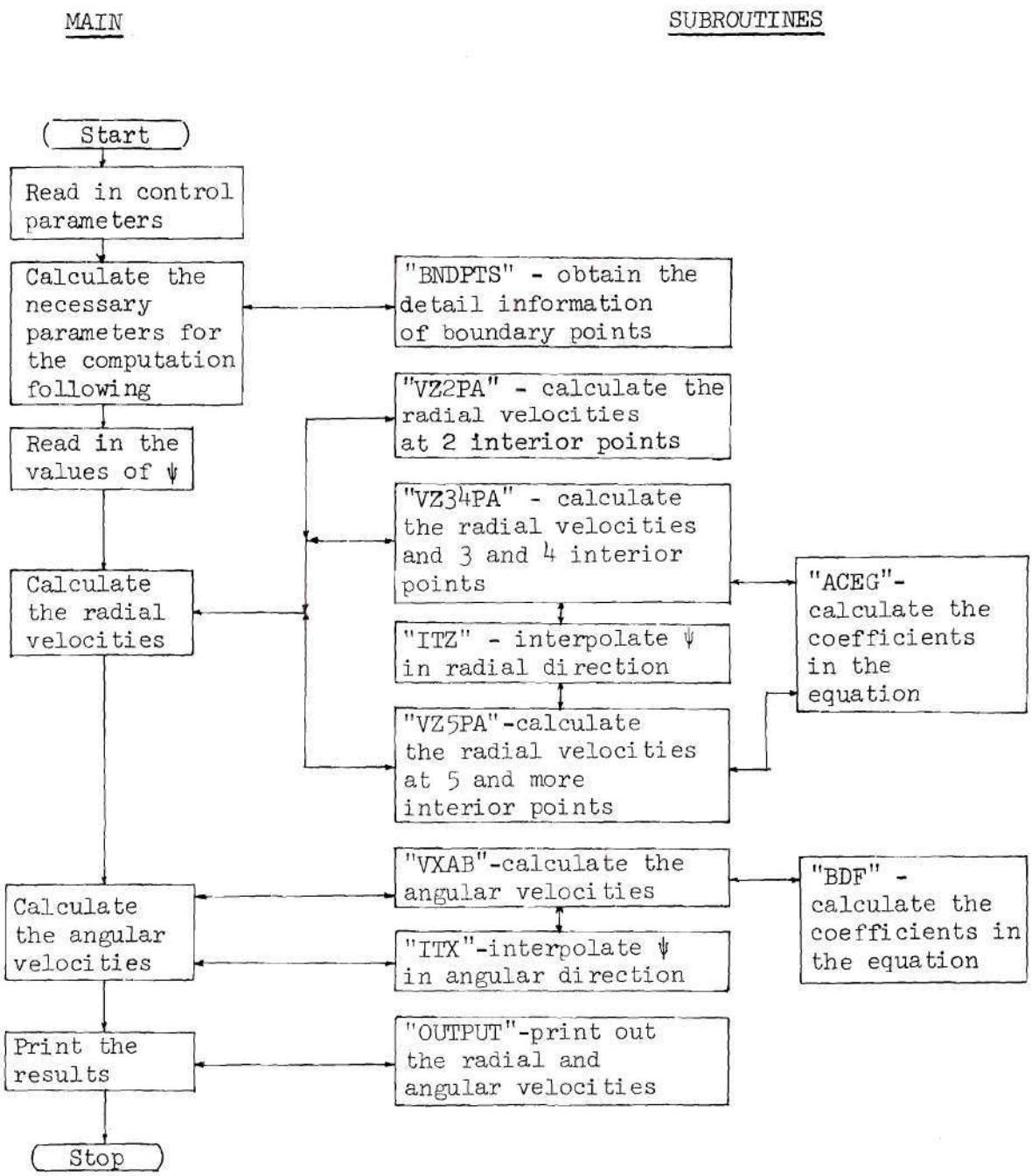

Figure C-2. Computer Block Diagram for Angular and Radial Velocities Calculation.

```
MAIN
  DIMENS   PROG
       COMMON DX,DZ,M,N,MP1,MP2,MHALF,N1,NP1,PT,VZERO,R
      1       ,PHIBDR,DX6,DX12,DZ6,DZ12,J1,J2,J3,NL
       COMMON PHI(61,143),ITYPE(61,143),A(61,143),B(61,143),
      1       IR(143),IL(143),IMAX(143),IMIN(143)
      2       ,EZ(143),ETWOZ(143)
       COMMON VX(61,143),VZ(61,143),VXA(61),VXB(61),VZA(61),
      1       VZB(61),PHITPX(143),PHITPZ(61)
   END
C      LOW REYNOLDS NUMBER FLOW PAST A SINGLE ROW OF
C      CYLINDERS WITH SURFACE MASS TRANSFER
C      AUTHOR: TA-YEH J. FANG, SCHOOL OF CHEMICAL ENGINEERING
C              , GEORGIA TECH, ATLANTA, GEORGIA 30332
C              JULY,1974
       INCLUDE DIMENS,LIST
       READ (5,102) M,NL,PT,R,ALPHA,BETA,VZERO,EPSMAX,
      1             EPVMAX
       PAI = 3.1415926536
       DX = PAI/M
       MHALF = M/2 + 1
       MP1 = M + 1
       MP2 = M + 2
       MM1 = M - 1
       MM2 = M - 2
       PHIBDR = PT - VZERO*(MHALF - 1)*DX
       ZX = ALOG(PT)
       DZ = ZX/NL
       N1 = NL + 1
       DX6 = 6.0*DX
       DZ6 = 6.0*DZ
       DX12 = 12.0*DX
       DZ12 = 12.0*DZ
C      ..... DETERMINE THE NUMBER OF GRID SPACING IN RADIAL
C            DIRECTION AND THE BOUNDARY POINTS OF BOTH LEFT
C            AND RIGHT HALF AND THEIR ASSOCIATED INTERCEPTS
       CALL BNDPTS
       WRITE (6,230) DZ,DX,R,M,N,PT,ALPHA,BETA,EPSMAX,EPVMAX,
      1              NL,VZERO,PHIBDR
       MD2 = M/2
       DO 6 J = 1,NP1,1
       DO 6 I = 1,MD2,1
       L1 = 2*(I - 1) + 1
       L2 = 2*I
     6 READ (5,104) (IQ,JQ,PHI(K,J), K=L1,L2,1)
       DO 7 J = 1,NP1,1
     7 READ (5,108) IQ,JQ,PHI(MP1,J)
       DO 11 I = 1,MP1,1
       VX(I,1) = 0.0
```

```
      VZ(I,1) = VZERO
      IF (I .GT. MHALF) GO TO 10
      VX(I,NP1) = SIN((I-1)*DX)
      VZ(I,NP1) = -COS((I-1)*DX)
      GO TO 11
   10 VX(I,NP1) = VX(MP2-I,NP1)
      VZ(I,NP1) = -VZ(MP2-I,NP1)
   11 CONTINUE
      DO 12 J = 1,NP1,1
      EZ(J) = EXP((J-1)*DZ)
   12 ETWOZ(J) = EXP(2.0*(J-1)*DZ)
C     ..... CALCULATE THE VELOCITIES .....
      WRITE (6,299)
      DO 436 J = N,N1,-1
      IHIGH = IMAX(J)
      ILOW = IN(J) + 1
      IHIGHM = IMIN(J)
      ILOWM = IL(J) - 1
      IF (IHIGH .GE. 3) GO TO 401
      CALL VZ2PA (IHIGH,J,1,-1)
      CALL VZ2PA (IHIGHM,J,-1,1)
      GO TO 458
  401 IF (IHIGH .GT. 4) GO TO 402
      CALL VZ34PA (IHIGH,J,1,-1,4)
      CALL VZ34PA (IHIGHM,J,-1,1,MM2)
      GO TO 458
  402 CALL VZ5PA (IHIGH,J,1,-1)
      CALL VZ5PA (1,J,-1,1)
      IHI2 = IHIGH - 2
      DO 403 I = 3,IHI2,1
  403 VZ(I,J) = (PHI(I+2,J)-8.0*PHI(I+1,J)+8.0*PHI(I-1,J)-
     1           PHI(I-2,J))/(DX12*EZ(J))
      IF (IHIGH .EQ. ILOW) GO TO 419
      IHI1 = IHIGH - 1
      DO 418 L = ILOW,IHI1,1
      BZ = B(L,1)
      DO 405 K = 1,3,1
      LK = L - K
      CALL ITZ (LK,J,BZ)
  405 CONTINUE
      VZB(L) = -(11.0*PHIRDR-18.0*PHITPZ(L-1)+9.0*PHITPZ
     1           (L-2)-2.0*PHITPZ(L-3))/(DX6*EZ(J))
      WRITE (6,289) L,J,VZB(L)
  418 CONTINUE
  419 CALL VZ5PA (IHIGHM,J,-1,1)
      CALL VZ5PA (MP1,J,1,-1)
      IHI2M = IHIGHM + 2
      DO 422 IM = IHI2M,MM1,1
  422 VZ(IM,J) = (PHI(IM+2,J)-8.0*PHI(IM+1,J)+8.0*PHI(IM-1,
```

```
     1              J)-PHI(IM-2,J))/(6X12*EZ(J))
      IF (IHIGHM .EQ. ILOWM) GO TO 438
      IHI1M = IHIGHM + 1
      DO 437 LM = ILOWM,IHI1M,-1
      BZM = B(LM,J)
      DO 424 K = 1,3,1
      LKM = LM + K
      CALL ITZ (LKM,J,BZM)
  424 CONTINUE
      VZB(LM) = (11.0*PHITBR-18.0*PHITPZ(LM+1)+9.0*PHITPZ
     1              (LM+2)-2.0*PHITPZ(LM+3))/(DX6*EZ(J))
      WRITE (6,289) LM,J,VZB(LM)
  437 CONTINUE
  438 CONTINUE
      DO 439 J = NL,2,-1
      VZ(1,J) = (25.0*PHI(1,J)-48.0*PHI(2,J)+36.0*PHI(3,J)-
     1              16.0*PHI(4,J)+3.0*PHI(5,J))/(DX12*EZ(J))
      VZ(MP1,J) = (- 3.0*PHI(M-3,J)+16.0*PHI(M-2,J)-36.0*PHI
     1              (M-1,J)+48.0*PHI(M,J)-25.0*PHI(MP1,J))/
     2              (DX12*EZ(J))
      VZ(2,J) = (3.0*PHI(1,J)+10.0*PHI(2,J)-18.0*PHI(3,J)+
     1              6.0*PHI(4,J)-PHI(5,J))/(DX12*EZ(J))
      VZ(M,J) = (PHI(M-3,J)-6.0*PHI(M-2,J)+18.0*PHI(M-1,J)-
     1              10.0*PHI(M,J)-3.0*PHI(MP1,J))/(DX12*EZ(J))
      DO 439 I = 3,MM1,1
  439 VZ(I,J) = (8.0*(PHI(I-1,J)-PHI(I+1,J))+PHI(I+2,J)-PHI
     1              (I-2,J))/(DX12*EZ(J))
      NM1 = N - 1
      VX(1,N) = 0.0
      VX(2,N) = (-PHI(2,N-3)+6.0*PHI(2,N-2)-18.0*PHI(2,NM1)
     1              +10.0*PHI(2,N)+3.0*PHI(2,NP1))/(DZ12*EZ(N))
      VX(MP1,N) = 0.0
      VX(M,N) = (-PHI(M,N-3)+6.0*PHI(M,N-2)-18.0*PHI(2,NM1)
     1              +10.0*PHI(2,N)+3.0*PHI(2,NP1))/(DZ12*EZ(N))
      LP = 0
      DO 451 J = NM1,N1,-1
      VX(1,J) = 0.0
      VX(MP1,J) = 0.0
      IHIGH = IMAX(J)
      ILOW = IM(J) + 1
      IHIGHM = IMIN(J)
      ILOWM = IL(J) - 1
      AX = A(IHIGH,J)
      J1 = J - 1
      J2 = J - 2
      J3 = J - 3
      IF (IHIGH .GE. 3) GO TO 447
      DO 442 JK = J1,J3,-1
      CALL ITX (IHIGH,JK,1,AX)
```

```
443 CONTINUE
    VXA(IHIGH) = (-2.0*PHITPX(J3)+9.0*PHITPX(J2)-18.0*
   1              PHITPX(J1)+11.0*PHIBDR)/(DZ6*EZ(J))
    WRITE (6,286) IHIGH,J,VXA(IHIGH)
    DO 445 JK = J1,J3,-1
    CALL ITX (IHIGHM,JK,-1,AX)
445 CONTINUE
    VXA(IHIGHM) = (-2.0*PHITPX(J3)+9.0*PHITPX(J2)-18.0*
   1               PHITPX(J1)+11.0*PHIBDR)/(DZ6*EZ(J))
    WRITE (6,286) IHIGHM,J,VXA(IHIGHM)
    LP = LP + 1
    IF (LP .EQ. 1) GO TO 451
    DO 446 JK = NM1,3,-1
    VX(IHIGH,JK) = (PHI(IHIGH,JK-2)-8.0*PHI(IHIGH,JK-1)+
   1                8.0*PHI(IHIGH,JK+1)-PHI(IHIGH,JK+2))
   2               /(DZ12*EZ(JK))
446 VX(IHIGHM,JK) = (PHI(IHIGHM,JK-2)-8.0*PHI(IHIGHM,JK-1)
   1                 +8.0*PHI(IHIGHM,JK+1)-PHI(IHIGHM,JK+2
   2                 ))/(DZ12*EZ(JK))
    GO TO 451
447 IF (IHIGH .GT. ILOW) GO TO 448
    CALL VXAD (IHIGH,J,1,AX)
    CALL VXAD (IHIGHM,J,-1,AX)
    GO TO 451
448 CALL VXAD (IHIGH,J,1,AX)
    CALL VXAD (IHIGHM,J,-1,AX)
    IHI1 = IHIGH - 1
    DO 449 ILH = ILOW,IHI1,1
449 CALL VXAD (ILH,J,1,AX)
    IHI1M = IHIGHM + 1
    DO 450 ILHM = IHI1M,ILOWM,1
450 CALL VXAD (ILHM,J,-1,AX)
451 CONTINUE
    DO 452 I = 2,M,1
452 VX(I,2) = (-3.0*PHI(I,1)-10.0*PHI(I,2)+18.0*PHI(I,3)
   1            -6.0*PHI(I,4)+PHI(I,5))/(DZ12*EZ(2))
    DO 453 J = NP1,2,-1
    VX(1,J) = 0.0
453 VX(MP1,J) = 0.0
    WRITE (6,298)
    CALL OUTPUT (VX)
    WRITE (6,297)
    CALL OUTPUT (VZ)
    MD2 = M/2
    DO 454 J = 1,NP1,1
    DO 454 I = 1,MD2,1
    L1 = 2*(I - 1) + 1
    L2 = 2*I
454 WRITE (14,105) (K,J,VX(K,J),VZ(K,J), K=L1,L2,1)
```

```
      DO 455 J = 1,NP1,1
  455 WRITE (14,107) MP1,J,VX(MP1,J),VZ(MP1,J)
      DO 456 I = 1,MP1,1
  456 WRITE (15,106) I,VXA(I),VXB(I),VZA(I),VZB(I)
  102 FORMAT ()
  104 FORMAT (2(2I3,E15.7))
  105 FORMAT (2(2I3,2E15.7))
  106 FORMAT (I3,4E15.7)
  107 FORMAT (2I3,2E15.7)
  108 FORMAT (2I3,E15.7)
  230 FORMAT (1H1,4X,'DZ = ',F8.6,8X,'DX = ',F8.6,8X,'R = ',
     1        F5.1,8X,'M = ',I3,8X,'N = ',I3,8X,'PT = ',F4.2
     2        ///,5X,'ALPHA = ',F6.3,7X,'BETA = ',F6.3,8X,
     3        'EPSMAX = ', 1PE7.0, 5X, 'EPVMAX = ', 1PE7.0,
     4        10X,'NL = ',I2,//,5X,'VZERO = ',0PF9.6,4X,
     5        'PHIRDR = ',F9.6)
  286 FORMAT (25X,'VXA (',I2,',',I2,') = ',F10.6)
  289 FORMAT (25X,'VZB (',I2,',',I2,') = ',F10.6)
  297 FORMAT (1H1,'THE VELOCITIES(VZ) ON THE REGULAR GRID ',
     1        'POINTS')
  298 FORMAT (1H1,'THE VELOCITIES(VX) ON THE REGULAR GRID ',
     1        'POINTS')
  299 FORMAT (1H1,'THE VELOCITIES OF THE X- OR Z-COMPONENT',
     1        //)
      STOP
      END
      SUBROUTINE VZ2PA (L,J,K,IP)
      INCLUDE DIMENS,LIST
      CALL ACEX (L,J,A1,A2,C1,C2,E1,E2,G1,ACX,ACEX)
      L1K = L - K
      VZA(L) = IP*(G1*PHIRDR-C2*PHI(L,J)+A2*PHI(L1K,J))/
     1         (ACX*EZ(J))
      WRITE (6,289) L,J,VZA(L)
      VZ(L,J) = IP*(PHIRDR-(1.0-A2)*PHI(L,J)-A2*PHI(L1K,J))/
     1          (ACX*EZ(J))
      VZ(L1K,J) = IP*(-PHIRDR+C2*PHI(L,J)-A1*E1*PHI(L1K,J))/
     1            (ACX*EZ(J))
  288 FORMAT (25X,'VZA (',I2,',',I2,') = ',F10.6)
      RETURN
      END
      SUBROUTINE VZ34PA (L,J,K,IP,KP)
      INCLUDE DIMENS
      CALL ACEX (L,J,A1,A2,C1,C2,E1,E2,G1,ACX,ACEX)
      L1K = L - K
      L2K = L - 2*K
      L3K = L - 3*K
      VZA(L) = IP*((4.0+1/2.0*A1+6.0*A2)*PHIRDR-C2*E2*PHI(L,
     1           J)+2.0*A2*E2*PHI(L1K,J)-A2*C2*PHI(L2K,J))
     2         /(ACEX*EZ(J))
```

```
      WRITE (6,288) L,J,VZA(L)
      VZ(L,J) = IP*(4.0*PHIBDR-C1*E1*(2.0-3.0*A1)*PHI(L,J)
     1              -4.0*A2*E1*PHI(L1K,J)+A2*C1*PHI(L2K,J))
     2          /(ACEX*EZ(J))
      VZ(L1K,J) = IP*(2.0*PHIBDR-E1*C2*PHI(L,J)+2.0*E1*A1*
     1              PHI(L1K,J)+A1*C2*PHI(L2K,J))/(-ACEX*
     2            EZ(J))
      VZ(L2K,J) = IP*(4.0*PHIBDR-C1*E2*PHI(L,J)+4.0*A1*E2*
     1              PHI(L1K,J)-A1*(8.0+3.0*A1)*C1*PHI(L2K,
     2              J))/(ACEX*EZ(J))
      BZ = B(L,J)
      IF (L .EQ. KP) GO TO 2
      IF (ITYP(L,J) .NE. 1) GO TO 5
      CALL ITZ (L1K,J,BZ)
      PHITPZ(L2K) = PHI(L2K,J)
      VZB(L) = IP*(3.0*PHIBDR-4.0*PHITPZ(L1K)+PHITPZ(L2K))/
     1         (2.0*DX*EZ(J))
      WRITE (6,289) L,J,VZB(L)
      GO TO 5
    2 IF (ITYP(L,J) .NE. 1) GO TO 1
      DO 4 IK = 1,2,1
      LK = L - IK*K
      CALL ITZ (LK,J,BZ)
    4 CONTINUE
      PHITPZ(L3K) = PHI(L3K,J)
      VZB(L) = IP*(11.0*PHIBDR-18.0*PHITPZ(L1K)+9.0*PHITPZ
     1             (L2K)-2.0*PHITPZ(L3K))/(DX6*EZ(J))
      WRITE (6,289) L,J,VZB(L)
    1 VZ(L3K,J) = IP*(-11.0*PHI(L3K,J)+18.0*PHI(L2K,J)-9.0*
     1              PHI(L1K,J)+2.0*PHI(L,J))/(DX6*EZ(J))
  288 FORMAT (25X,'VZA (',I2,',',I2,') = ',F10.6)
  289 FORMAT (25X,'VZB (',I2,',',I2,') = ',F10.6)
    5 RETURN
      END
      SUBROUTINE VZSPA (L,J,K,IP)
      INCLUDE DIMENS
      CALL ACEG (L,J,A1,A2,C1,C2,E1,E2,G1,ACX,ACEX)
      L1K = L - K
      L2K = L - 2*K
      L3K = L - 3*K
      L4K = L - 4*K
      IF (L .LE. 2 .OR. L .GT. M) GO TO 3
      BZ = B(L,J)
      IF (ITYP(L,J) - 3) 1,2,3
    1 DO 4 IK = 1,3,1
      LK = L - IK*K
      CALL ITZ (LK,J,BZ)
    4 CONTINUE
      VZB(L) = IP*(11.0*PHIBDR-18.0*PHITPZ(L1K)+9.0*PHITPZ
```

```
     1              (L,2K)-2.0*PHITPZ(L,3K))/(DX6*EZ(J))
      WRITE (6,289) L,J,VZB(L)
    2 VZA(L) = TP*((4.0+12.0*A1+6.0*A2)*PHIBDR-C2*E2*PHI(L,
     1              J)+2.0*A2*E2*PHI(L1K,J)-A2*C2*PHI(L2K,J))
     2          /(ACEX*EZ(J))
      WRITE (6,288) L,J,VZA(L)
    3 VZ(L,J) = TP*(25.0*PHI(L,J)-48.0*PHI(L1K,J)+36.0*PHI
     1              (L2K,J)-16.0*PHI(L3K,J)+3.0*PHI(L4K,J))
     2          /(DX12*EZ(J))
      VZ(L1K,J) = TP*(3.0*PHI(L,J)+10.0*PHI(L1K,J)-18.0*PHI
     1              (L2K,J)+6.0*PHI(L3K,J)-PHI(L4K,J))/(
     2          DX12*EZ(J))
288 FORMAT (26X,'VZA (',I2,',',I2,') = ',F10.6)
289 FORMAT (26X,'VZB (',I2,',',I2,') = ',F10.6)
    RETURN
    END
    SUBROUTINE ITZ (L,J,BZ)
    INCLUDE DIMENS,LIST
    IF (ITYPE(L,J) .NE. 2) GO TO 1
    DZI = PHIBDR - PHI(L,J)
    PHITPZ(L) = PHI(L,J) + DZI*(BZ/B(L,J))
    WRITE (6,908) L,PHITPZ(L)
    GO TO 2
  1 DZI = PHI(L,J+1) - PHI(L,J)
    PHITPZ(L) = PHI(L,J) + DZI*BZ
    WRITE (6,908) L,PHITPZ(L)
908 FORMAT ('   PHITPZ(',I2,') = ',F12.7)
  2 RETURN
    END
    SUBROUTINE VXAB (L,J,K,AX)
    INCLUDE DIMENS,LIST
    IF (ITYPE(L,J) - 3) 1,4,2
  1 CALL BDF (L,J,B1,B2,D2,F2,BDF2)
    VXB(L) = ((4.0+12.0*B1+6.0*B2)*PHIBDR-D2*F2*PHI(L,J)
     1          +2.0*B2*F2*PHI(L,J-1)-B2*D2*PHI(L,J-2))/(
     2          DZ2*EZ(J))
      WRITE (6,287) L,J,VXB(L)
  2 VX(L,J) = (3.0*PHI(L,J-4)-16.0*PHI(L,J-3)+36.0*PHI(L,
     1          J-2)-48.0*PHI(L,J-1)+25.0*PHI(L,J))/(DZ12*
     2          EZ(J))
      VX(L,J-1) = (-PHI(L,J-4)+6.0*PHI(L,J-3)-18.0*PHI(L,J-2
     1          )+10.0*PHI(L,J-1)+3.0*PHI(L,J))/(DZ12*EZ
     2          (J-1))
      DO 3 JK = J2,J3,-1
    3 VX(L,JK) = (PHI(L,JK-2)-8.0*PHI(L,JK-1)+8.0*PHI(L,JK+1
     1          )-PHI(L,JK+2))/(DZ12*EZ(JK))
      IF (ITYPE(L,J) .NE. 1) GO TO 8
    4 DO 7 JM = J1,J3,-1
      CALL ITX (L,JM,K,AX)
```

```
    7 CONTINUE
      VXA(L) = (-2.0*PHITPX(J-3)+9.0*PHITPX(J-2)-18.0*PHITPX
     1           (J-1)+11.0*PHIBDR)/(DZ6*EZ(J))
      WRITE (6,286) L,J,VXA(L)
  286 FORMAT (25X,'VXA (',I2,',',I2,') = ',F10.6)
  287 FORMAT (25X,'VXB (',I2,',',I2,') = ',F10.6)
    8 RETURN
      END
      SUBROUTINE TTX (L,J,K,AX)
      INCLUDE DIMENS.LIST
      IF (ITYPE(L,J) .NE. 3) GO TO 1
      DXI = PHIBDR - PHI(L,J)
      PHITPX(J) = PHI(L,J) + DXI*(AX/A(L,J))
      WRITE (6,907) J,PHITPX(J)
      GO TO 2
    1 DXI = PHI(L+K,J) - PHI(L,J)
      PHITPX(J) = PHI(L,J) + DXI*AX
      WRITE (6,907) J,PHITPX(L)
  907 FORMAT ('   PHITPX(',I2,') = ',F12.7)
    2 RETURN
      END
      SUBROUTINE BDF (L,J,B1,B2,D2,F2,BDFZ)
      INCLUDE DIMENS
      B1 = B(L,J)
      D1 = 1.0 + B(L,J)
      F1 = 2.0 + B(L,J)
      B2 = B1**2
      D2 = D1**2
      F2 = F1**2
      BDFZ = 2.0*B1*D1*F1*DZ
      RETURN
      END
```

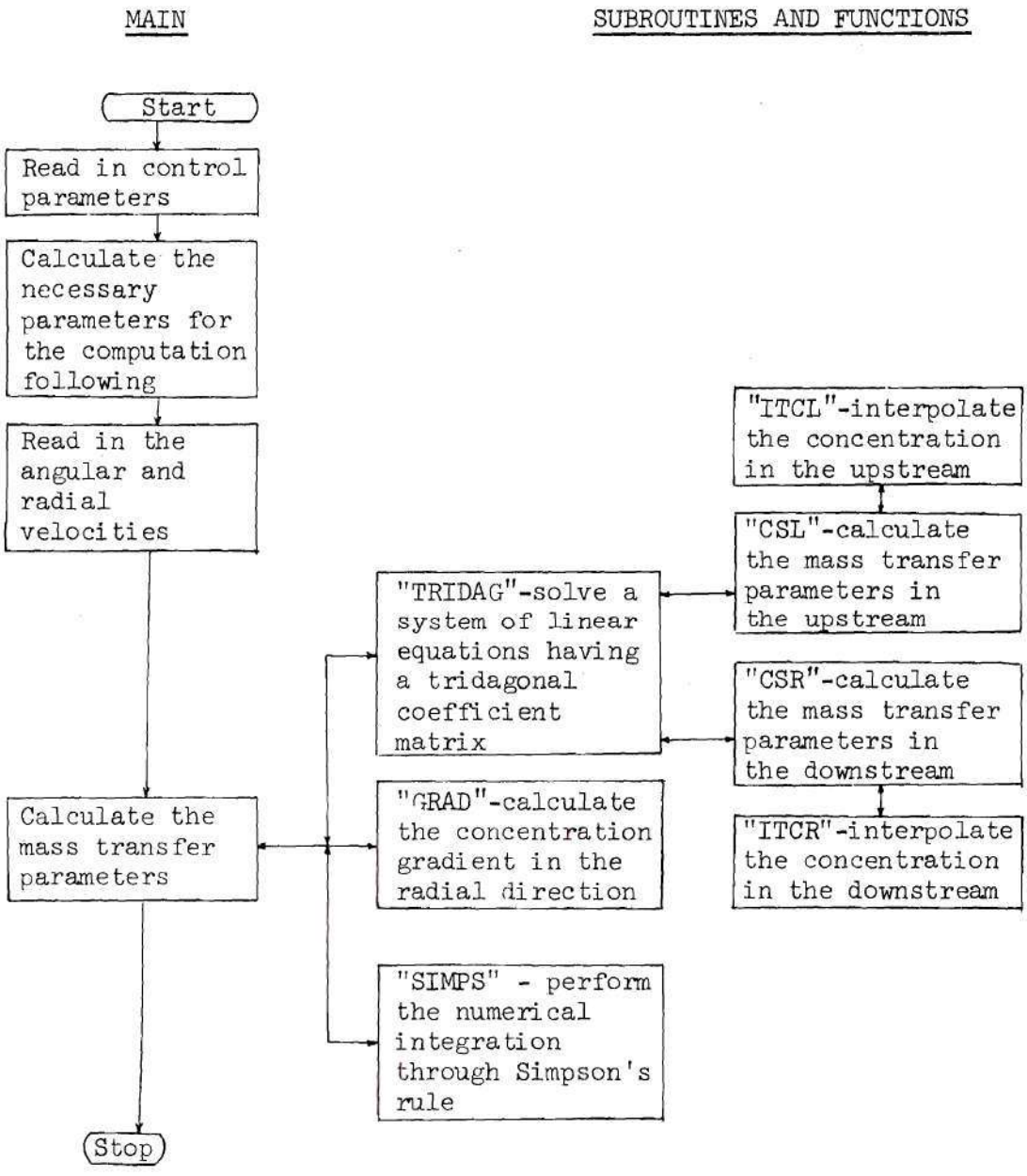

Figure C-3. Computer Block Diagram for Mass Transfer Parameters Calculation.

```
MAIN
  DIMENS  PROC
        COMMON DX,DZ,M,N,MP1,MP2,MHALF,N1,NL,NP1,R,PE,PT,T1,
       1       VZERO,DXOVDZ,DZSQ,EPSMAX,VOPE,ICOUNT,EPS,MR
        COMMON AC(143), BC(143), CC(143), DC(143), CSTAR(61,
       1      143), CGUESS(61,1), DCDZ(61), CS(61), CBDR(61)
       2       , CITPZ(61), Y(143), CBOLD(61), CSOLD(61,143)
       3       , S(61), FLOCNU(61), EZ(143)
        COMMON VX(61,143), VZ(61,143), VXA(61), VXB(61), VZA
       1       (61), VZB(61), DX2, DZ2, DZ6, DZ8
   END
C       LOW REYNOLDS NUMBER FLOW PAST MULTIPLE CYLINDERS WITH
C       SURFACE MASS TRANSFER
C       AUTHOR: TA-YEH J. FANG, SCHOOL OF CHEMICAL ENGINEERING
C               , GEORGIA TECH, ATLANTA, GEORGIA 30332
C               JULY,1974
        INCLUDE DIMENS,LIST
        DIMENSION TAU(61)
        READ (5,102) M,NL,PT,R,ALPHA,BETA,VZERO,EPSMAX
        EPS = 1.0E-6
        PAI = 3.1415926536
        DX = PAI/M
        MHALF = M/2 + 1
        MP1 = M + 1
        MP2 = M + 2
        ZX = ALOG(PT)
        DZ = ZX/NL
        N1 =NL + 1
        DZSQ = DZ**2
        DXOVDZ = DX/DZ
        SCHMDT = 560.0
        PE = R*SCHMDT
        DX2 = 2.0*DX
        DZ2 = 2.0*DZ
        DZ4 = 4.0*DZ
        DZ6 = 6.0*DZ
        DZ8 = 8.0*DZ
        VOPE = 0.5*VZERO*PE
        T1 = 1.0/(PE*DZSQ)
        DO 10 J = N1,151,1
        FJM1 = J - 1
        PTOVRE = PT/EXP(FJM1*DZ)
        XOVRDX = ASIN(PTOVRE)/DX
        IM1 = XOVRDX + EPS
        IF (IM1 .LT. 1) GO TO 11
     10 CONTINUE
     11 NP1 = J - 1
        N = NP1 - 1
        WRITE (6,230) DZ,DX,R,M,N,PT,ALPHA,BETA,NL,VZERO,
```

```
     1                EPSMAX
      DO 12 J = 1,NP1,1
   12 EZ(J) = EXP((J-1)*DZ)
      MD2 = M/2
      DO 690 J = 1,NP1,1
      DO 690 I = 1,MD2,1
      L1 = 2*(I - 1) + 1
      L2 = 2*I
  690 READ (5,105) (IQ,JQ,VX(K,J),VZ(K,J), K=L1,L2,1)
      DO 691 J = 1,NP1,1
  691 READ (5,107) IQ,JQ,VX(MP1,J),VZ(MP1,J)
C.....DETERMINE THE CONCENTRATION PROFILES IN THE LEFT HALF
C     DOMAIN.........
      I = 1
      CGUESS(1,1) = 1.60
      CSTAR(1,1) = CGUESS(1,1)
      CSTAR(1,NP1) = 1.0
      CBOR(1) = CSTAR(1,NP1)
      DO 600 J = 2,N,1
      T3 = VZ(1,J)*EZ(J)/DZ4
      AC(J) = T1 + T3
      BC(J) = -2.0*T1
      CC(J) = T1 - T3
  600 DC(J) = 0.0
      ITERA = 0
      GO TO 602
  601 IF ((ITERA/200)*200 .NE. ITERA) GO TO 6011
      WRITE (6,231) I,ITERA
      WRITE (6,240) (K,CSTAR(I,K), K=1,N1,1)
      WRITE (6,235) CBOR(I)
      STOP
 6011 CSTAR(1,1) = CGUESS(1,1)
  602 DC(2) = -AC(2)*CSTAR(1,1)
      DC(N) = -CC(N)*CSTAR(1,NP1)
      CALL TRIDAG (2,N,AC,BC,CC,DC,Y)
      ITERA = ITERA + 1
      DO 603 J = 2,N,1
      CSTAR(1,J) = Y(J)
      IF (CSTAR(1,J) .LT. 1.0) GO TO 604
  603 CONTINUE
  604 DO 605 L = J,N,1
  605 CSTAR(1,L) = 1.0
      CGUESS(1,1) = (18.0*CSTAR(1,2) - 9.0*CSTAR(1,3) + 2.0
     1                *CSTAR(1,4))/(11.0 + VOPE*DZ6)
      IF (ABS(CGUESS(1,1) - CSTAR(1,1)) .GE. EPSMAX) GO TO
     1601
      CSTAR(1,1) = CGUESS(1,1)
      WRITE (6,231) I,ITERA
      WRITE (6,232) (J,CSTAR(1,J), J=1,NP1,1)
```

```
      DCDZ(1) = (-11.0*CSTAR(1,1) + 18.0*CSTAR(1,2) - 9.0*
     1            CSTAR(1,3) + 2.0*CSTAR(1,4))/DZ6
      WRITE (6,233) DCDZ(1)
      CS(1) = DCDZ(1)/(CSTAR(1,1) - 1.0)
      FLOCNU(1) = -2.0*CS(1)
      WRITE (6,234) FLOCNU(1)
      WRITE (16,103) I,FLOCNU(I)
      I = 2
      CGUESS(I,1) = CSTAR(I-1,1)
      CSTAR(I,1) = CGUESS(I,1)
      CSTAR(I,NP1) = 1.0
      CBDR(I) = CSTAR(I,NP1)
      DO 606 J = 2,N,1
      T3 = (VZ(I,J)+VZ(I-1,J))*EZ(J)/DZ2
      T4 = (VX(I,J)+VX(I-1,J))*EZ(J)/DX2
      AC(J) = T1 + T3
      BC(J) = -(2.0*T1 + T4)
      CC(J) = T1 - T3
  606 DC(J) = -AC(J)*CSTAR(I-1,J-1) + (2.0*T1 - T4)*CSTAR
     1        (I-1,J) - CC(J)*CSTAR(I-1,J+1)
      ITERA = 0
      GO TO 609
  607 IF ((ITERA/200)*200 .NE. ITERA) GO TO 6071
      WRITE (6,231) I,ITERA
      WRITE (6,240) (K,CSTAR(I,K), K=1,N1,1)
      WRITE (6,235) CBDR(I)
      STOP
 6071 CSTAR(I,1) = CGUESS(I,1)
      DO 608 J = 2,N,1
      T4 = (VX(I,J) + VX(I-1,J))*EZ(J)/DX2
  608 DC(J) = -AC(J)*CSTAR(I-1,J-1) + (2.0*T1 - T4)*CSTAR
     1        (I-1,J) - CC(J)*CSTAR(I-1,J+1)
  609 DC(2) = DC(2) - AC(2)*CSTAR(I,1)
      DC(N) = DC(N) - CC(N)*CSTAR(I,NP1)
      CALL TRIDAG (2,N,AC,BC,CC,DC,Y)
      ITERA = ITERA + 1
      DO 610 J = 2,N,1
      CSTAR(I,J) = Y(J)
      IF (CSTAR(I,J) .LT. 1.0) GO TO 611
  610 CONTINUE
  611 DO 612 L = J,N,1
  612 CSTAR(I,L) = 1.0
      CGUESS(I,1) = (18.0*CSTAR(I,2) - 9.0*CSTAR(I,3) + 2.0*
     1               CSTAR(I,4))/(11.0 + VOPE*DZ6)
      IF (ABS(CGUESS(I,1) - CSTAR(I,1)) .GE. EPSMAX) GO TO
     1607
      CSTAR(I,1) = CGUESS(I,1)
      WRITE (6,231) I,ITERA
      WRITE (6,232) (J,CSTAR(I,J), J=1,NP1,1)
```

```
      DCDZ(I) = (-11.0*CSTAR(I,1) + 18.0*CSTAR(I,2) - 9.0*
     1           CSTAR(I,3) + 2.0*CSTAR(I,4))/D76
      WRITE (6,233) DCDZ(I)
      CS(I) = DCDZ(I)/(CSTAR(I,1) - 1.0)
      FLOCNU(I) = -2.0*CS(I)
      WRITE (6,234) FLOCNU(I)
      WRITE (16,103) I,FLOCNU(I)
      DO 613 I = 3,MHALF,1
      CALL CSL (I)
  613 CONTINUE
C.....DETERMINE THE CONCENTRATION PROFILES IN THE RIGHT
C     HALF DOMAIN ........
      MR = MHALF + 1
      DO 14 I = MR,MP1,1
      DO 13 J = 1,N1,1
   13 CSTAR(I,J) = 1.0
   14 CBDR(I) = 1.0
      ICOUNT = 0
  650 ICOUNT = ICOUNT + 1
      IF (ICOUNT .GT. 200) STOP
      IF ((ICOUNT/50)*50 .NE. ICOUNT) GO TO 6501
      WRITE (6,210) ICOUNT
 6501 DO 652 I = MR,M,1
      DO 651 J = 1,N1,1
  651 CSOLD(I,J) = CSTAR(I,J)
  652 CBOLD(I) = CBDR(I)
      DO 653 I = MR,M,1
      CALL CSR (I)
      IF (CBDR(I) .LE. CSTAR(I,N1)) GO TO 6521
      FI1 = I - 1
      ZOVRDZ = (ALOG(PT/SIN(FI1*DX)))/DZ
      BZZ = ZOVRDZ + 1.0 - N1
      P1 = NP1 - N1
      DCS = CSTAR(I,N1) - 1.0
      CBDR(I) = CSTAR(I,N1) - DCS*(BZZ/P1)
 6521 IF ((ICOUNT/50)*50 .NE. ICOUNT) GO TO 653
      WRITE (6,236)
      WRITE (6,232) (K,CSTAR(I,K), K=1,N1,1)
      DCDZ(I) = (-11.0*CSTAR(I,1) + 18.0*CSTAR(I,2) - 9.0*
     1           CSTAR(I,3) + 2.0*CSTAR(I,4))/D76
      CS(I) = DCDZ(I)/(CSTAR(I,1) - 1.0)
      FLOCNU(I) = -2.0*CS(I)
      WRITE (6,237)
      WRITE (6,110) I,CBDR(I),DCDZ(I),CS(I)
      WRITE (6,234) FLOCNU(I)
  653 CONTINUE
      I = MP1
      DO 669 J = 1,N1,1
  669 CSOLD(I,J) = CSTAR(I,J)
```

```
      CBOLD(I) = CBDR(I)
      CGUESS(I,1) = 2.0*CSTAR(I-1,1)
      CSTAR(I,1) = CGUESS(I,1)
      CSTAR(I,NP1) = 1.0
      CBDR(I) = CSTAR(I,NP1)
      DO 670 J = 2,NL,1
      T3 = (VZ(I,J) + VZ(I-1,J))*EZ(J)/DZ8
      T4 = (VX(I,J) + VX(I-1,J))*EZ(J)/DX2
      AC(J) = T1 + T3
      BC(J) = -(2.0*T1 + T4)
      CC(J) = T1 - T3
  670 DC(J) = -AC(J)*CSTAR(I-1,J-1) + (2.0*T1-T4)*CSTAR(I-1,
     1          J) - CC(J)*CSTAR(I-1,J+1)
      S(I) = NP1 - N1
      S1 = S(I) + 1.0
      S2 = S(I) + 2.0
      S1Q = S1**2
      S2Q = S2**2
      SQ = S(I)**2
      ST = S(I)**3
      SB = S(I)*S1*S2
      TB7 = (VZ(I,N1) + VZ(I-1,N1))*EZ(N1)/(SB*DZ8)
      TB8 = T1/SB
      TB9 = (VX(I,N1) + VX(I-1,N1))*EZ(N1)/DX2
      EC = TB7*SQ*S1 + TB8*S(I)*(1.0-SQ)
      IF((EC .GT. 0.0 .AND. AC(NL) .GT. 0.0) .OR. (EC .LT.
     1   0.0 .AND. AC(NL) .LT. 0.0)) GO TO 671
      KC = 1
      GO TO 672
  671 KC = -1
  672 TB10 = KC*EC/AC(NL)
      ACP = 4.0*TB7*SQ*S2 + 2.0*TB8*S(I)*(4.0-SQ)
      BCP = TB7*S1*S2*(2.0-3.0*S(I)) - TB8*(6.0+7.0*S(I)-ST)
     1      + TB9
      AC(N1) = -ACP + TB10*BC(NL)
      BC(N1) = -BCP + 2.0*TB9 + TB10*CC(NL)
      DC(N1) = -EC*CSTAR(I-1,NL-1) + ACP*CSTAR(I-1,NL) +
     1          BCP*CSTAR(I-1,N1) + 12.0*TB8 - 8.0*TB7 + TB10
     2          *DC(NL)
      ITERA = 1
      GO TO 675
  673 IF ((ITERA/200)*200 .NE. ITERA) GO TO 674
      WRITE (6,231) I,ITERA
      WRITE (6,240) (K,CSTAR(I,K), K=1,N1,1)
      WRITE (6,235) CBDR(I)
      STOP
  674 CSTAR(I,1) = CGUESS(I,1)
      T4 = (VX(I,2) + VX(I-1,2))*EZ(2)/DX2
      DC(2) = -AC(2)*CSTAR(I-1,1) + (2.0*T1 - T4)*CSTAR
```

```
     1          (I-1,2) - CC(2)*CSTAR(I-1,3)
  675 DC(2) = DC(2) - AC(2)*CSTAR(I,1)
      CALL TRIDAG (2,N1,AC,BC,CC,DC,Y)
      ITERA = ITERA + 1
      DO 676 K = 2,N1,1
      CSTAR(I,K) = Y(K)
      IF (CSTAR(I,K) .LT. 1.0) GO TO 677
  676 CONTINUE
      GO TO 679
  677 DO 678 L = K,N1,1
  678 CSTAR(I,L) = 1.0
  679 CGUESS(I,1) = (18.0*CSTAR(I,2) - 9.0*CSTAR(I,3) +
     1                 2.0*CSTAR(I,4))/(11.0 + VOPE*DZ6)
      IF (ABS(CGUESS(I,1) - CSTAR(I,1)) .GE. EPSMAX) GO TO
     1673
      CSTAR(I,1) = CGUESS(I,1)
      IF ((ICOUNT/50)*50 .NE. ICOUNT) GO TO 654
      WRITE (6,231) I,ITERA
      WRITE (6,236)
      WRITE (6,232) (K,CSTAR(I,K), K=1,N1,1)
      DCDZ(I) = (-11.0*CSTAR(I,1) + 18.0*CSTAR(I,2) - 9.0*
     1            CSTAR(I,3) + 2.0*CSTAR(I,4))/DZ6
      CS(I) = DCDZ(I)/(CSTAR(I,1) - 1.0)
      FLOCNU(I) = -2.0*CS(I)
      WRITE (6,237)
      WRITE (6,110) I,CBDR(I),DCDZ(I),CS(I)
      WRITE (6,234) FLOCNU(I)
      AVEGRA = GRAD (M,DCDZ)
      WRITE (6,238) AVEGRA
      OVRLNU = -(2.0*SIMPS (CS,DX,1,MP1))/PAI
      WRITE (6,239) OVRLNU
  654 DO 656 I = MR,MP1,1
      DO 656 J = 1,N1,1
  656 IF (ABS(CSTAR(I,J) - CSOLD(I,J)) .GE. EPSMAX) GO TO
     1650
      DO 655 I = MR,MP1,1
  655 IF (ABS(CBDR(I) - CBOLD(I)) .GE. EPSMAX) GO TO 650
      WRITE (6,210) ICOUNT
      WRITE (6,231) I,ITERA
      DO 657 I = MR,MP1,1
      WRITE (6,241) I
      WRITE (6,236)
      WRITE (6,232) (K,CSTAR(I,K), K=1,N1,1)
      DCDZ(I) = (-11.0*CSTAR(I,1) + 18.0*CSTAR(I,2) - 9.0*
     1            CSTAR(I,3) + 2.0*CSTAR(I,4))/DZ6
      CS(I) = DCDZ(I)/(CSTAR(I,1) - 1.0)
      FLOCNU(I) = -2.0*CS(I)
      WRITE (6,237)
      WRITE (6,110) I,CBDR(I),DCDZ(I),CS(I)
```

```
      WRITE (6,234) FLOCNU(I)
      WRITE (16,103) I,FLOCNU(I)
  657 CONTINUE
      DO 658 I = 1,MP1,1
      TAU(I) = CSTAR(I,1) - 1.0
  658 WRITE (17,104) I,TAU(I)
      AVEGRA = GRAD (M,DCDZ)
      WRITE (6,238) AVEGRA
      OVRLNU = -(2.0*SIMPS (CS,DX,1,MP1))/PAI
      WRITE (6,239) OVRLNU
  101 FORMAT (2I3,F5.2,F5.1,2F8.3,I3,F7.3)
  102 FORMAT ()
  103 FORMAT (I3,F12.7)
  104 FORMAT (I3,F13.7)
  105 FORMAT (2(2I3,2E15.7))
  106 FORMAT (I3,4E15.7)
  107 FORMAT (2I3,2E15.7)
  108 FORMAT (2I3,F15.7)
  109 FORMAT (2(2I3,F12.7))
  110 FORMAT (I3,3F12.7)
  111 FORMAT (2F6.3,2E7.1)
  205 FORMAT (23H0                    ITERA = ,I3)
  206 FORMAT (1H1,14X,'CONVERGENCE CONDITION HAS BEEN',
     1        1X,'REACHED AFTER A NUMBER OF ITERATIONS')
  210 FORMAT (/14X,'ICOUNT = ',I3/)
  220 FORMAT ('    J =', I3/(10(I3,F9.6)))
  230 FORMAT (1H1,4X,'DZ = ',F8.6,8X,'DX = ',F8.6,8X,'R = ',
     1        F5.1,8X,'M = ',I3,8X,'N = ',I3,8X,'PT = ',F4.2
     2        ,//,5X,'ALPHA = ',F6.3,7X,'BETA = ',F6.3,8X,
     3        'NL = ',I2,10X,'VZERO = ',F9.6,6X,'EPSMAX = ',
     4        E8.1)
  231 FORMAT (/25X,'I = ',I2,4X,'ITERA = ',I3)
  232 FORMAT (/5(I4,F13.7))
  233 FORMAT (1H0,22X,'LOCAL CONCENTRATION GRADIENT DCDZ = '
     1        ,F10.6)
  234 FORMAT (1H0,22X,'LOCAL NUSSELT NUMBER FLOCNU = ',
     1        F10.6)
  235 FORMAT (/,  CBDR = ',F13.7)
  236 FORMAT (/,   CONCENTRATION IN THE LOWER DOMAIN'/)
  237 FORMAT (/,   BOUNDARY CONCENTRATION (CBDR),DCDZ AND CS'/)
  238 FORMAT (1H0,12X,'AVERAGE CONCENTRATION GRADIENT ',
     1        'AVEGRA = ',F10.6)
  239 FORMAT (1H0,12X,'OVERALL NUSSELT NUMBER OVERNU = ',
     1        F10.6)
  240 FORMAT (5(I4,E13.7))
  241 FORMAT (/,   I = ',I2/)
      STOP
      END
      SUBROUTINE CSL (IH)
```

```
      INCLUDE  DIMENS,LIST
      CGUESS(IH,1) = CSTAR(IH-1,1)
      CSTAR(IH,1) = CGUESS(IH,1)
      FIH1 = IH - 1
      ZOVRDZ = (ALOG(PT/SIN(FIH1*DX)))/DZ
      BZJ = ZOVRDZ + 1.0
      J = BZJ
      BZ = BZJ - J
      IF (IH .NE. MHALF) GO TO 6141
      CHF = 1.0
      CSTAR(IH,J) = CHF
 6141 J1 = J - 1
      DO 615 K = 2,J1,1
      T3 = VZ(IH,K)*EZ(K)/DZ
      T4 = VX(IH,K)*EZ(K)/DX
      AC(K) = 2.0*T1 + T3/2.0
      BC(K) = -(4.0*T1 + 3.0*T4/2.0)
      CC(K) = 2.0*T1 - T3/2.0
  615 DC(K) = T4*(CSTAR(IH-2,K)/2.0 - 2.0*CSTAR(IH-1,K))
      IF (ABS (BZ) .LT. EPS)   GO TO 618
      DO 617 IK = 1,2,1
      IHK = IH - IK
      CALL ITCL (IHK,J,BZJ)
  617 CONTINUE
      B2 = BZ**2
      D1 = 1.0 + BZ
      D2 = D1**2
      BD = BZ*D1
      H1 = 1.0 + 2.0*BZ
      TB1 = BD/(2.0*DXOVDZ)
      TB2 = VZ(IH,J)*EZ(J)/(BD*DZ)
      TB3 = 4.0*T1/BD
      TB4 = VX(IH,J)*EZ(J)/DX2
      TB5 = (TB2 - TB3)/(3.0*TB1 + H1*TAN((IH-1)*DX))
      AC(J) = TB2*B2 + TB3*BZ + TB5*B2*TAN((IH-1)*DX)
      BC(J) = -(TB2*(B2 - 1.0) + TB3*D1 + 3.0*TB4 + TB5*D2*
     1          TAN((IH-1)*DX))
      DC(J) = TB4*(CSTAR(IH-2,J) - 4.0*CSTAR(IH-1,J)) + TB1
     1        *TB5*(4.0*CITPZ(IH-1) - CITPZ(IH-2))
  618 ITERA = 0
      GO TO 625
  619 IF ((ITERA/200)*200 .NE. ITERA) GO TO 6190
      WRITE (6,231) IH,ITERA
      WRITE (6,240) (K,CSTAR(IH,K), K=1,KJ,1)
      STOP
 6190 CSTAR(IH,1) = CGUESS(IH,1)
      IF (ABS (BZ) .GE. EPS) GO TO 6192
      CSTAR(IH,J) = CHF
      T4 = VX(IH,J1)*EZ(J1)/DX
```

```
      DC(J1) = T4*(CSTAR(IH-2,J1)/2.0 - 2.0*CSTAR(IH-1,J1))
      DC(J1) = DC(J1) - CC(J1)*CSTAR(IH,J)
 6192 T4 = VX(IH,2)*EZ(2)/DX
      DC(2) = T4*(CSTAR(IH-2,2)/2.0 -  2.0*CSTAR(IH-1,2))
  620 DC(2) = DC(2) - AC(2)*CSTAR(IH,1)
      IF (ITERA .GE. 1 .OR. ABS (BZ) .GE. EPS) GO TO 6200
      DC(J1) = DC(J1) - CC(J1)*CSTAR(IH,J)
 6200 IF (ABS (BZ) .LT. EPS) GO TO 6201
      KJ = J
      GO TO 6202
 6201 KJ = J1
 6202 CALL TRIDAG (2,KJ,AC,BC,CC,DC,Y)
      ITERA = ITERA + 1
      DO 621 K = 2,KJ,1
      CSTAR(IH,K) = Y(K)
      IF (CSTAR(IH,K) .LT. 1.0) GO TO 622
  621 CONTINUE
      IF (ABS (BZ) .LT. EPS) GO TO 628
      CBDR(IH) = TB1*(4.0*CITPZ(IH-1) - CITPZ(IH-2)) + TAN(
     1           (IH-1)*DX)*(D2*CSTAR(IH,KJ) - B2*CSTAR(IH,
     2           KJ-1))/(3.0*TB1 + H1*TAN((IH-1)*DX))
      IF (CBDR(IH) - CSTAR(IH,KJ)) 6222,6222,6221
  628 CBDR(IH) = (4.0*CSTAR(IH,KJ) - CSTAR(IH,KJ-1))/3.0
      IF (CBDR(IH) - CSTAR(IH,KJ)) 6222,6222,6221
 6221 BLZ = ZOVRDZ + 1.0 - KJ
      BZL = NP1 - KJ
      DCS = CSTAR(IH,KJ) - 1.0
      CBDR(IH) = CSTAR(IH,KJ) - DCS*(BLZ/BZL)
 6222 IF (CBDR(IH) .LE. (1.0+EPS)) GO TO 624
      GO TO 625
  622 DO 623 L = K,KJ,1
  623 CSTAR(IH,L) = 1.0
  624 CBDR(IH) = 1.0
  625 CGUESS(IH,1) = (18.0*CSTAR(IH,2) - 9.0*CSTAR(IH,3) +
     1                2.0*CSTAR(IH,4))/(11.0 + VOPE*DZ6)
      IF (ABS(CGUESS(IH,1) - CSTAR(IH,1)) .GE. EPSMAX) GO TO
     1619
      IF (ABS (BZ) .GE. EPS) GO TO 626
      CHF = (4.0*CSTAR(IH,J-1) - CSTAR(IH,J-2))/3.0
      IF (ABS(CHF - CSTAR(IH,J)) .GE. EPSMAX) GO TO 619
      CSTAR(IH,J) = CHF
  626 CSTAR(IH,1) = CGUESS(IH,1)
      WRITE (6,231) IH,ITERA
      WRITE (6,232) (K,CSTAR(IH,K), K=1,KJ,1)
      WRITE (6,235) CBDR(IH)
      DCDZ(IH) = (-11.0*CSTAR(IH,1) + 18.0*CSTAR(IH,2) - 9.0
     1           *CSTAR(IH,3) + 2.0*CSTAR(IH,4))/DZ6
      WRITE (6,233) DCDZ(IH)
      CS(IH) = DCDZ(IH)/(CSTAR(IH,1) - 1.0)
```

```
      FLOCNU(IH) = -2.0*CS(IH)
      WRITE (6,234) FLOCNU(IH)
      WRITE (16,103) IH,FLOCNU(IH)
  103 FORMAT (I3,F12.7)
  231 FORMAT (1H0,25X,'I = ',I2,4X,'ITERA = ',I3)
  232 FORMAT (/5(I4,F13.7))
  233 FORMAT (1H0,22X,'LOCAL CONCENTRATION GRADIENT DCDZ = '
     1        ,F10.6)
  234 FORMAT (1H0,22X,'LOCAL NUSSELT NUMBER FLOCNU = ',
     1        F10.6)
  235 FORMAT (/,  CBDR = ', F13.7)
  240 FORMAT (5(I4,E13.7))
      RETURN
      END
      SUBROUTINE TTCL (L,J,BZ)
      INCLUDE DIMENS,LIST
      IF (L .EQ. 1) GO TO 3
      FL1 = L - 1
      ZOVRDZ = (ALOG(PT/SIN(FL1*DX)))/DZ
      JZ = ZOVRDZ + 1.0
      DO 1 K = 1,JZ,1
      IF (CSTAR(L,K) .LE. 1.0) GO TO 3
    1 CONTINUE
      BZI = BZ - JZ
      IF (JZ .NE. J) GO TO 2
      BZZ = ZOVRDZ + 1.0 - JZ
      DCI = CSTAR(L,JZ) - CBDR(L)
      CITPZ(L) = CSTAR(L,J) - DCI*(BZI/BZZ)
      GO TO 4
    2 DCI = CSTAR(L,J) - CSTAR(L,J+1)
      CITPZ(L) = CSTAR(L,J) - DCI*BZI
      GO TO 4
    3 CITPZ(L) = 1.0
    4 WRITE (6,242) L,CITPZ(L)
  242 FORMAT ('   CITPZ(',I2,') =',F12.7)
      RETURN
      END
      SUBROUTINE CSR (IH)
      INCLUDE DIMENS,LIST
      CGUESS(IH,1) = CSTAR(IH-1,1)
      CSTAR(IH,1) = CGUESS(IH,1)
      DO 660 K = 2,NL,1
      T3 = VZ(IH,K)*EZ(K)/DZ
      T4 = VX(IH,K)*EZ(K)/DX
      AC(K) = 2.0*T1 + T3/2.0
      BC(K) = -(4.0*T1 + 3.0*T4/2.0)
      CC(K) = 2.0*T1 - T3/2.0
  660 DC(K) = T4*(CSTAR(IH-2,K)/2.0 - 2.0*CSTAR(IH-1,K))
      IF (IH .LT. M) GO TO 661
```

```
      S(IH) = NP1 - N1
      GO TO 662
  661 IH1 = IH - 1
      ZOVRDZ = (ALOG(PT/SIN(IH1*DX)))/DZ
      BZJ = ZOVRDZ + 1.0
      S(IH) = BZJ - N1
      DO 662 IK = 1,2,1
      IHK = IH + IK
      CALL ITCR (IHK,BZJ)
  662 CONTINUE
  663 S1 = S(IH) + 1.0
      S2 = S(IH) + 2.0
      S10 = S1**2
      S20 = S2**2
      SQ = S(IH)**2
      ST = S(IH)**3
      SB = S(IH)*S1*S2
      TB6 = SB/DXOVDZ
      TB7 = VZ(IH,N1)*EZ(N1)/(DZ2*SB)
      TB8 = 2.0*T1/SB
      TB9 = VX(IH,N1)*EZ(N1)/DX2
      EC = -(TB7*SQ*S1 + TB8*S(IH)*(1.0-SQ))
      IF (IH .LT. M) GO TO 636
      IF ((EC .GT. 0.0 .AND. AC(NL) .GT. 0.0) .OR. (EC .LT.
     1    0.0 .AND. AC(NL) .LT. 0.0)) GO TO 634
      KC = 1
      GO TO 635
  634 KC = -1
  635 TB10 = KC*EC/AC(NL)
      AC(N1) = 4.0*TB7*SQ*S2 + 2.0*TB8*S(IH)*(4.0-SQ) + TB10
     1         *BC(NL)
      BC(N1) = TB7*S1*S2*(2.0-3.0*S(IH)) - TB8*(6.0+7.0*
     1         S(IH)-ST) - 3.0*TB9 + TB10*CC(NL)
      DC(N1) = 1.0*TB7 - 6.0*TB8 - TB9*(4.0*CSTAR(IH-1,N1) -
     1         CSTAR(IH-2,N1)) + TB10*DC(NL)
      GO TO 6361
  636 TB11 = (4.0*TB7 - 6.0*TB8)/(3.0*TB6 + 2.0*TAN(IH1*DX)
     1       *(2.0 + 6.0*S(IH) + 3.0*SQ))
      TB12 = TB11*TAN(IH1*DX)
      EC = TB12*SQ*S1Q - EC
      IF ((EC .GT. 0.0 .AND. AC(NL) .GT. 0.0) .OR. (EC .LT.
     1    0.0 .AND. AC(NL) .LT. 0.0)) GO TO 637
      KC = 1
      GO TO 638
  637 KC = -1
  638 TB13 = KC*EC/AC(NL)
      AC(N1) = -(2.0*TB12*S20*SQ + 4.0*TB7*SQ*S2 + 2.0*TB8*
     1         S(IH)*(4.0-SQ)) + TB13*BC(NL)
      BC(N1) = TB12*S1Q*S20 + TB8*(6.0+7.0*S(IH)-ST) + 3.0*
```

```
     1          TB9 - TB7*S1*S2*(2.0 - 3.0*S(IH)) + TB13*
     2          CC(NL)
      DC(N1) = TB9*(4.0*CSTAR(IH-1,N1) - CSTAR(IH-2,N1)) -
     1          TB6*TB11*(4.0*CITPZ(IH+1) - CITPZ(IH+2)) +
     2          TB13*DC(NL)
 6381 ITERA = 0
      GO TO 641
  639 IF ((ITERA/200)*200 .NE. ITERA) GO TO 640
      WRITE (6,231) IH,ITERA
      WRITE (6,236)
      WRITE (6,240) (K,CSTAR(IH,K), K=1,N1,1)
      WRITE (6,235) CBDR(IH)
      STOP
  640 CSTAR(IH,1) = CGUESS(IH,1)
      T4 = VX(IH,2)*EZ(2)/DX
      DC(2) = T4*(CSTAR(IH-2,2)/2.0 - 2.0*CSTAR(IH-1,2))
  641 DC(2) = DC(2) - AC(2)*CSTAR(IH,1)
      CALL TRIDAG (2,N1,AC,BC,CC,DC,Y)
      ITERA = ITERA + 1
      DO 642 K = 2,N1,1
      CSTAR(IH,K) = Y(K)
      IF (CSTAR(IH,K) .LT. 1.0) GO TO 643
  642 CONTINUE
      IF (IH .EQ. M) GO TO 6441
      CBDR(IH) = (TAN((IH-1)*DX)*(S1Q*S2Q*CSTAR(IH,N1) - 2.0
     1           *SQ*S2Q*CSTAR(IH,NL) + SQ*S1Q*CSTAR(IH,
     2           NL-1)) + TB6*(4.0*CITPZ(IH+1) - CITPZ(IH
     3           +2)))/(3.0*TB6 + 2.0*TAN((IH-1)*DX)*(2.0
     4           +6.0*S(IH)+3.0*SQ))
      IF (CBDR(IH) .LE. (1.0 + EPS)) GO TO 6441
      GO TO 645
  643 DO 644 L = K,N1,1
  644 CSTAR(IH,L) = 1.0
 6441 CBDR(IH) = 1.0
  645 CGUESS(IH,1) = (18.0*CSTAR(IH,2) - 9.0*CSTAR(IH,3) +
     1                2.0*CSTAR(IH,4))/(11.0 + VOPE*DZ6)
      IF (ABS(CGUESS(IH,1) - CSTAR(IH,1)) .GE. EPSMAX) GO TO
     1639
      CSTAR(IH,1) = CGUESS(IH,1)
      IF ((ICOUNT/50)*50 .NE. ICOUNT) GO TO 646
      WRITE (6,231) IH,ITERA
  231 FORMAT (/25X,'I = ',I2,4X,'ITERA = ',I3)
  235 FORMAT (/,  CBDR = ', F13.7)
  236 FORMAT (/,   CONCENTRATION IN THE LOWER DOMAIN',/)
  240 FORMAT (5(I4,E13.7))
  646 RETURN
      END
      SUBROUTINE ITCR (L,RZ)
      INCLUDE DIMENS,LIST
```

```
      DO 1 K = 1,N1,1
      IF (CSTAR(L,K) .LE. 1.0) GO TO 4
    1 CONTINUE
      FL1 = L - 1
      ZOVRDZ = (ALOG(PT/SIN(FL1*DX)))/DZ
      BZZ = ZOVRDZ + 1.0 - N1
      BZI = BZ - N1
      DCI = CSTAR(L,N1) - CBDR(L)
      CITPZ(L) = CSTAR(L,N1) - DCI*(BZI/BZZ)
      IF (CITPZ(L) .LE. (1.0 + EPS)) GO TO 4
      GO TO 5
    4 CITPZ(L) = 1.0
    5 IF ((ICOUNT/50)*50 .NE. ICOUNT) GO TO 6
      WRITE (6,242) L,CITPZ(L)
  242 FORMAT ('   CITPZ(',I2,') =',F12.7)
    6 RETURN
      END
      SUBROUTINE TRIDAG (IF,IU,AQ,BQ,CQ,DQ,Q)
      DIMENSION AQ(1),BQ(1),CQ(1),DQ(1),Q(1),FBETA(143),
     1          GAMMA(143)
      FBETA(IF) = BQ(IF)
      GAMMA(IF) = DQ(IF)/FBETA(IF)
      IFP1 = IF + 1
      DO 1 K = IFP1,IU
      FBETA(K) = BQ(K) - AQ(K)*CQ(K-1)/FBETA(K-1)
    1 GAMMA(K) = (DQ(K) - AQ(K)*GAMMA(K-1))/FBETA(K)
      Q(IU) = GAMMA(IU)
      LAST = IU - IF
      DO 2 KQ = 1,LAST
      IV = IU - KQ
    2 Q(IV) = GAMMA(IV) - CQ(IV)*Q(IV+1)/FBETA(IV)
      RETURN
      END
      FUNCTION GRAD (M,F)
      DIMENSION F(1)
      DCDZ = 0.0
      MP1 = M + 1
      DO 1 I = 1,MP1,1
      IF (I .EQ. 1 .OR. I .EQ. MP1) GO TO 2
      DCDZ = DCDZ + F(I)
      GO TO 1
    2 DCDZ = DCDZ + 0.5*F(I)
    1 CONTINUE
      GRAD = DCDZ/M
      RETURN
      END
```

BIBLIOGRAPHY

1. G. G. Stokes, "On the Effect of the Internal Friction of Fluids on on the Motion of Pendulums," Trans. Camb. Phil. Soc., 9, 8 (1851).

2. C. W. Oseen, "Ueber die Stokes'sche Formel, und über eine verwandte Aufgabe in der Hydrodynamik," Ark. Math. Astronom. Fys., 6, 29 (1911).

3. H. Lamb, "On the Uniform Motion of a Sphere through a Viscous Fluid," Philos. Mag., 21, 112 (1911).

4. S. Tomotika and T. Aoi, "The Steady Flow of Viscous Fluid Past a Sphere and Circular Cylinder at Small Reynolds Numbers," Quart. J. Mech. Appl. Math., 3, 140 (1956).

5. H. Yamada, "On the Slow Motion of Viscous Liquid Past a Circular Cylinder," Rep. Res. Inst. Appl. Mech., Kyushu Univ., 3, 11 (1954).

6. A. Thom, "An Investigation of Fluid Flow in Two Dimensions," British Aero. Res. Council, R. & M., No. 1194 (1928).

7. M. Kawaguti, "Numerical Solution of the Navier-Stokes Equations for the Flow Around a Circular Cylinder at Reynolds Number 40," J. Phys. Soc. Japan, 8, 747 (1953).

8. A. E. Hamielec and J. D. Raal, "Numerical Studies of Viscous Flow Around Circular Cylinders," Phys. Fluids, 12, 11 (1969).

9. H. B. Keller and H. Takami, "Numerical Studies of Steady Viscous Flow about Cylinders," Numerical Solutions of Nonlinear Differential Equations, ed. by D. Greenspan, John Wiley & Sons, Inc., New York, pp. 115-140 (1966).

10. H. C. Wu, "Low Reynolds Number Flow Perpendicular to a Circular Cylinder with Surface Mass Transfer," Ph.D. Thesis, School of Chemical Engineering, Georgia Institute of Technology, Atlanta (Dec. 1971).

11. S. Taneda, "Experimental Investigation of the Wakes behind Cylinders and Plates at Low Reynolds Numbers," J. Phys. Soc. Japan, 11, 302 (1956).

12. D. J. Tritton, "Experiments on the Flow Past a Circular Cylinder at Low Reynolds Numbers," J. Fluid Mech., 6, 547 (1959).

13. M. Nishioka and H. Sato, "Measurement of Velocity Distribution in the Wake of a Circular Cylinder at low Reynolds Numbers," J. Fluid Mech., 65, 97 (1974).

14. H. Fujikawa, "The Forces Acting on Two Circular Cylinders of Arbitrary Radii Placed in a Uniform Stream at Low Values of Reynolds Number," J. Phys. Soc. Japan, 11,690 (1956).

15. K. Tamada and H. Fujikawa, "The Steady Two Dimensional Flow of Viscous Fluid at Low Reynolds Numbers Passing Through an Infinite Row of Equal Parallel Circular Cylinders," Quart. J. Mech. Appl. Math., 10, 425 (1957).

16. S. Kuwabara, "The Forces Experienced by Randomly Distributed Parallel Circular Cylinders or Spheres in a Viscous Flow at Small Reynolds Numbers," J. Phys. Soc. Japan, 14, 527 (1959).

17. J. Happel, "Viscous Flow Relative to Arrays of Cylinders," A.I.Ch.E. J., 5(2), 174 (1959).

18. B. P. LeClair and A. E. Hamielec, "Viscous Flow Through Particle Assemblages at Intermediate Reynolds Numbers," I.E.C. Fundamental, 9(4), 608 (1970).

19. K. Ishihara, "Incompressible Viscous Flow Across Banks of Tubes at Low Reynolds Numbers," Ph.D. Thesis, School of Chemical Engineering, Oklahoma State University, Stillwater (May 1971).

20. O. L. Bergelin, A. P. Colburn and H. L. Hull, "Heat Transfer and Fluid Friction During Viscous Flow Across Banks of Tubes," University of Delaware Experiment Station Bulletin No. 2 (1950).

21. H. Honji, "Viscous Flow past a Group of Circular Cylinders," J. Phys. Soc. Japan, 34, 821 (1973).

22. V. G. Levich, Physicochemical Hydrodynamics, Prentice-Hall, Englewood Cliffs, New Jersey (1962).

23. V. G. Jenson, "Viscous Flow Round a Sphere at Low Reynolds Numbers (40)," Proc. Royal Soc. London, A249, 346 (1959).

24. J. Crank and P. Nicholson, "A Practical Method for Numerical Evaluation of Solutions of Partial Differential Equations of the Heat-Conduction Type," Proc. Camb. Phil. Soc., 43, 50 (1947).

25. G. H. Bruce, D. W. Peaceman, H. H. Rachford and J. D. Rice, "Calculation of Unsteady-State Gas Flow Through Porous Media," Trans. Amer. Inst. Mining and Met. Engrs., 198, 79 (1953).

Supplementary References:

1. W. F. Ames, Nonlinear Partial Differential Equations in Engineering, Academic Press, New York (1965).

2. R. B. Bird, W. E. Stewart and E. N. Lightfoot, Transport Phenomena, John Wiley & Sons, New York (1960).

3. B. Carnahan, H. A. Luther and J. O. Wilkes, Applied Numerical Methods, John Wiley & Sons, New York (1969).

4. "General Purpose Contouring Program," by California Computer Products, Inc., 1968.

5. L. Lapidus, Digital Computation for Chemical Engineers, McGraw-Hill, New York (1962).

6. V. G. Levich, Physicochemical Hydrodynamics, Prentice-Hall, Englewood Cliffs, New Jersey (1962).

7. W. H. McAdams, Heat Transmission, 3rd ed., McGraw-Hill, New York (1954).

8. D. G. Moursund and C. S. Duris, Elementary Theory and Application of Numerical Analysis, McGraw-Hill, New York (1967).

9. "Research and Development Progress Reports," by the Office of Saline Water, U. S. Department of the Interior, Washington.

10. R. D. Richtmyer and K. W. Morton, Difference Methods for Initial Value Problems, 2nd ed., Interscience, New York (1967).

11. M. G. Salvadori and M. L. Baron, Numerical Methods in Engineering, 2nd ed., Prentice-Hall, Englewood Cliffs, New Jersey (1961).

12. H. Schlichting, Boundary-Layer Theory, 6th ed., McGraw-Hill, New York (1968).

13. J. Singer, Elements of Numerical Analysis, Academic Press, New York (1964).

VITA

Ta-Yeh Jerry Fang was born on July 25, 1946 in Tien-Chin City, Northern China, and graduated from high school at Taipei, Taiwan in 1964. He attended Cheng Kung University at Tainan, Taiwan and received a Bachelor of Science degree in Chemical Engineering in 1968.

The author was employed by Acme Chemical Works at Taipei, before entering graduate school at Georgia Tech in 1969. He received an M.S. in Chemical Engineering in 1970. During 1970 and 1971 he served as a Graduate Teaching Assistant in the School of Chemical Engineering. In 1973, he was employed by Coca Cola Export Corp. at Atlanta, Georgia.

He is a member of the American Institute of Chemical Engineers, the Association of Professional Engineers in Ontario, Canada, and the Fine Particles Society.